UNIVERSITY OF ROME

“Sapienza”

SCHOOL OF BIOLOGY AND MOLECULAR MEDICINE

PhD in INNOVATION IN IMMUNO-MEDIATED AND HEMATOLOGICAL DISORDERS

XXXIV CICLE

Dr. Maggi Federica

“Effects of TRPV receptor agonists in Chronic Myeloid Leukemia”

Coordinator:

Prof. Silvano Sozzani

Tutor:

Prof. Giorgio Santoni

A.A. 2020-2021

CONTENTS

Introduction

Hematological malignancies: chronic and acute myeloid leukemia

Haematological malignancies represent a mixed group of neoplasms (Figure 1) divided generally in: acute myeloid and lymphocytic leukaemia (AML and ALL), chronic myeloid and lymphocytic leukaemia (CML and CLL), Hodgkin's and non-Hodgkin's lymphoma (HL and NHL) and multiple myeloma (MM) [1].

Leukaemia is based on the accumulation of immature cells, mainly affecting blood-forming cells in the bone-marrow, it accounts for 30% of all childhood cancers, and counting 437.0 thousand new cases of and 309.0 thousand cancer deaths worldwide in 2018 [2,3].

AML is an aggressive cancer identified by a block in myeloid differentiation lineage, with an uncontrolled proliferation of abnormal myeloid progenitors, that pile up in the bone marrow and blood flow. Its outset can be different from an underlying haematological disorder or as a consequence of prior therapy; however mostly, it develops as a *de novo* disorder in healthy individuals. Indeed, AML can arise at any age, is more common in male than in female, and could be the result of the exposure to smoke, benzene and formaldehyde, pesticide, and other chemicals [4,5].

Until today, several markers have been identified to improve patient's characterization allowing precise treatment decisions and care [4]. Despite this, the majority of patients experience relapses and the overall survival (OS) after 5 years is about 45% in young patients and less than 10% in elderly one [5].

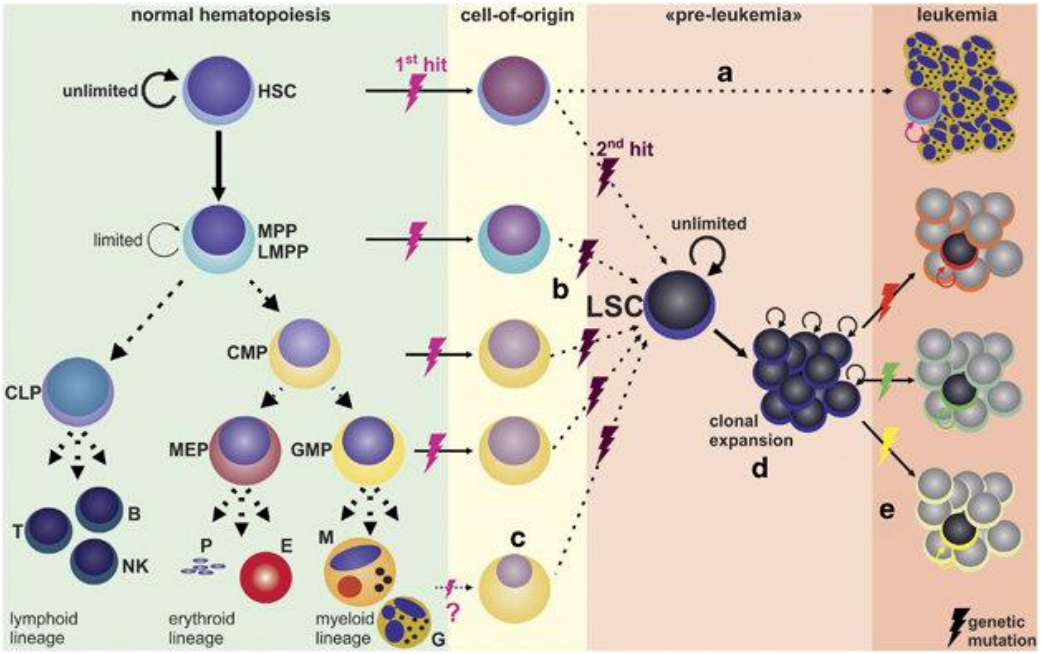

***Figure 1**: The leukemic stem cell model. Comparison of normal hematopoiesis with malignant hematopoiesis*[6].

CML is a myeloproliferative disorder first described in 1845, it represents about 14-15% of all leukaemia cases [7], and is characterized by an incomplete differentiation of hematopoietic stem cells (HSC) into the adult form with consequent accumulation of immature cells in the bone marrow and peripheral blood. Until now, there are no data referring to hereditary, familial, geographic, ethnic, or economic associations, but the common risk factor are represented by age (>64 years), radiation exposure used in other therapies and gender (men are somewhat more predispose to develop CML than women). The main treatments for CML include allogeneic stem cell transplantation, chemotherapy, interferon and tyrosine kinase inhibitors (TKI) administration. CML patients show a good prognosis, but it is not uncommon to have episode of TKI resistance or intolerance due to BCR-ABL mutations [8].

CML cells show uncontrolled proliferation, reduced sensitivity to apoptotic signals that promote the growth and selection of a progenitor population known as leukaemia stem cells (LSC). Numerous studies have shown that LSCs themselves are involved in initiation, drug resistance and recurrence of CML. Although good results have been achieved thanks to the introduction of the TKI, such as imatinib,

nilotinib, dasatinib, bosutinib and ponatinib, into clinical practice, bringing the survival rate to over 90%, for several subjects this treatment must be discontinued or modified due to the development of adverse drug reactions or resistance [9,10]. Indeed, the BCR-ABL1 fusion products can remain still detectable in CML patients even after the remission [8]. For this reason, recent data support the use of mixed therapeutic approaches aimed at considering not only kinase-dependent mechanisms, but also independent ones. In fact, a lot of research is aimed at studying in greater depth new targets expressed exclusively on LSCs [2,9,11,12].

From the molecular profiling, the *BCR-ABL1* fusion gene products are detected in 95% of all CML cases [13], instead, only 1% of all AML cases are positive for this condition [14]. The *BCR-ABL1* gene generates as a product of the t(9;22)(q34;q11) giving rise to the Philadelphia (Ph) chromosome which is detectable in most of the cases. *BCR-ABL* is responsible for the dysregulation of important cellular pathways (Figure 2): RAS/MAPK pathway, which induces proliferation, the PI3K (phosphatidylinositol-3 kinase)/AKT, which leads to apoptosis, and JAK/STAT, with increased transcriptional activity, which are essential for leukemogenesis. Unfortunately, about the 5-10% of CML patients show uncommon t(9;22)(q34;q11) arrangements with the involvement of additional chromosome variant as microdeletions proximal to the *ABL1* or distant to the *BCR* gene (30-40%) or the presence of *BCR-ABL* mutant clones (T315I) which are insensible even to second generation TKIs [15,16].

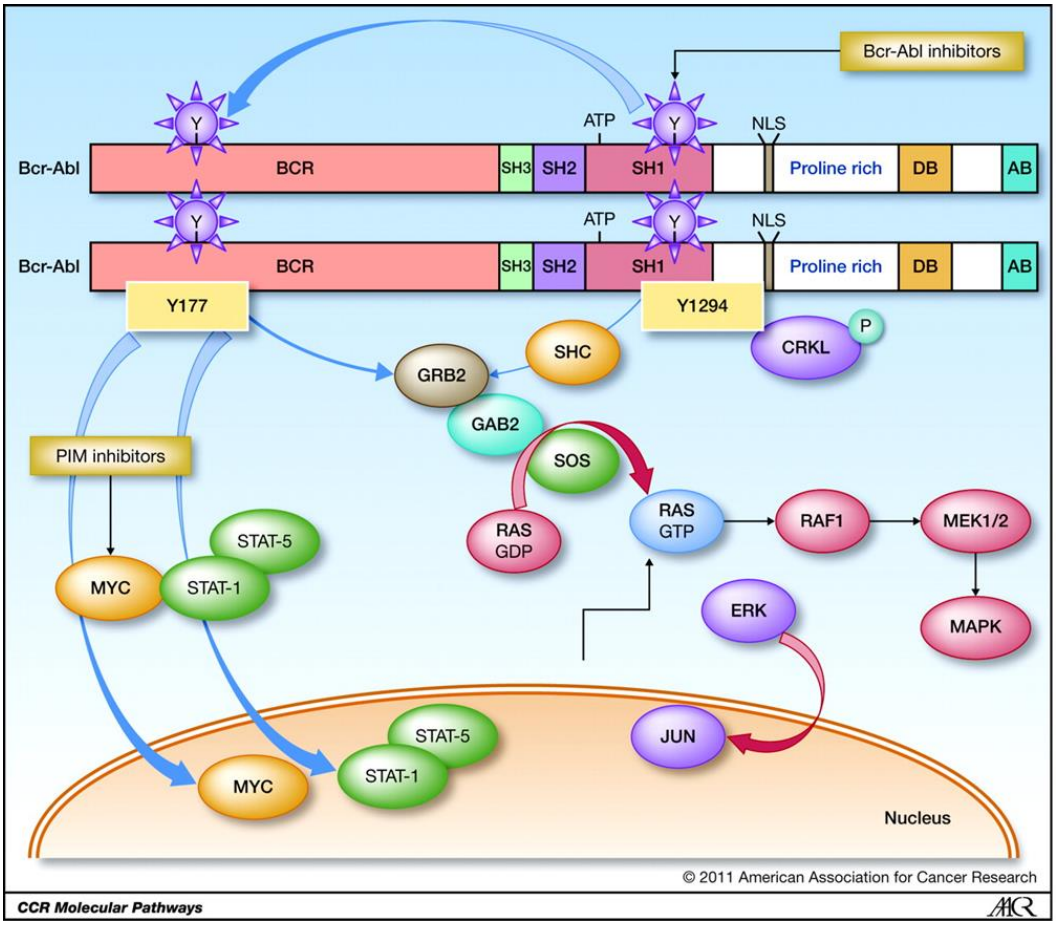

Figure 2. *Schematic representation of the molecular pathway activated by BCR-ABL* [15].

Transient Receptor Potential (TRP) Channels in Cancer

Extract from the article: Maggi F, Morelli MB, Nabissi M, Marinelli O, Zeppa L, Aguzzi C, Santoni G, Amantini C. Transient Receptor Potential (TRP) Channels in Haematological Malignancies: An Update. Biomolecules. 2021;11(5):765. doi: 10.3390/biom11050765.

Transient Receptor Potential (TRP) channels are a family of ion channels belonging to voltage-gated super families, mainly involved in Ca^{2+} trafficking. They are divided in seven major groups (Figure 3): TRPC1-6 ("C" for canonical), TRPV1-6 ("V" for vanilloid), TRPM1-8 ("M" for melastatin), TRPN ("N" for no mechanoreceptor potential C, not present in mammalian), TRPA ("A" for ankyrin), TRPP ("P" for polycystic) and TRPML1-3 ("ML" for mucolipin) [17,18]. Most of TRPs are selective for cations and most of them are permeable to both monovalent, as sodium (Na^{+}), and divalent cations, as magnesium (Mg^{2+}) or calcium (Ca^{2+}) [19]. Moreover, they can be activated by a variety of environmental stimuli like temperature (as TRPV2), mechanical forces (as TRPA1), and plant-derived compound as menthol for TRPM8 or capsaicin (CPS) for TRPV1 (Table 1) [20–22].

A

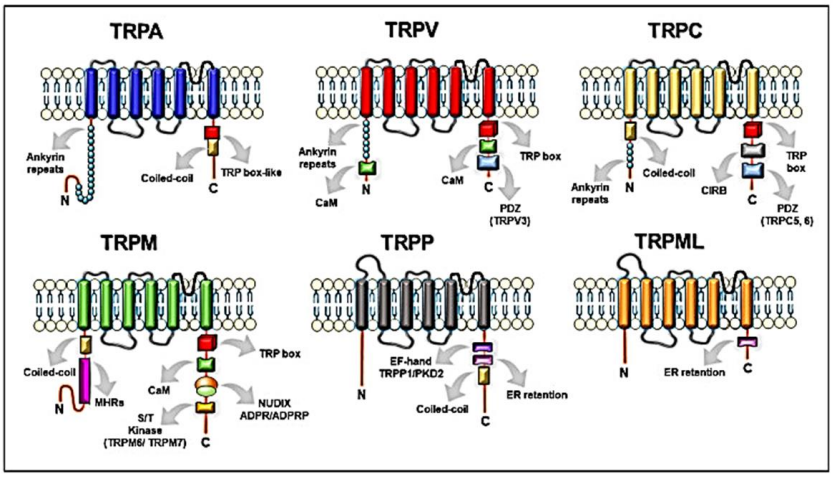

B

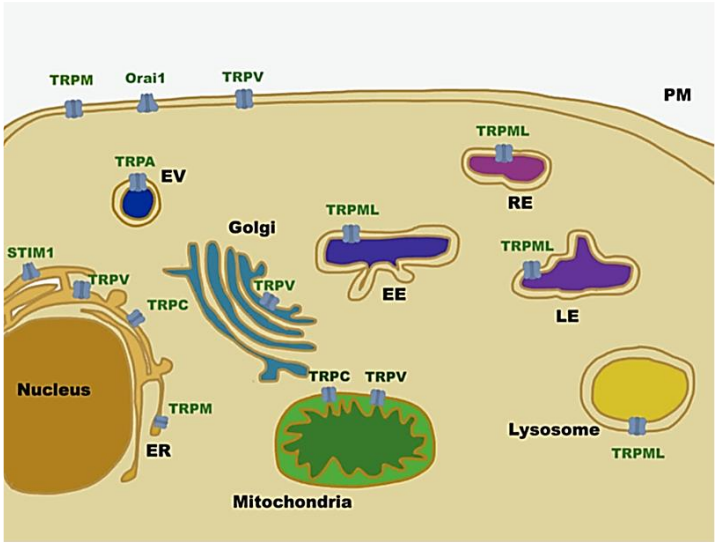

Figure 3. *Structure and localization of TRP channels. (A) Structural domains and motifs in the N- and C-terminus of TRP channel subfamilies* [23]. *(B) Intracellular localization of TRP channel subfamilies and SOCE machinery.*

Abbreviation*: TRPA, transient receptor potential ankyrin; TRPC, transient receptor potential canonical; TRPM, transient receptor potential melastatin; TRPML, transient receptor potential mucolipidin; TRPP, transient receptor potential polycystic; TRPV, transient receptor potential vanilloid; ER, endoplasmatic reticulum; EV, vesicle of exocytosis; EE, early endosome; RE, recycling endosome; LE, late endosome; PM, plasma membrane; STIM1, stromal interaction molecule 1; Orai1, calcium release-activated calcium channel protein 1.*

Table 1. Environmental activating stimuli and calcium permeability characteristics of TRP channels

TRP	Ca^{2+} Selectivity	Activation Temperature	Exogenous Activators	References
TRPA1	Medium/Low	<17°C	Caffeine, Cinnamaldehide, Nicotine	[24–26]
TRPC1	Medium		Lanthanide ions (La^{3+}, Gd^{3+}), carbachol	[27]
TRPC3	Medium		OAG	[28]
TRPC6	Medium		OAG, Hyperforin, 2,4-Diacylphloroglucinol	[28–30]
TRPM2	Medium/Low	>38°C	N-(p-amylcinnamoyl)anthranilic acid, Clotrimazole, Flufenamic acid	[31–34]
TRPM4	Non selective	15-35°C	BTP2	[31,35,36]
TRPM7	Medium/Low		Naltriben	[37]
TRPM8	Medium	17-25°C	Menthol, eucaliptol, geraniol	[22]
TRPML2	Non selective		SID24801657, SID24787221, ML2SA1	[38,39]
TRPV1	Medium/High	> 42 °C	CPS, Piperine, Gingerol	[22,40]
TRPV2	Medium	(≈52 °C)	2-aminoethoxydiphenyl borate, diphenylyboronic anhydride, and *Cannabis sativa* derivatives	[22]
TRPV4	Medium	24-27°C	Bisandrographolide A, Apigenin, 4-alpha-phorbol	[22]

		12,13-didecanoate	
TRPV5	High	-	
TRPV6	High	CPS	[41]

***Abbreviations**: TRPA, transient receptor potential ankyrin; TRPC, transient receptor potential canonical; TRPM, transient receptor potential melastatin; TRPML, transient receptor potential mucolipidin; TRPV, transient receptor potential vanilloid; CPS, Capsaicin; La3+, Lanthanum; Gd3+, Gadolinium; BTP2, N-[4-[3,5-Bis(trifluoromethyl)pyrazol-1-yl]phenyl]-4-methylthiadiazole-5-carboxamide; OAG, Oleyl acetyl glycerol. – No data reported. Ca2+ selectivity of TRP channels in according to PCa/PNa ratios are considered: High selective 10-100 score; Medium selective 1-10 score; Low selective < 1 score. Data found in literature [42,43].*

Initially, it was thought that TRP channels were solely expressed on plasma membrane (PM) mediating cation entry, but many studies have demonstrated that almost all mammalian TRP channels are located in the intracellular vesicular membranes (Figure 1B). It is unclear whether TRPs are expressed in these compartments as intermediate of biosynthetic pathways and then shuttled to their final location, or if they have a role as signal transducers and/or membrane trafficking regulators [44].

Above all, they are considered important Ca^{2+} selective ion channels which have been linked to countless physiological and pathological functions [45]. TRP channels are important biophysical cues for cellular microenvironment and Ca^{2+} controlled influx which are able to translate physical signals into biochemical ones. The homeostasis of intracellular calcium (Ca^{2+}) shows an extremely precise and fine regulation, which constitutes the functional and vital centre of cell signalling. Oscillations of Ca^{2+} concentration play a crucial role in multiple cellular processes such as regulation of cellular enzyme activity, cytoskeleton modification and expression of surface proteins. It also plays a key role in cell proliferation, migration, invasion, cell death including also autophagy, who's that dysregulation represents an excellent starting point for the development of the malignant phenotype [46]. Numerous studies have demonstrated that the aberrant expression of TRP channels is associated with poor prognosis, recognizing them as promising

diagnostic and therapeutic tools [47]. Emerging evidences suggest that TRPs, especially TRPML, TRPC and TRPV channels, play a key role in the regulation of autophagy by modulating the intracellular Ca^{2+} trafficking. In addition, it has been demonstrated that loss of TRPML1 promotes autophagy impairment [48]. Few data are present about the involvement of TRP channels in hematological malignancies. The expression of several members of the TRP family such as melastatin 2 (TRPM2), TRPM7, vanilloid 1 (TRPV1), TRPV2, TRPV5, TRPV6, and canonical 7 (TRPC7) in different lymphoid and myeloid leukemia have been demonstrated *in vitro* and *in vivo* [49,50].

Transient Receptor Potential (TRP) Channels in Chronic Myeloid Leukemia

Extract from the article: Maggi F, Morelli MB, Nabissi M, Marinelli O, Zeppa L, Aguzzi C, Santoni G, Amantini C. Transient Receptor Potential (TRP) Channels in Haematological Malignancies: An Update. Biomolecules. 2021;11(5):765. doi: 10.3390/biom11050765.

In CML the different TRP expression leads to different phenotype in CML, in particular the expression of TRPV channels is linked to cell death, TRPM channels are tied up with cell differentiation and proliferation, and TRPC expression is associated with cell proliferation and *BCR-ABL* gene function. The last findings regarding TRP and CML are listed in table 2.

Table 2. Expression of TRP channels in CML.

Cell line/model	TRP	Methods	Functions	References
32d and 32d-p210	TRPC1	WB	Cell proliferation	[51]
K562	TRPM7	RT-PCR, IF	Erythroid differentiation	[52]
K562	TRPV2	RT-PCR, WB	Cell death	[53]

***Abbreviations**: CML chronic myeloid leukaemia; TRPC, transient receptor potential canonical; TRPM, transient receptor potential melastatin; TRPV, transient receptor potential vanilloid; IF, Immunofluorescence; RT-PCR, Real Time- Polimerase Chain Reaction; WB, western blot.*

Among TRPV channels, TRPV2 has been studied in K562 cell line. In this cell line the expression of TRPV2 is higher, up to six folds, than in normal PBMCs and in THP-1 and U937 cell lines. Moreover, K562 express high levels of the f-TRPV2 and s-TRPV2 forms, as for THP-1 and U937 cells, but the expression of the short form is still lower respect the s-TRPV2 showed in the PBMCs [52,53]. TRPV2 silencing induces the loss of mitochondria membrane potential, triggering the accumulation

of cells in subG0/G1 phase, DNA fragmentation and apoptosis activation through the mitochondrial intrinsic pathway [53]. Treatments with TRPV2 inhibitors (TL and SKF) increase consistently the s-TRPV2 form with a concomitant decrease of the full one, and turns out to cell growth reduction due to apoptotic pathway activation. Indeed, active caspase-3, inactive PARP, γ-H_2AX and p38 are increased, whereas the Bcl-2 and ERK1/2 levels result lower than in the control [53]. These data together with the fact that the expression of TRPV2 in leukemic and normal blood cells has been demonstrated to be significantly different, TRPV2 can be considered a promising target for myeloid leukaemia treatment [53].

Regarding TRPM subfamily, TRPM7 is abundantly expressed in K562 cell line [52]. TRPM7 shows a unique structure recognized as "chanzyme" thanks to the contemporary presence of both channel and kinase-like domains. TRPM7 is expressed wildly in all cells and numerous studies have demonstrated its implication in cell survival, growth, differentiation and death [54]. In K562 cells, TRPM7 is expressed mainly in the PM and is essential for basal Ca^{2+} entry. The block or alteration of TRPM7 results in the reduction of cell proliferation, and counter increase of erythroid differentiation under hemin stimulation, through ERK activity [52]. Taken together, these data suggest that TRPM7 could be a promising check-point not only for K562 differentiation, but also for the normal haematopoiesis.

Also, the expression of TRPC channels has been evaluated in CML cells models. In K562, TRPC family is barely expressed [52]. In 32d cells (32d-p210), an interleukine-3 (IL-3)-dependent myeloid progenitor cell line which expresses the BCR-ABL gene, Cabanas and colleagues evaluated the expression of TRPC1 and its correlation with Ca^{2+} influx. The 32d-p210 cells showed reduced expression of TRPC1 and SOCE activity respect to the wild-type cells (32d-WT). Given that previous studies demonstrated that different members of TRPC family have been implicated in SOCE activity [55], this suggests a possible relationship between the SOCE activity and the TRPC1 expression. Two principal proteins are involved in SOCE activity:

stromal interaction molecule 1 (STIM1) and the calcium release-activated calcium channel protein 1 (Orai1) [56]. These two proteins are essential for Ca^{2+} trafficking between the endoplasmic reticulum (ER) and the PM (Fig. 3B). Their activation is subordinated by Ca^{2+} concentration in the ER, indeed a decrease in Ca^{2+} concentration in ER prompts the translocation of STIM1 from ER to the ER\PM junction where it binds Orai1 channels increasing Ca^{2+} entry. In this regard, the TRPC1 translocation contributes to the STIM1\Orai1 co-localization participating to the SOCE activity amplification signal [57]. Interestingly, it has been demonstrated that TRPC1 KO reduces SOCE activity, proliferation and migration in endothelial progenitor cells [58]. An opposite effect has been reported in 32d-p210 cells, in fact even if the TRPC1 expression and SOCE activity are low, the rate of proliferation remains higher, compared to 32d-WT, suggesting a possible link between Ca^{2+}-independent pathway activation and enhanced proliferation in 32d-p210 cells. The *BCR-ABL* gene seems to tightly regulate SOCE activity by reducing the expression of TRPC1, protein kinase C (PKC) activity and SOCEs network too [51]. So TRPC1 seems a good candidate in CML treatment.

TRPs as promising diagnostic, prognostic and therapeutic markers in the clinical management of hematological malignancies

It is now well accepted that alterations of TRP expression and functions are responsible for the impairment of cellular signaling pathways involved in cancer growth, metastasis and chemoresistance [59]. In particular, dysregulations of TRPC, TRPM and TRPV members have been mainly correlated with malignant growth and progression. For this reason, in the recent years many efforts have been spent to improve the knowledge about these channels and the ability to target them. Thus, they are considered promising tools not only to inhibit cancer progression but also to ameliorate the diagnosis and overcome chemoresistance in cancer [45,47,60–62].

Interesting recent findings indicate and suggest that TRP channels could be also useful as diagnostic, prognostic and therapeutic markers in the clinical management of hematological malignancies (Table 3).

Table 3. Expression and functions of TRP channels in leukaemia and lymphoma patients

Cancer type	TRP	Effects	References
ALL	TRPC3	↓Glucocorticoid resistance	[63]
AML	TRPM2	↓ OS ↓Doxo-sensitivity	[64]
	TRPV4	↑ Chemotherapy efficacy	[65]
CLL	TRPC1	OS	[66]
Lymphoma	TRPM8	Prognostic	[67]
	TRPM4	↓OS ↓PFS	[68]

***Abbreviations**: ALL, acute lymphoblastic leukemia; CLL, chronic lymphocytic leukaemia; TRPC, transient receptor potential canonical; TRPM, transient receptor potential melastatin; TRPV, transient receptor potential vanilloid; OS, overall survival; PFS, Progression Free Survival. ↑, increase; ↓, decrease.*

At this regard, integrated methylome, transcriptome and epigenetic analysis showed that the expression level of many genes is dysregulated in pediatric leukemia and among them the presence of TRPC1, TRPC4, TRPC3, TRPM2, TRPM4 and TRPM8 also stands out. These TRP channels are repressed and this indicates a reduced potential for cell-microenvironment interactions and apoptotic potential of the ALL cells [69,70]. In accordance with these data, the potential utility to add TRP as diagnostic tools is also confirmed by other studies. It has been found that TRPM4 is significantly overexpressed in diffuse large B-cell lymphoma (DLBCL) compared to normal germinal center (GC) B cells and, in addition, it is more expressed in activated B-cell-like than in GC DLBCL [68].

Moreover, Hirai and coworkers demonstrated that TRPM8 positive neoplastic cells are mostly present in post-GC neoplasms but not in pre-GC or in the majority of GC neoplasms, suggesting TRPM8 as a marker to discriminate and diagnose reactive plasmablasts and mature B-neoplasms [67]**.** Finally, TRPM2 was found to be strongly up-regulated in AML samples from patients with normal karyotypes or all AML mutational sub-groups respect to normal HSC or common myeloid progenitor, suggesting the possibility to differentiate normal from neoplastic cells by using TRPM2 expression levels [71].

The potential prognostic impact of TRP channels in hematological malignancies has been recently highlighted. In DLBCL, negativity of TRPM4 expression significantly correlated with better overall survival (OS) and progressive-free survival (PFS) compared with TRPM4 strong intensity. TRPM4 positivity was also associated with higher lactate dehydrogenase levels, higher ECOG (Eastern Cooperative Oncology Group) score and stage III-IV. In addition, TRPM4-positive DLBCL patients treated with R-CHOP (cyclophosphamide, doxorubicin, vincristine, and prednisone) protocol displayed worse survival consistent with its expression [68]. Moreover, a close relationship between TRPM8 and International Prognostic

Index (IPI) scores was found in DLBCL patients indicating that lower TRPM8 expression levels are associated with higher IPI scores [67]. *In vivo* studies underline the importance of developing new pharmacological approaches based on targeting of TRP channels. In fact, mice injected with TRPM2-depleted leukemia cells showed significant reduced leukemia compared with controls suggesting that these channels play an important role in leukemogenesis [71].

The targeting of TRP channels has been shown not only affect leukemia cells but also the tumor microenvironment. It has been recently demonstrated that TRPV4, by acting as a volume receptor, is involved in bone marrow adipocyte remodeling in AML mice and it is clear that the inhibition of this remodeling increases the survival in the AML mouse model [65]. Moreover, many *in vitro* studies, performed in patient-derived cells, demonstrated the ability of TRP-targeting therapy to inhibit cell proliferation and improve the effects of traditional chemotherapy in hematological malignancies. For instance, the TRPC3 channel blocker, Pyr3, enhances apoptosis induced by dexamethasone in ALL cells isolated from patients by altering calcium signaling, mitochondrial membrane potential and ROS production [63]. In addition, the activation of TRPV1, by using the specific agonist RTX, reduced cell proliferation, blocked cell cycle and increased apoptosis in T cells from ALL patients [72].

Obviously, further studies are necessary in order to develop and use drugs capable of modulating the TRP functions. However, interesting assumptions are gradually growing. In fact, by molecular imaging methods, the *in vivo* potential of soricidin-derived peptides in targeting TRPV6-rich tumors has been evaluated [73]. In addition, an apoptosis-inducing TRPV1 nanoagonist contained semiconducting polymer nanoparticles (SPNs) as nanocarriers and CPS as the agonist, has been developed to target TRPV1-positive cancer cells [74]. Finally, given that ongoing clinical trials specifically targeting TRPM4 have been approved in patients with stroke [75], it can be expected that soon other TRP-based therapeutic strategies may have an

adequate safety profile and be applied in the field of cancer including hematological malignancies.

Transient Receptor Potential Vanilloid (TRPV) Channels relevance in cancer

Transient receptor potential vanilloid (TRPV) channels were named based on the activation by capsaicin, a vanilloid-like molecule, the active ingredient in spicy foods [76]. TRPV channels are tetrameric complexes and can be both homo or hetero-tetrameric [77], are widely expressed and are located mostly on the plasma membrane, where they play an important role in calcium homeostasis. Some of them have been also shown to be located in the endoplasmic reticulum, a large cellular calcium store involved in calcium-triggered pathways[77]. TRPV channels in general, thanks to their mechanosensible features, are strictly connected to cancer progression and invasion [78,79].

In actual facts, changes in TRPV expression may have cancer promoting effects by enhancing Ca^{2+}-dependent proliferative response. Furthermore, altered expression, mutations and polymorphisms of TRPV channels may be advantageous for cancer cells offering a survival advantage increasing the resistance to apoptotic-induced cell death. TRPV gene mutations may play a role in cancer development and there may be a relationship between the expression of specific TRPV gene single nucleotide polymorphisms and increased cancer [60].

TRPV1

TRPV1 is a polymodal, no selective cation channel expressed by all major classes of nociceptive neurons and is important for the detection of noxious stimuli. Ion channels, including TRPV1, are typically found in the plasma membrane creating a passageway. Increasing evidences suggest that TRPV1 is also located intracellularly in various cell types such as neurons, myocytes, immune cells and cancer cells. TRPV1 can be activated by a number of endogenous and exogenous stimuli including capsaicin, heat (>42 °C), acidic conditions, N-acyl amides, arachidonic

acid (AA) derivatives, vanilloids, protons, cannabinoids and N-oleoyldopamine (OLDA) (Table 1) [77,80,81].

In immune cells TRPV1 participates in the regulation of cell response due to their involvement in the calcium signaling cascade and perception of the external stimuli [82]. TRPV1 colocalizes with immunological synapse and it is involved in the regulation of $CD4^+$ cell activation and functioning, shaping its proinflammatory properties [83–85].

TRPV2

TRPV2 is ubiquitously expressed in various tissues types including both neuronal and non-neuronal tissues [76,77]. This channel has been implicated in various physiological processes, such as neuronal development, cardiac function, immunity, and a variety of disease states, including cancer [76,86]. TRPV2 modulates may cellular functions in these cells. Among the six members of the TRPV family channels, the expression of only TRPV2 channel was detected in macrophages [77].

In many cases, depending on the cell type, TRPV2 translocates from intracellular membrane compartments to the plasma membrane after stimulation and/or regulation by general or specific signaling pathways involving phospholipase C, the PI3K pathway or other kinases [87].

TRPV agonists

Cannabidiol

Cannabinoids are a group of more than sixty structurally related terpenophenolic compounds. Initially, the phenylterpenoid tetrahydrocannabinol (THC) and some of its naturally occurring derivatives, by which cannabidiol (CBD) (Figure 4), were the only plant natural products known to directly interact with cannabinoid receptors. In the last years, several non-cannabinoid plant natural products have been reported to act as cannabinoid receptor (CNR) ligands.

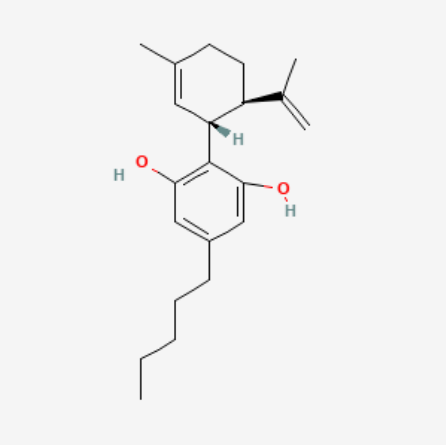

***Figure 4**. Cannabidiol (CBD) structure (PubChem).*

This encouraged scientists to define phytocannabinoids as any plant-derived natural product capable of either directly interacting with CNR or sharing chemical similarity with cannabinoids or both. Direct cannabinoid receptor ligands are compounds that show high binding affinities for cannabinoid receptors and exert discrete functional effects [88]. Cannabinoids have been used for decades in the field of palliative care. Recently the two phytocannabinoids, THC and CBD, were found to possess anti-tumorigenic properties. Contrary to THC, a well-known strong CNR1 (or CB1) agonist with psychotropic effect, CBD has a low binding affinity for CB1 and CB2 receptors [89] and is considered as a non-intoxicating drug because it is

devoid of the psychoactive side effects exhibited by THC [90]. Moreover, data suggests that CBD exhibits pro-apoptotic and anti-proliferative actions in different types of tumors and also deploys anti-migratory, anti-invasive, anti-metastatic and anti-angiogenic properties [91–93]. Molecular targets for CBD are uncertain. Among putative candidates, some members of the TRP channels family, in particular TRPV1 and TRPV2, orphan cannabinoid receptor (G-protein-coupled receptor) GPR55, 5-hydroxytryptamine receptors (5HT) and peroxisome proliferator-activated receptors γ (PPARγ) have been proposed [94].

OLDA

OLDA is an endogenous fatty amide resulting from the formal condensation of the carboxy group of oleic acid with the amino group of dopamine (Figure 5).

***Figure 5**. N-oleoyldopamine (OLDA) structure (PubChem).*

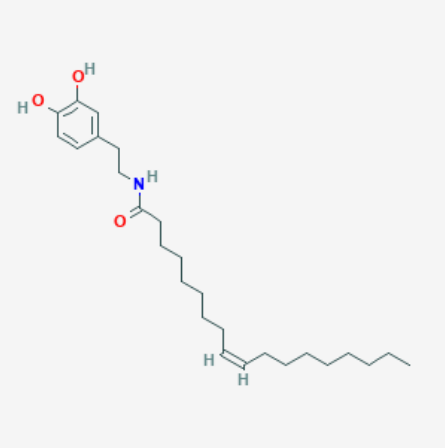

It is a fatty amide, a secondary carboxamide and a member of catechol. Synthesized in catecholaminergic neurons, it crosses the blood-brain barrier and might be considered as a carrier of dopamine into the brain. It acts as a potent TRPV1 receptor agonist increasing its activity which leads to calcium intake, reducing the latency of paw withdrawal from a radiant heat source and producing nocifensive behavior. Moreover, OLDA is a weak ligand for CB1 receptor in rat [81,95–97]. So far, there are any evidences regarding the use of this endogenous compound in cancer.

Capsaicin

CPS is the major active ingredient of chilli pepper and is used wordwide as food additive (Figure 6). It has also an ancient story as medicinal due to its feature as anti-oxidant, anti-inflammatory, anti-obesity, analgesic, hypocholesterolemic and hypoglycemic [98]. Conflicting data are present regarding its role as pro or anti carcinogenic substance. In fact, CPS is responsible for skin, prostate and colorectal cancer development, whereas findings suggest that it also avoid the progression of breast, lung, gastric, liver and more cancer. CPS also synergizes with common chemotherapeutic drugs, such as cisplatin, enhancing their anti-tumor activity. Due to its short half-life and hydrophobicity, recently CPS-loaded nanoparticles have been developed to optimize the effects and delivery of this drug to the specific target [99]. CPS potently activates TRPV1 and evokes strong burning sensations. Upon activation, calcium preferentially moves through the pore, and stimulates a series of Ca^{2+}-dependent processes that ultimately lead to desensitization of the channel. Upon desensitization, the channel enters a refractory period in which it can no longer respond to further stimulation, leading to the paradoxical analgesic effect [80]. Through TRPV1 activation, CPS is able to induce apoptosis in many different types of cancer cell lines via intracellular ROS production [99].

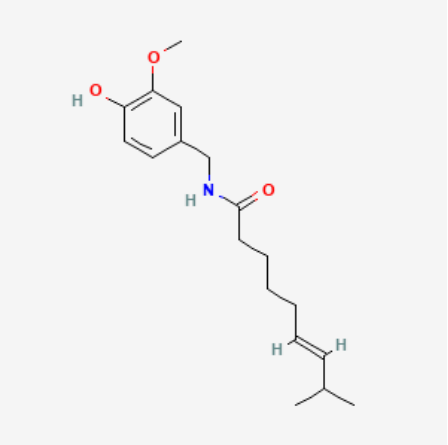

***Figure 6**. Capsaicin structure (PubChem).*

Autophagy in cancer

Autophagy is an important conserved self-degradation mechanism, crucial for the turnover of damaged organelles, excess of cellular constitutes and aggregates (Figure 7), and it can play a double-edge sword role promoting or suppressing cell survival [100–102]. Due to the dualistic role, autophagy can represent the driving force for the formation of cancer stem cells (CSCs) and promote drug resistance, recurrences, cell migration, and escape from immune surveillance [103,104]. Although it is not yet well understood by which regulatory molecules and how this mechanism can guide cell fate [104], the role of autophagy in the transformation and maintenance of CSC represents a possible new therapeutic goal. Moreover, autophagy has proven to be decisive in the immunogenicity of cell death in tumours and adequate response to induction of autophagy could predict resistance to blocking the therapeutic immune checkpoint in human cancer [105,106].

Transcription factors are essential for the transcription of autophagy mediators [104]. For instance, FOXOs family are implicated in the transcription of autophagy related genes as ATG5, ULK1, LC3 and BECLIN1, in particular in leukaemia FOXO3 protein is fundamental for CSC initiation [107–109]. In this scenario, FOXO proteins may regulate vary cellular pathways and, most importantly, it is suggested that FOXO-dependent stemness regulation and autophagy are interconnected in tumorigenesis [104]. Moreover, autophagy inhibition, through STAT3/JAK2 pathway, has been shown to decrease IL-6 secretion [110], crucial for CSCs maintenance [111]. CSCs are able to escape from immune surveillance by producing immunosuppressive factors, recruiting immunosuppressive cells and reducing tumor antigen expression through the activation of distinctive cellular pathway such as Notch and Wnt [112–114].

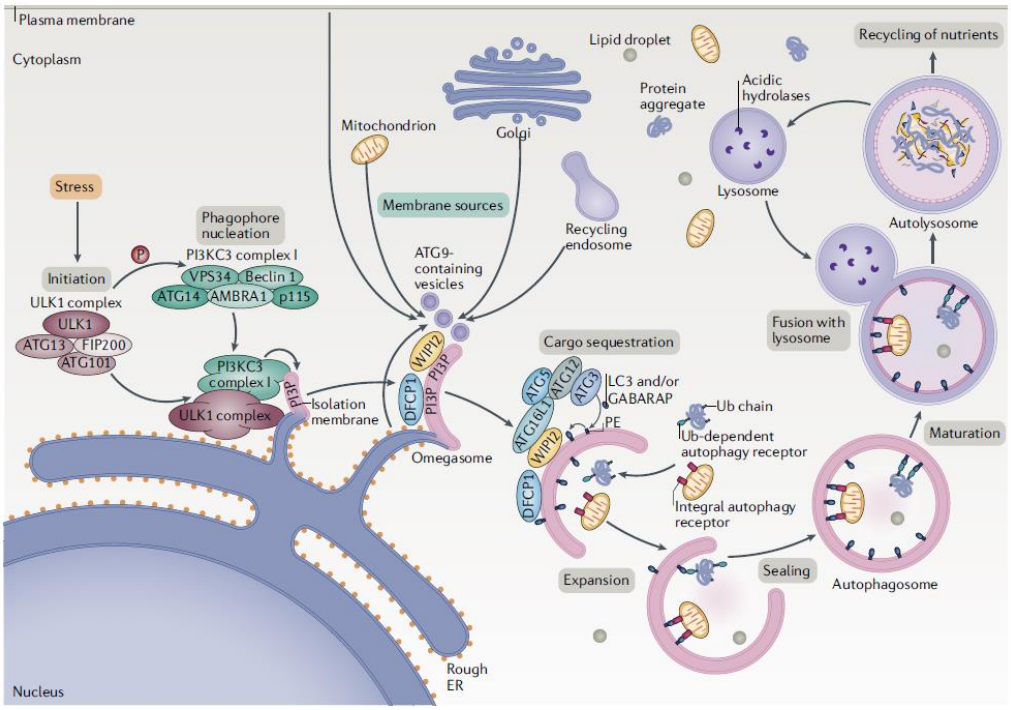

Figure 7. *Autophagy pathway.* [115]

Mitophagy in cancer

The important organelle for the regulation of cellular energy homeostasis and cell death are the mitochondria. There is a need to eliminate impaired mitochondria to conserve cellular activities by autophagy and this process is referred as mitophagy [116]. Mitophagy plays a major role in red blood cells differentiation, paternal mitochondrial degradation, neurodegenerative diseases, and ischemia or drug-induced tissue injury. The impaired mitochondria is eliminated in two steps: induction of general autophagy and priming of damaged mitochondria for selective autophagic recognition. The priming of impaired mitochondria is conciliated by the Pink1-Parkin signalling pathway or the mitophagic receptors Nix and Bnip3 [117]. Mitophagy plays a key part in hematological malignancies, in fact mitochondria bioenergetics is strictly associated with drug resistance and it has been demonstrated that the targeting of mitochondria increases the therapy efficacy (Figure 8) [118].

Figure 8. *Schematic representation of chemoresistance responses modulated by mitophagy.*

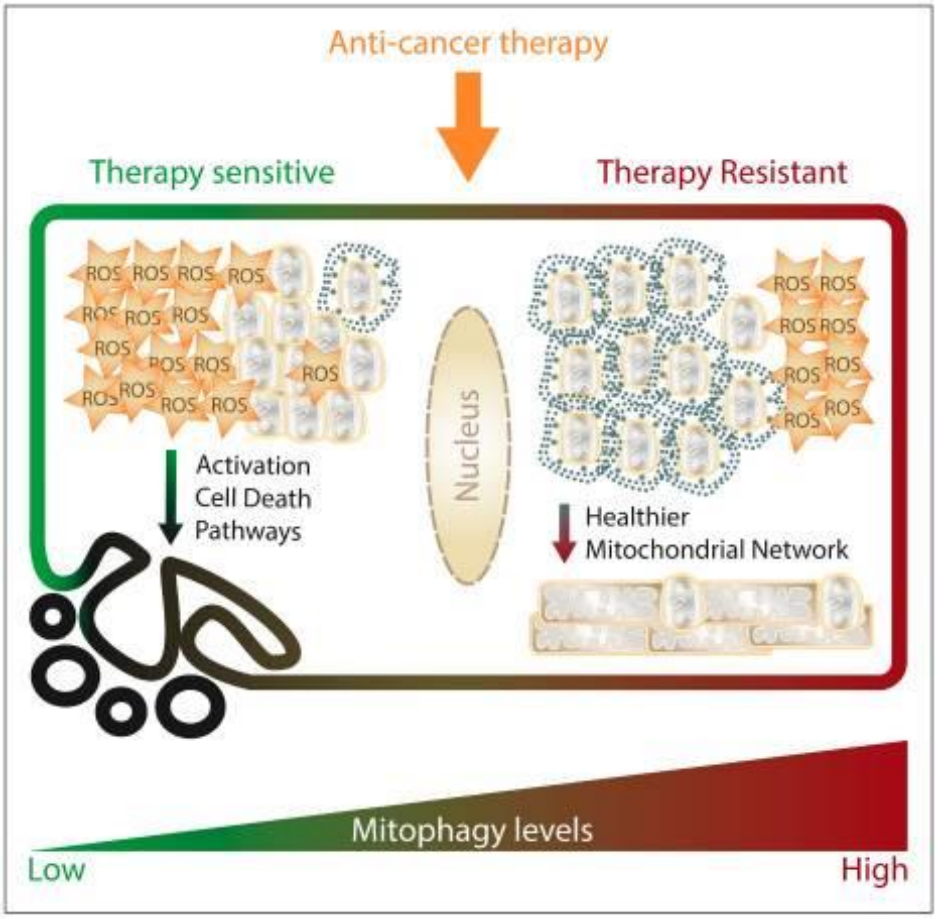

On the other hand, in cancer cell treated with anti-cancer drugs, mitochondria depolarize producing ROS. If accumulated to lethal levels, they trigger apoptosis as major cell death pathway. High levels of mitophagy within the treated tumor cell help resist the damage caused by the treatment and counteract the onset of cell death programs, maintaining a healthier mitochondrial network (limiting the production of ROS and the accumulation of depolarized mitochondria, preventing the release of cytochrome C) [119]. So far, mitophagy seems to be a critical point for both cancer progression and cell differentiation, playing, as already discussed, a double edge sword in cancer treatment.

Immuno-checkpoint in CML

PD-1 and its ligand PD-L1 are the newest frontier in immune-oncology field. They have relevant role as immune checkpoint for immune tolerance, but the activation of the PD-1 axis by cancer prompts to a potent impairment of tumour immunity with immune exhaustion (Figure 9). High expression of PD-L1 is correlated to worse prognosis, whereas low or absent expression is associated with less effective therapy. Based on this concept, the PD-1/PD-L1 pathway has been used therapeutically with amazing results in various types of cancer [120–122].

Figure 9. *Mechanism of action of PD-1 and PD-L1 inhibitors. A. PD-L1 binds to PD-1 and inhibits T-cell killing of tumor cells. B. Blocking PD-L1 or PD-1 allows T-cell killing of tumor cells.* [123]

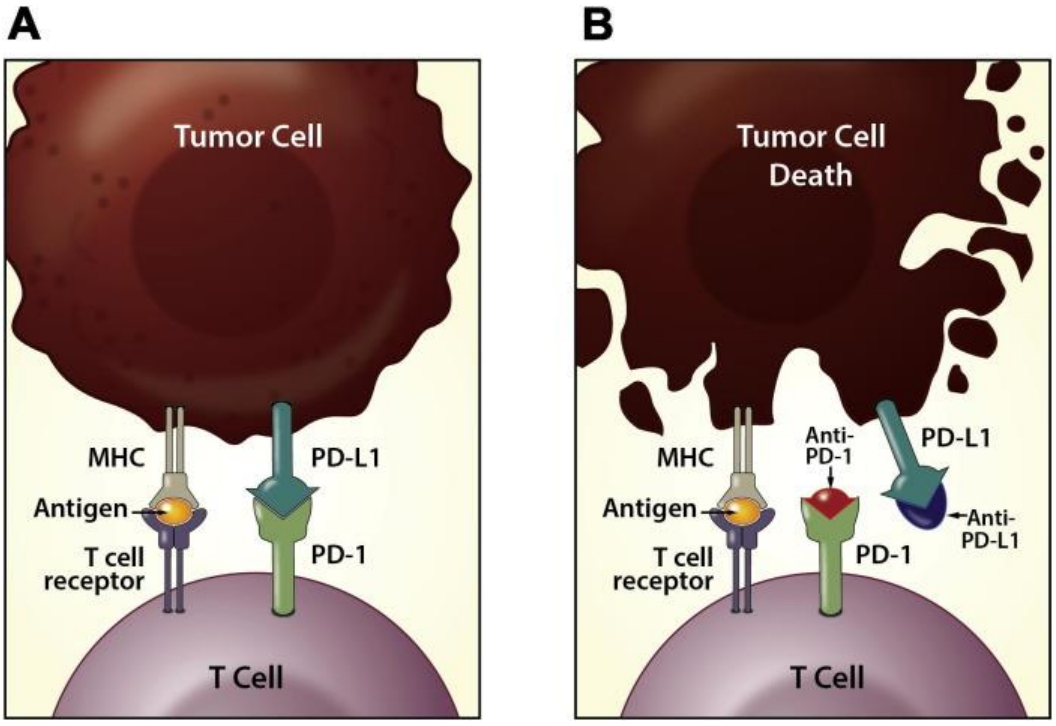

Moreover, a correlation between immune check point expression and autophagy pathway is rising [124], but the molecular mechanisms are still unknown and may represent a further avenue of treatment.

Among cancers, CML shows few clinical data. Expression of PD-1/PD-L1 has been already assessed in haematological malignancies, and the PD-1/PD-L1 pathway is now considered a promising molecular target for treatment of these spectrum of

diseases at every stage [125]. PD-L1 expression has been assessed also in myeloid leukaemia [126] and it has been linked to immune exhaustion and disease progression [127]. Several evidences suggest the implication of autophagy in PD-L1 expression on cancer cells. Indeed, low expression of PD-L1 is correlated with an increase in the autophagy pathway activation with reduction in invasion, tumorigenesis, stemness and cellular damages leading to an increasing in time progression disease [124,128].

Aim of the project

One of the most important TKI therapy side effect is the acquisition of a more aggressive phenotype which drives CML patients from the accelerated phase into the blast one thanks to cytogenetic clonal evolution and acquirement of crucial resistant mutation. For this reason, there is the urgent request of alternative strategies and/or supportive strategies in order to avoid or overcome this situation, ameliorating the typical side effects of general chemotherapy in patient. The main objective is to identify new targets to selectively develop innovative drugs useful for the elimination of leukaemia cells and leukaemia stem cells. In this scenario, the aim of this project was to investigate the contribution of TRP channels, focusing the attention in particular on TRPV channel family, in the regulation of autophagy in different myeloid leukaemia cell lines. Since the autophagic pathway can play a dualistic role in cancer inducing both survival and cell death, and also given that in hematological malignancies mitochondria bioenergetics is strictly associated with drug resistance and the targeting of mitochondria increases the therapy efficacy, we focused also the attention on the mitophagy and the modulation of markers involved in the differentiation of CML cells. Since growing preclinical evidence suggests that many therapies induce autophagy, targeting this process can improve the effectiveness of cancer therapies.

Materials and methods

Chronic Myeloid Leukemia cell lines

Human chronic myeloid leukemia K562 (erythroid progenitor [129]), KU812 (granulocyte progenitor [130,131]) and MOLM-6 (megakaryoblast progenitor [132]) cell lines were obtained from DSMZ – German Collection of Microorganisms and Cell Cultures GmgH (DSMZ, Braunschweig, Germany), were maintained in RPMI1640 medium (Euroclone Ltd, Devon, UK) supplemented with 10% heat-inactivated fetal calf serum (Euroclone), 2 mM L-glutamine, 100 IU/ml of penicillin and 100 µg/ml of streptomycin. K562 imatinib-resistant (IR) were developed by exposures of K562 cells to a concentration of 1 µM imatinib for 10 days [133].

Human acute leukemia THP-1 cell line was was kindly provided by IFOM (Rome, Italy) and was cultured in RPMI-1640 Medium supplemented with 2-mercaptoethanol to a final concentration of 0.05 mM, 10% heat-inactivated fetal calf serum, 2 mM L-glutamine, 100 IU/ml of penicillin and 100 µg/ml of streptomycin. Cell lines were cultured at 37°C, 5% CO2 and 95% of humidity.

Blood of healthy donors, kindly provided by transfusion center (Macerata Hospital, Italy) after authorization of the hospital management, was used to isolate PBMCs/red blood cells by using Ficoll paque (Cederlane, Burlington, Canada) and to obtain an enrichment of normal myeloid cells by means of Rosette SepTM HLA Myeloid Cell Enrichment Kit (StemCell Technologies, Vancouver, Canada).

CD38 Micro Bead Kit (Miltenyi Biotech Inc, Auburn, USA) was used to isolate $CD38^+$ common myeloid progenitors from human cord blood $CD34^+$ progenitor cells (Sigma Aldrich, Milan, Italy) [134].

Chemical and Reagents

Capsazepine, imatinib mesylate, ionomycin, 3-4,5-dimethylthiazol-diphenyltetrazolium bromide (MTT) and 2',7'-Dichlorofluorescin Diacetate (DCFDA) were purchased from Sigma Aldrich (Milan, Italy). Bafilomycin A (BAF, 25 nM), Fluo-3 AM calcium indicator and 4',6-diamidino-2-phenylindole (DAPI) was from ThermoFisher Scientific (Waltham, USA). Pure CBD was supplied from ENECTA (Amsterdam, Netherlands). Tranilast, OLDA and A784168 were purchased from Bio-Techne SRL (Milan, Italy). CBD, tranilast, capsazepine and BAF were dissolved in DMSO that was used as control (vehicle). The maximum percentage of DMSO was 0.05, a much lower percentage than those considered toxic to blood cells [135]. The following rabbit antibodies (Abs) were used according to company instructions: anti-microtubule-associated protein-1 light chain 3 (LC3), anti-cytochrome c oxidase subunit 4 (COX IV), anti-octamer-binding transcription factor 4 (OCT4), anti-autophagy protein 16 like 1 (ATG16L1), anti-autophagy protein 12 (ATG12), anti-PTEN induced putative kinase 1 (pink1), anti-parkin, anti-caspase 3, anti-glyceraldehyde-3-phosphate dehydrogenase (GAPDH), anti-optineurin, anti-PU.1, anti-γH2AX (γH2AX), anti- degradation in endoplasmic reticulum protein 1 (Derlin1) and anti-Binding Immunoglobulin Protein (BIP) were from Cell Signaling Technology (Danvers, USA). The following Abs were used: rabbit anti-human Transient Receptor Potential Vanilloid 1 (TRPV1, 1:1000, Invitrogen), goat anti-human TRPV2 (TRPV2, 1:50, Santa Cruz Biotechnology, Dallas, USA). The following secondary antibodies were used: Horseradish peroxidase (HRP)-conjugated anti-rabbit IgG (1:5000, Jackson Immuno Research Europe Ltd); HRP-conjugated anti-mouse IgG (1:2000, Cell Signaling Technology); PE-conjugated goat anti-rabbit Ab (BD Biosciences, Milan, Italy), FITC-conjugated goat anti-mouse Ab (BD Biosciences, Milan, Italy), Alexa Fluor-594-conjugated goat anti-rabbit Ab (1:100; Cell Signaling Technology), Alexa Fluor-488-conjugated donkey anti-goat Ab (1:100; Invitrogen).

BloodSpot and Stemformatics analysis

The BloodSpot and Stemformatics are an open-access downloaded bio-database, providing visualization and analyzing tool for large-scale hematology genomics data sets (https://www.bloodspot.eu; https://www.stemformatics.org/ access in October, 2021).

In particular, BloodSpot provide gene expression profiles of healthy and malignant hematopoiesis in human or mice, encompassing more than 5000 samples in total analyzed with Oligonucleotide microarray chip and RNA-seq assay [136].

Stemformatics is an established gene expression data portal containing over 420 public gene expression datasets derived from microarray, RNA sequencing and single cell profiling technologies. It has a major focus on pluripotency, tissue stem cells, and staged differentiation [137].

Raw data were normalized from Affymetrix Human Gene and Affymetrix Human Genome U133 Plus. Analysis of data from these databases was performed in silico. Dataset used for the analysis are listed in Table 4.

Table 4. Dataset and Databases used for genomic analysis.

Database	**Dataset ID**	**Accession code**	**Reference**
Stemformatics	6326	GSE47927	[138]
BloodSpot		GSE17054	[139]
		GSE19599	[140]
		GSE11864	[141]
		E-MEXP-1242	[142]

RNA isolation, reverse transcription and quantitative Real- Time PCR

Total RNA from purified $CD34^{+}CD38^{+}$ common myeloid progenitors was extracted by using SingleShot Cell Lysis Kit (BioRad) whereas the RNeasy Mini Kit (Qiagen, Milan, Italy) was used for all the other cell types. cDNA was synthesized using the iScript Advanced cDNA Synthesis Kit for RT-qPCR (BioRad, Milan, Italy) according to manufacturer's protocol. Quantitative real-time polymerase chain reactions (qRT-PCR) were performed with QuantiTect Primer Assays for human TRPV1 (QT00046109), TRPV2 (QT00035987), CD274 (QT00082775), CD34 (QT00056497) and GAPDH (QT00079247) (Qiagen), using the iQ5 Multicolor Real-Time PCR Detection System (BioRad). The PCR parameters were according to the primer datasheet. All samples were assayed in triplicates in the same plate. Gene expression analysis was performed by using the BioRad IQ5 software that is based on the $2^{-\Delta\Delta Ct}$ method. GAPDH was used as a housekeeping gene and for each experiment a selected calibrator (=1) was chosen. IQ5 software uses the average of all samples including control for statistical analysis.

Immunofluorescence and FACS analysis

Cells, were fixed in paraformaldehyde 4% in PBS and permeabilized with cold methanol and permeabilization solution (1% FBS, 0.1% saponin, 0.1% sodium azide in PBS) before the incubation with anti-TRPV1, anti-TRPV2, anti-COX IV or anti-OCT-4 Abs. After 30 min at 4 °C, cells were then incubated with FITC-conjugated secondary Ab and analyzed using a FACScan cytofluorimeter with CellQuest software (Beckton Dickinson, San Jose, USA). Fluorescent intensity was expressed in arbitrary units on a logarithmic scale.

Confocal Microscope Analysis

CML cells were fixed with 4% paraformaldehyde for 10 min at room temperature and cytospin at 1800 rpm for 5 min was performed. Then, cells were permeabilized using ice-cold methanol and incubated with 5% of bovine serum albumin (BSA) and 0.1% of Tween-20 in PBS for 1 h at room temperature. After that, CML cells were co-labeled with anti-TRPV1 Abs followed by Alexa Fluor 594-conjugated secondary Ab and with anti-TRPV2 Ab followed by Alexa Fluor 488-conjugated secondary Ab. Nuclei were stained with DAPI. Slides were then analyzed under 100X magnification with C2 Plus confocal laser scanning microscope (Nikon Instruments, Firenze, Italy). Optimized emission detection bandwidths were configured by Zeiss Zen control software. Images were processed using NIS Element Imaging Software (Nikon Instruments, Firenze, Italy). In some experiments, CML cells were treated with CBD at IC_{50} dose or with vehicle (used as control) for 24 h and then fixed and permeabilized for the staining with PU.1 Ab.

Intracellular calcium influx $[Ca^{2+}]_i$

Intracellular Ca^{2+} influx was measured by using Fluo 3-AM and FACS analysis. Briefly, 1.5×10^6/mL CML cells were firstly washed in calcium and magnesium free PBS supplemented with 4.5 g/L of glucose and then incubated in calcium and magnesium free PBS/glucose medium supplemented with 7 µmol/L FLUO 3-AM for 30 min in the dark at 37 °C, 5% CO_2. After washing, cells, resuspended in calcium and magnesium free PBS/glucose medium containing 2 mmol/L Ca^{2+}, were stimulated with CBD (IC_{50} dose) or with vehicle up to 3 minutes. In some experiments, CML cells, loaded as above described, were treated with CBD in combination with tranilast. Ionomycin (5 µg/ml) treatment was used as positive control for calcium influx. Fluo 3-AM fluorescence was measured by FACS on the green channel and Cell Quest Software.

Gene silencing

TRPV2 (siTRPV2), TRPV1 (siTRPV1) and siGLO non-targeting siRNA (used as negative control) FlexiTube siRNA were purchased from Qiagen. CML cell lines were plated at the density of 6 x 10^5/mL for 24 h; the day after cells were plated at the density of 4 x 10^5/mL and siTRPV2, siTRPV1 or siGLO (50 nM) were added to the wells, following the HiPerfect transfection reagent transfection protocol (Qiagen). Cells were then harvested at 48 h post-transfection for subsequent analyses. Silencing efficiency was evaluated by qRT-PCR analysis and western blot. No differences were observed comparing siGLO transfected with untransfected cells.

Cell Viability Assay

10^5 cells/well were cultured in 12 well plate, the day after cells were exposed to different concentrations 1, 10, 25, 50, 100 µM of CBD or vehicle were added for 24 h. To study cell growth, live cells were counted using Trypan blue staining. 24 h post treatment the cells were resuspended and added to trypan blue at ratio on 1:1. The number of cells was counted using the TC-20 Automatic Cell Counter Bio-Rad and the percentage of cell growth was calculated by considering vehicle-treated cells as 100%. The half-maximal inhibitory concentration, IC_{50}, was calculated using GraphPad Prism® 8 software (GraphPad Software, San Diego, CA, USA). Biological and technical repeats were used to reach the statistical significance results.

In addition, to assess the involvement of TRPV2 and TRPV1 in CBD-mediated effects, CML cells were pretreated with tranilast (10 µM) or with capsazepine (10 µM) for 1 h before the addition of CBD for 24 h. Tripan blue exclusion assay was also performed in siTRPV2, siTRPV1 or siGLO CML cells as described above.

Moreover, CBD and imatinib were used in combined and sequential treatment. For the sequential administration, cells were treated with the proper IC_{50} doses for 24h, the day after the medium were removed and cells were treated with different concentration of imatinib (5 nM - 2.5 μM) for additional 24h. Tripan blue exclusion assay was performed as described.

CBD (10, 15, 20, 25 μM) was used in combination with imatinib mesylate (0.01, 0.1, 0.5 and 1 μM) for 24 h. Synergistic activity of the CBD/imatinib combination was determined by the isobologram analysis and combination index (CI) methods (CompuSyn Software, ComboSyn, Inc. Paramus, NJ 2007). The CI was used to express synergism ($CI < 1$), additivity ($CI = 1$) or antagonism ($CI > 1$) and was calculated according to the standard isobologram equation. The same protocol was used to assessed the effects of CBD in K562 IR (10, 15, 20, 25 μM).

Cell growth was also measured in CML cells pretreated with BAF (25 nM) for 1 h and then treated with CBD (IC_{50} dose) for 24h. Moreover, this test was performed in K562 IR and K562 treated with different doses of imatinib. IC_{50} values were calculated as above described. In addition, K562 IR cells were treated for 24 h with different doses of CBD

In addition, 10^5 cells/well were cultured in 12 well plate, the day after cells were exposed to different concentrations OLDA (0,5, 1, 5, 10, 25, 50, 75 and 100 μM), CPS (10, 50, 100, 150, 200, 250 and 300 μM) or the respective Vehicle for 24 hours. The half-maximal inhibitory concentration, IC_{50}, was calculated using GraphPad Prism® 8 software (GraphPad Software, San Diego, CA, USA). Biological and technical repeats were used to reach the statistical significance results.

Western blot analysis

Total lysate from CML cells, treated with CBD at IC_{50} dose or with vehicles for several times (8, 12 and 24 h) was extracted by using lysis-buffer (10 mM Tris, pH 7.4; 100 mM NaCl; 1 mM ethylenediaminetetraacetic acid; 1 mM ethyleneglycol-bis(aminoethylether)-tetraacetic acid; 1 mM NaF; 20 mM $Na_4P_2O_7$; 2 mM Na_3VO_4; 1% Triton X-100; 10% glycerol; 0.1% sodium dodecyl sulfate; 0.5% deoxycholate and 1 mM phenylmethylsulfonyl fluoride) containing protease inhibitor cocktail (EuroClone). Proteins were separated on 8–14% SDS polyacrylamide gels in a Mini-PROTEAN Tetra Cell system (BioRad). Protein transfer was carried out using Mini Trans-Blot Turbo RTA system (BioRad). Non-specific binding sites were blocked with 5% low-fat dry milk or 5% BSA in phosphate-buffered saline 0.1% Tween 20 for 1 h at room temperature. Membranes were incubated overnight at 4°C with the following primary Abs: anti-TRPV1, anti-TRPV2, anti-LC3, anti-caspase 3, anti-ATG16L1, anti-ATG12, anti-PINK1, anti-optineurin, anti-parkin, anti-PU.1, anti-γH2AX, anti-BiP, anti-Derlin1 or for 1 h at room temperature with anti-TRPV2, and anti-GAPDH followed by the incubation for 1 h at room temperature with HRP-conjugated anti-rabbit or anti-mouse secondary Abs. The detection was performed using the LiteAblot PLUS or Turbo kits and densitometric analysis was carried out by a Chemidoc using the Quantity One software (BioRad). For quantification, GAPDH was used as loading control. One representative out of three independent experiments is shown in each immunoblot Figure.

In some experiment, to assess the autophagic flux by using anti-LC3 Ab, CML cells were treated with CBD at IC_{50} dose in combination with BAF for 12 h. Moreover, autophagy was analyzed in lysates from siTRPV2 or siGLO (control) CML cells treated or not with CBD. To validate the downregulation of TRPV2 in silencing experiments, western blot was performed in lysates from siGLO and siTRPV2 CML cells by using anti-TRPV2 Ab. Moreover, to better clarify cell death in KU812,

lysates from KU812 cells treated with vehicle or with CBD 15 µM for 24 h were used for immunoblotting with anti-caspase-3.

Statistical analysis of the immunoblot densitometry was performed by averaging the values, including the control, obtained in the different experiments.

Cell cycle analysis

For cell cycle analysis, CML cells treated with CBD at IC_{50} dose or with vehicle for 24 h were fixed in ice-cold 70% ethanol, treated for 30 min at 37 °C with 100 µg/mL ribonuclease A solution, stained for 30 min at room temperature with PI 20 µg/mL, and analyzed by flow cytometry using linear amplification. In some experiments, CML cells were pre-treated with tranilast (10 µM) for 1 h before the addition of CBD at dose IC_{50} for 24 h.

BrdU Cell Proliferation assay

For cell cycle analysis, CML cells treated with CBD at IC_{50} dose or with vehicle for 24 h were fixed in ice-cold 70% ethanol, treated for 30 min at 37 °C with 100 µg/mL ribonuclease A solution, stained for 30 min at room temperature with PI 20 µg/mL, and analyzed by flow cytometry using linear amplification. In some experiments, CML cells were pre-treated with tranilast (10 µM) for 1 h before the addition of CBD at dose IC_{50} for 24 h.

Cell death analysis

Cell death was evaluated using propidium iodide (PI, Sigma Aldrich) staining. Briefly, cells, treated with CBD at IC_{50} dose, with OLDA at 1, 10 and 20 μM or with vehicle for 24 h, were incubated with 2 µg/mL for 30 min at 37°C. The cells were then washed, and the fluorescence intensity was analyzed by using flow cytometry and CellQuest software. To assess the potential toxic effects of CBD in healthy cells, PBMCs or red blood cells were treated with CBD 25 µM or vehicle for 24 h and then Annexin V and/or PI staining was performed by using Annexin V-FITC according to the company datasheet (Enzo Life Science, Farmingdale, USA). As positive control, PBMCs and red blood cells were treated with H_2O_2 [143,144].

Reactive Oxygen Species (ROS) Production

The fluorescent probe DCFDA was used to assess oxidative stress levels in CML cells after treatment with CBD (IC_{50}) and OLDA at 20µM dose. Cells were incubated with 20 µM DCFDA 20 min prior to the harvest time point. After washing, the fluorescence was assayed using FACS and CellQuest software. Moreover, oxidative stress was evaluated in red blood cells after CBD (25µM) treatment. As positive control, red blood cells were treated with H_2O_2 [144].

Mitochondrial transmembrane potential (ΔΨm) and Mitochondrial Integrity

Mitochondrial transmembrane potential was evaluated by JC-I staining in CML cells, treated with CBD at IC_{50} dose or with vehicle for 8, 12 and 24 h. JC-1 is a membrane potential sensible probe that accumulates in energized mitochondria and subsequently forms J-aggregate from monomers. Drop of ΔΨm decreases the J-aggregate emission at 590 nm (red fluorescence) and increases the monomer emission at 530 nm (green fluorescence). Briefly, cells were incubated for 10 min at room temperature with JC-1. JC-1 was excited by an argon laser (488 nm) and green (530 nm)/red (>570 nm) emission fluorescence was collected simultaneously. Samples were analyzed by a FACScan cytofluorimeter using the CellQuest software); the fluorescence intensity was expressed in arbitrary units on logarithmic scale. In some experiments, JC-1 was also used to evaluate ΔΨm in PBMCs from healthy donors treated with CBD (25 μM) or vehicle (used as control). The mitochondrial integrity was also investigated by labeling CML cells with Mitobright, a fluorescent probe for selectively staining of mitochondria in living cells, according to company instructions.

Mitophagy assay

Mitophagy in CML cells, treated with CBD at IC_{50} dose or with vehicle for 24 h, was detected using the Mtphagy detection kit® (Dojindo Molecular Technologies, Kumamoto, Japan) containing Mtphagy Dye® and Lyso Dye®. Briefly, CML cells (10^5 cells/well) were labeled with 100 nM Mtphagy Dye for 15 min in medium without FBS before the addition of CBD for 24 h. After treatment cells were analyzed by a FACScan cytofluorimeter using the CellQuest software. To better investigate mitophagy, confocal microscopy was also used. Briefly, CML cells, stained with

Mtphagy dye and treated with CBD as above described, were finally labelled with 1 µM Lyso Dye. After washes, cytospin was performed at 1800 rpm for 8 minutes. Nuclei were counteracted with DAPI before the analysis with C2 Plus confocal laser scanning microscope by using 100X magnification.

Colony Formation Assay

The clonogenic activity of CML cells was measured with the Human Colony-Forming Unit (CFU) Assay using MethoCult kit (StemCell technologies). Briefly, CML cells were treated for 24 h with CBD (IC_{50} dose) or vehicle as above described and then 2000 cells/well were plated for colony formation assay according to the datasheet. After 10 days, the development of colonies was visualized by inverted bright field microscope and the number of colonies in the well was counted. Each sample was assayed in triplicate.

Statistical analysis

The statistical significance was determined by Student's t-test and by One-way and Two-way ANOVA test with Dunnett's post-hoc test ($p<0.05$). No statistically significant difference was found between untransfected and siGLO transfected CML cells or between vehicle-treated with untreated cells or vehicle-treated cells at different times. In all experiments, untreated cells were used to verify that there were no differences with those treated with the vehicle. In addition, for statistical analysis purpose, the same acquisition parameters were used in all replicates for each experiment of flow cytometry analysis.

Results

TRPV channels regulation during hematopoiesis

It is already known that TRPV1 and 2 channels have a relevant role in normal immune cells [85,145] and that they are expressed in normal CD34+ HSC [146]. Starting from these knowledges, we investigated how the expression of these channels is modulated during the normal hematopoiesis. To date, we analyzed data from HemaExplorer dataset in BloodSpot as shown in Figure 10 A and B. As shown, TRPV channels expression changes during hematopoiesis. In particular, TRPV1 is weakly expressed in hematopoietic stem cells from bone marrow and in myelocyte lineage, but its expression is higher in polymorphonuclear and dendritic cells. TRPV2 is highly expressed in hematopoietic stem cells, highly expressed in hematopoietic stem cells, dendritic cells and especially in promyelocyte, myelocyte and polymorphonucleated cells from bone marrow and natural killer cells.

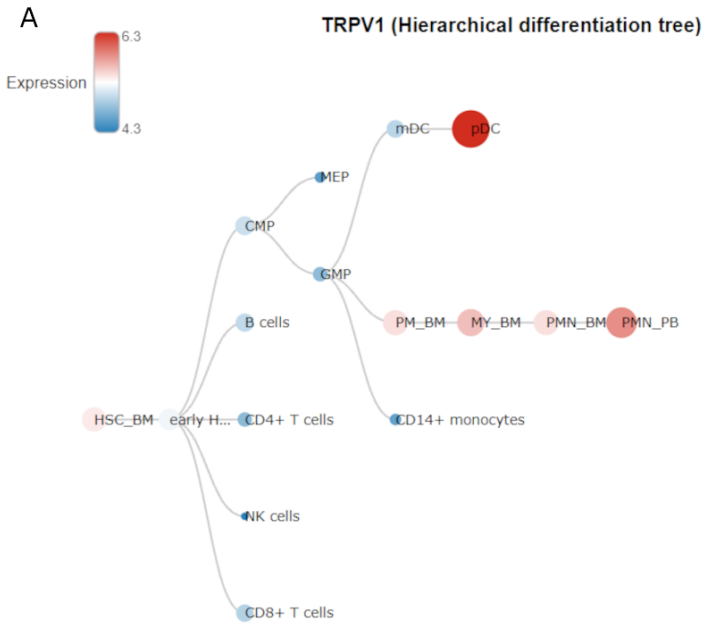

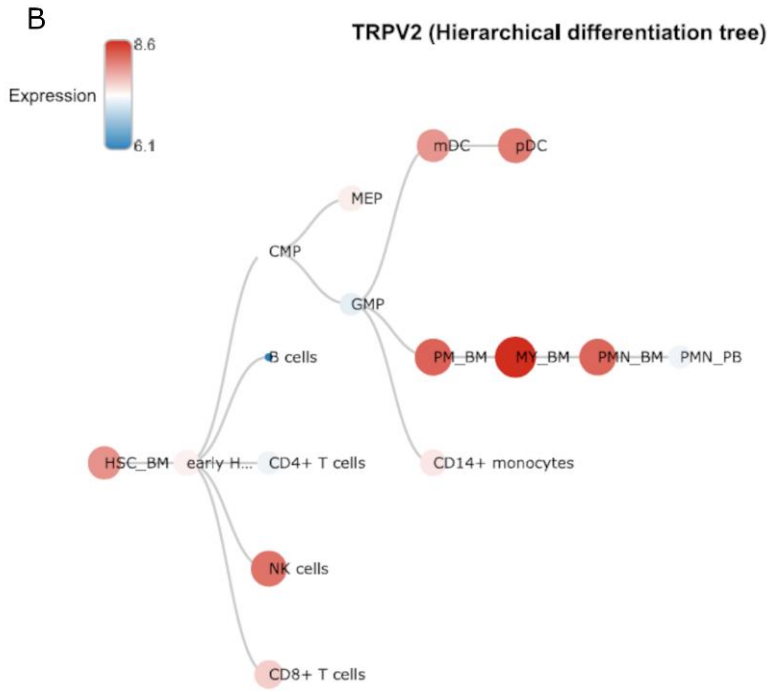

Figure 10. Hierarchical differentiation tree and TRPV channels modulation. *A) TRPV1 hierarchical differentiation tree, highest expressions are showed in red and blue the lowest. Data are showed as log2. B) TRPV2 hierarchical differentiation tree, highest expressions are showed in red and blue the lowest. Data are showed as log2. Data collected from BloodSpot using HemaExplorer database consulted on October 2021.*

Abbreviations: *HSC_BM (Hematopoietic stem cells from bone marrow); early HPC_BM (Hematopoietic progenitor cells from bone marrow); CMP (Common myeloid progenitor cell); GMP (Granulocyte monocyte progenitors); MEP (Megakaryocyte-erythroid progenitor cell); PM_BM (Promyelocyte from bone marrow); MY_BM (Myelocyte from bone marrow); PMN_BM (Polymorphonuclear cells from bone marrow); PMN_PB (Polymorphonuclear cells from peripheral blood); mDC (CD11c+ myeloid dendritic cells); pDC (CD123+ plasmacytoid dendritic cells).*

To gain importance, we analyzed the expression of TRPV1 and TRPV2 specifically in progenitor's healthy cells from myeloid lineage using Stemformatics database, selecting dataset that contains data regarding hematopoietic cells and TRPV expression. Samples were analyzed and divided according to the cell type and health state. In particular, we focused the attention on myeloid precursors as Common Myeloid Progenitors (CMP), Granulocyte Monocyte Progenitor (GMP), and Megakaryocyte-Erythroid Progenitor (MEP) (Figure 11).

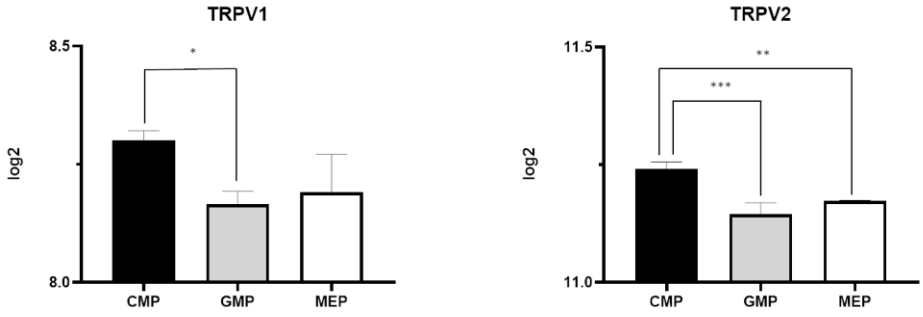

Figure 11. TRPV expression in normal hematopoietic progenitors from myeloid lineage. *mRNA (log_2) expression of TRPV expression among hematological progenitors. Data are collected from Stemformatics dataset ID 6326. *p<0.05; **p<0.005; ***p<0.001 respect to CMP.*

TRPV1 expression is reduced during differentiation and results to be lower in GMP compartment ($p<0.05$), whereas TRPV2 is markedly reduced in GMP ($p<0.001$) as well, and MEP ($p<0.05$) compartment. Moreover, TRPV2 is more expressed than TRPV1 ($p<0.0001$) as shown in Figure 12.

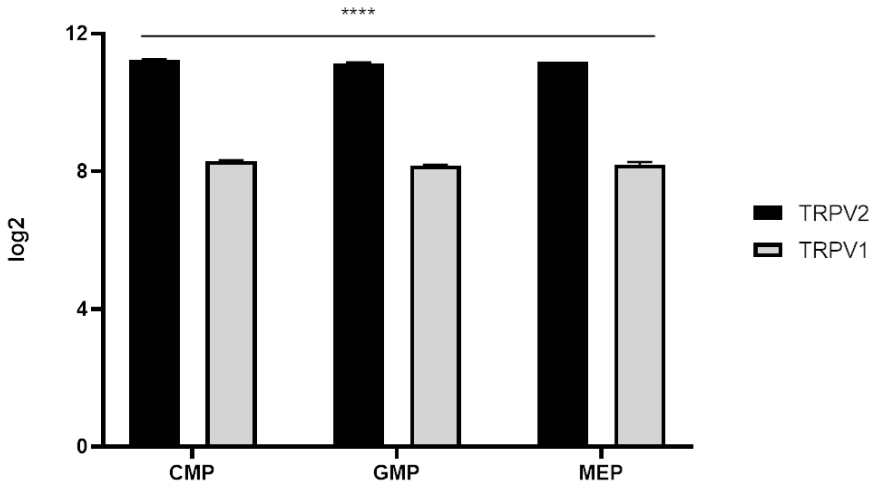

Figure 12. TRPVs comparison in normal hematopoietic progenitors. *mRNA (log_2) expression of TRPV expression among hematological progenitors. Data are collected from Stemformatics dataset ID 6326. ****p<0.0001 TRPV1 vs TRPV2.*

TRPV channels expression in CML sample from databases

Since both TRPV channels are genetically regulated during normal hematopoiesis, we evaluated their expression among the three phases of CML. Data were collected from Stemformatics database, selecting dataset that contain data regarding hematopoietic cells and TRPV expression data. The 62 samples were divided according to the disease state in Normal (13 samples), CML in Chronic Phase (CP-CML) (23 samples), CML in Accelerated Phase (AP-CML) (17 samples) and CML in Blast Crisis Phase (BCP-CML) (9 samples), and the mRNA levels were expressed in $\log_2$. All data groups were compared respect to the Normal category. As shown in Figure 13, the expression of TRPV channels changes with the progression of the disease. In particular TRPV1 expression has a decreasing trend with the progression. On the contrary, TRPV2 expression increases during the disease progression ($p<0.002$), and it is particular significant in AP-CML phase ($p<0.005$).

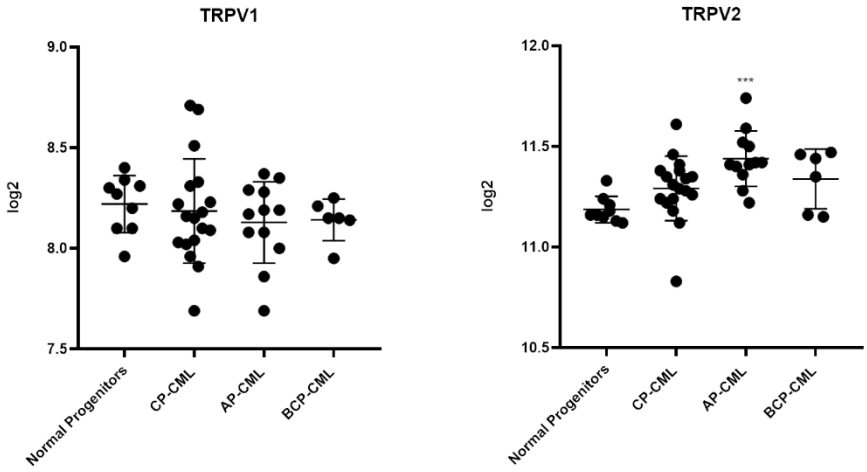

Figure 13. TRPV comparison in normal progenitors and CML. *mRNA (log_2) expression of TRPV expression between normal progenitors and tumoral progenitors in CML. Data are collected from Stemformatics dataset ID 6326. ***p<0.005 respect to Normal.*

Moreover, both TRPV channel expression varies among both the three progenitor's population and the three phases, as reported in Figure 14. TRPV1 channel expression decrease in CMP ($p<0.0001$ in BCP-CML) and GMP in CP ($p<0.05$) and AP ($p<0.005$) phases, then rises in BCP. Its level in MEP remain quite stable.

TRPV2 instead has an opposite trend, indeed it expressions is high in GMP, especcialy during the CP ($p<0.0001$) and AP ($p<0.0001$), and MEP, in AP ($p<0.005$) and BCP ($p<0.005$).

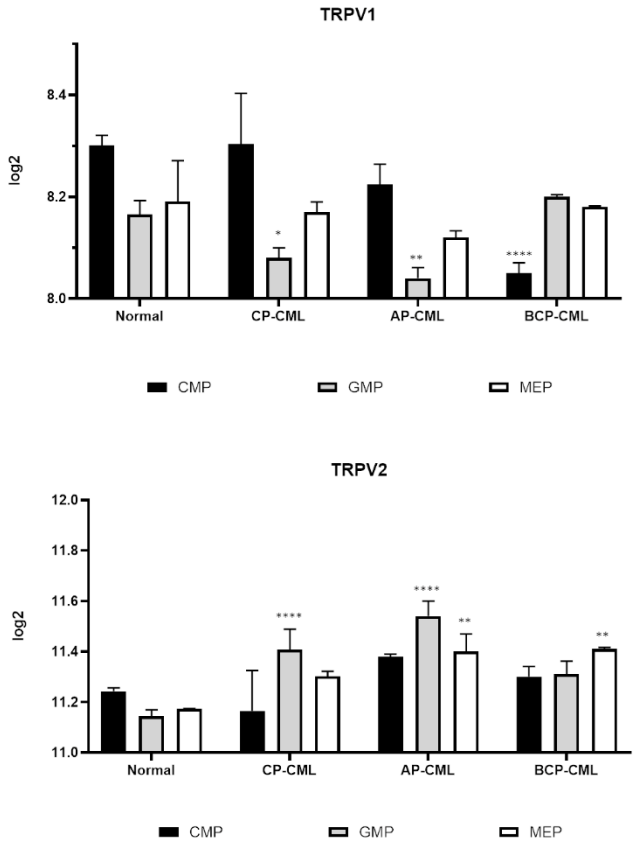

Figure 14. TRPV comparison among normal progenitors and CML progenitors in the three disease's phases. *A) TRPV1 and TRPV2 mRNA (log_2) expression of TRPV expression between normal progenitors and tumoral ones among the three phases. Data are collected from Stemformatics dataset ID 6326. *p<0.05; **p<0.005; ****p<0.0001 respect to Normal.*

TRPV channels expression in CML cell lines

After the assessment in silico, we evaluated the expression levels of TRPV1 and 2 receptors in three different CML cell lines (K562, KU812, MOLM-6), $CD34^{+}CD38^{+}$ common myeloid progenitors, normal myeloid cell enrichment, in PBMCs as healthy cells and THP-1 cells used as positive control [147]. By qRT-PCR we demonstrated that TRPV1 and TRPV2 are expressed at mRNA levels in all three cell lines (Figure 15 A). The expression was also confirmed at protein levels by using western blot and cytofluorimetric analysis (Figure 15 B, C). These results corroborated the expression of TRPV2 in K562 cells, as previously demonstrated [53]. In addition, confocal microscopy showed that TRPV1 and TRPV2 partially colocalize (Fig.15 D).

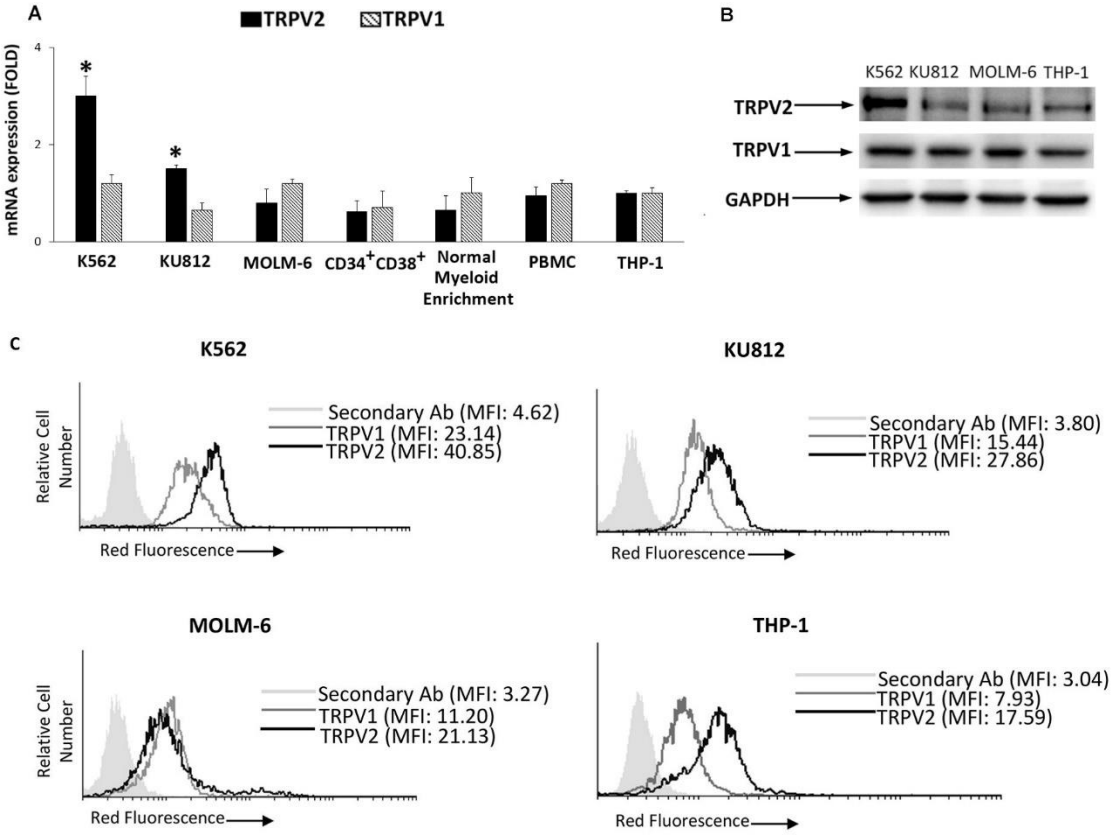

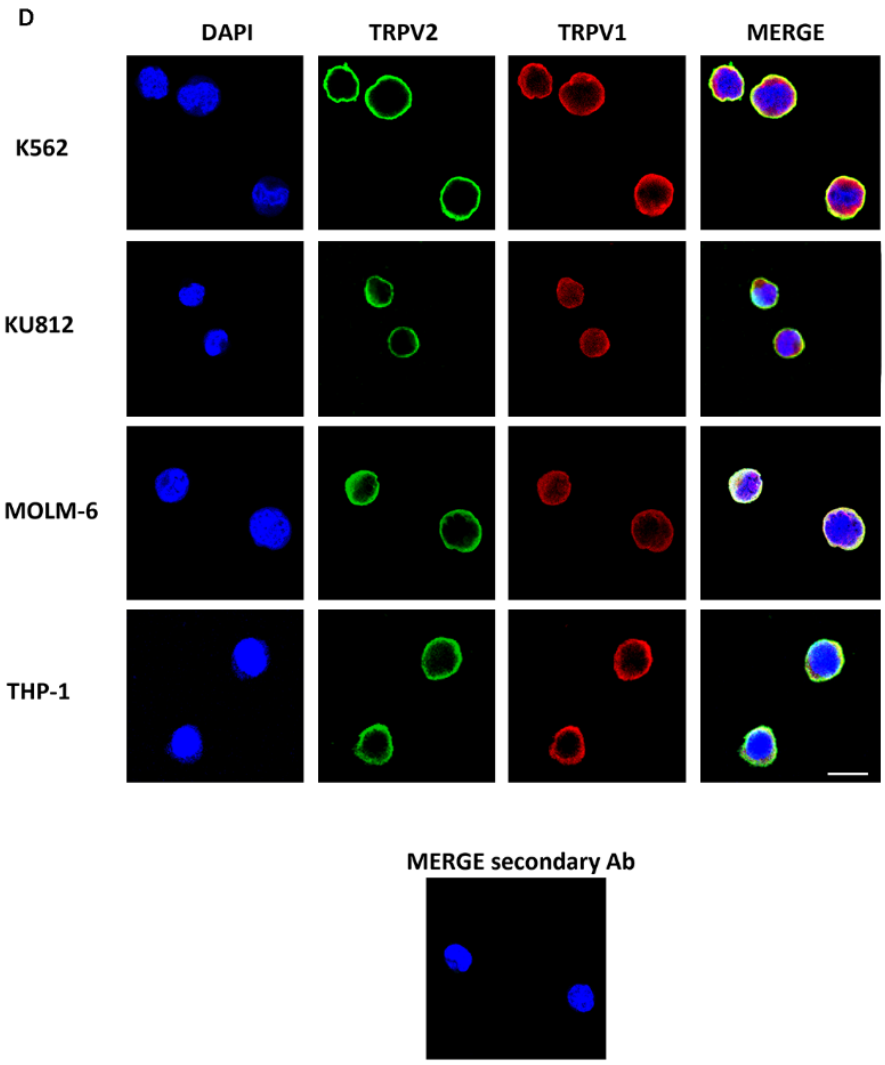

Figure 15. Expression of TRPV1 and TRPV2 in CML cells. *A) TRPV2 and TRPV1 mRNA expression was evaluated by qRT-PCR in CML cell lines, CD34+CD38+ common myeloid progenitors, normal myeloid cell enrichment, PBMCs as healthy cells and THP-1 used as positive control (calibrator=1). mRNA levels were normalized for GAPDH expression and Fold represents changes of gene expression respect to the calibrator. Data are expressed as fold mean ± SD of three separate experiments. *p < 0.05 vs THP-1 cells. B) Western blot analysis was performed in CML and THP-1 cells by using specific anti-TRPV1 and anti-TRPV2 Abs to assess the expression of TRPV2 and TRPV1 at protein level. GAPDH was used as loading control. Blot is representative of three separate experiments. C) Cytofluorimetric analysis of TRPV1 and TRPV2 protein level in CML and THP-1 cells by using specific anti-TRPV1 and anti-TRPV2 Abs followed by PE-conjugated secondary Abs. Data are representative of three separate experiments. MFI=Mean Fluorescence Intensity. D) TRPV1 and TRPV2 protein levels were also investigated in CML and THP-1 cells by confocal microscopy after incubation with specific anti-TRPV1 and anti-TRPV2 Abs. Magnification= 100X, Bar= 20 µm. Images are representative of three separate experiments.*

PART I: TRPV2

CBD, by activating TRPV2, affects CML cells viability

Given that the natural compound CBD is able to activate TRPV1 and TRPV2 [148,149], CML cells were treated with different doses of CBD (10-75 µM) for 24 h and cell viability was analyzed by cell viability assay. CBD induced a significant decrease of cell viability with an IC_{50} of 20 µM (K562), 15 µM (KU812) and 25 µM (MOLM-6) (Figure 16A). The IC_{50} doses of CBD were used for the subsequent experiments.

Thereafter, the involvement of TRPV receptors in CBD-mediated effects, was evaluated using cell viability assay, by pretreating for 1 h the CML lines with 10 µM capsazepine (TRPV1 antagonist) [150] and 10 µM tranilast (TRPV2 antagonist) [149] before the addition of CBD for 24 h. Only tranilast was able to revert the CBD effects (Figure 16B), suggesting that in CML lines, CBD inhibits viability by activating TRPV2.

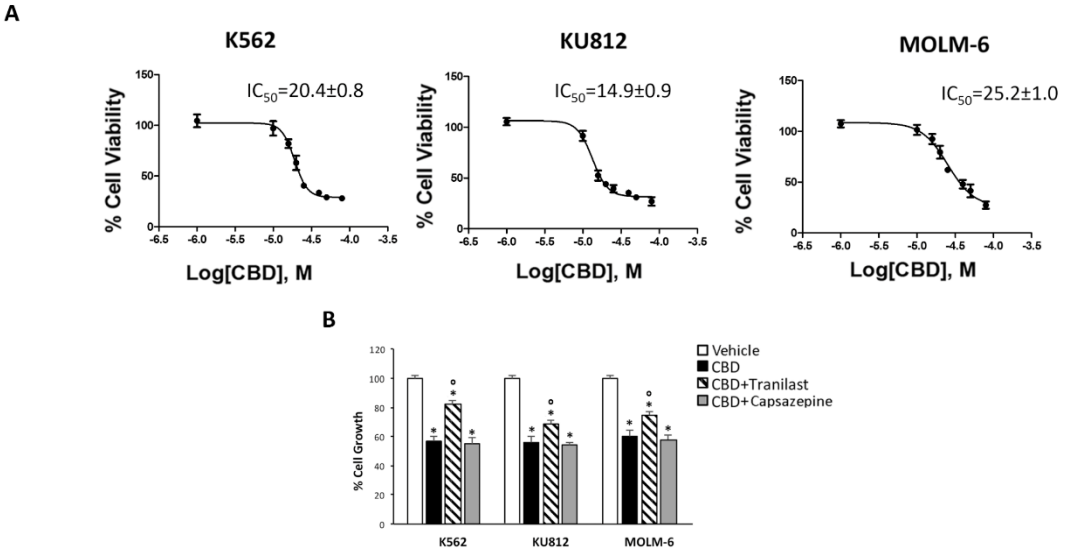

Figure 16. CBD treatment reduces cell viability in CML cells. *A) Tripan blue exclusion assay was performed in CML cells treated for 24 h with different doses of CBD. IC_{50} values were analyzed by*

*GraphPad software. Data are the mean ± SD of three different experiments. B) CML cells were pretreated with tranilast or capsazepine for 1 h before the addition of CBD at IC_{50} dose. Vehicle-treated cells were used as control (100% cell growth). The percentage of cell growth was analyzed by Tripan blue exlusion assay. Data are the mean ± SD of three different experiments. *p < 0.05 vs vehicle-treated cells; °p<0.05 vs CBD-treated cells.*

The involvement of TRPV2 was further investigated by TRPV2 and TRPV1 gene silencing (siTRPV1 and siTRPV2) (Figure 17A-D). Trypan blue exclusion assay demonstrated that the downregulation of TRPV2 levels, but not of TRPV1, reduces the effects of CBD treatment respect to siGLO (control) cells (Figure 17E, F).

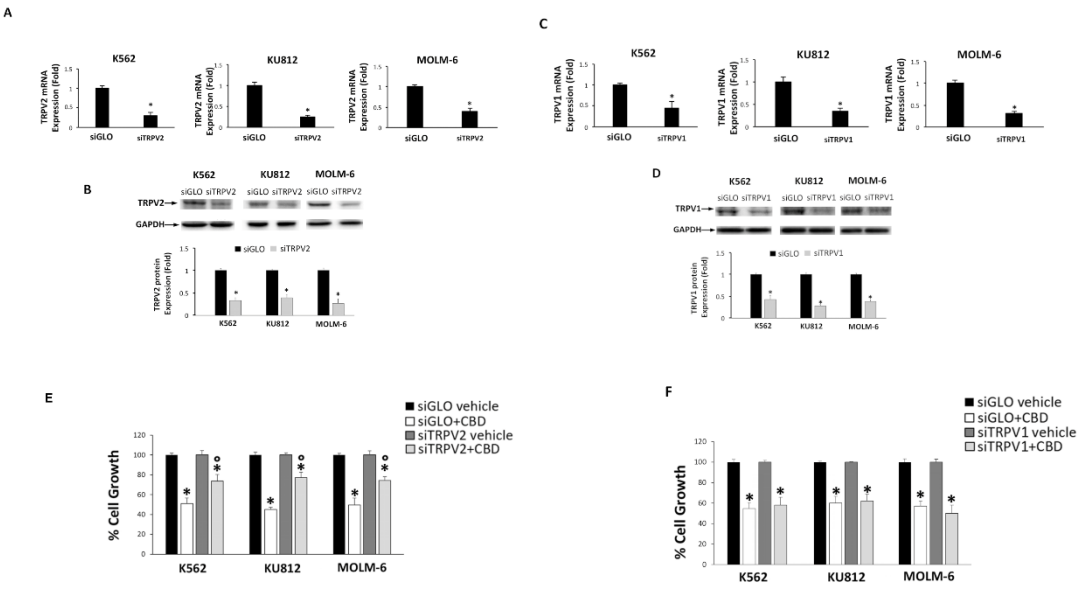

Figure 17. CBD treatment reduces cell viability in TRPV2 silenced CML cells. *A) The efficiency of TRPV2 silencing was evaluated by qRT-PCR. mRNA levels were normalized for GAPDH expression. Data are expressed as fold that represent changes in gene expression respect to siGLO (control) used as calibrator (=1). Data are the mean ± SD of three separate experiments. *p < 0.01 vs siGLO cells. B) The TRPV2 downregulation was also assessed by western blot analysis. Immunoblots are representative of separate experiments. GAPDH was used as loading control. Data of the densitometric analysis are the mean ± SD of three different experiments and are expressed as fold by using siGLO as control (=1). *p < 0.01 vs siGLO cells. C) The efficiency of TRPV1 silencing was evaluated by qRT-PCR. mRNA levels were normalized for GAPDH expression. Data are expressed as fold that represent changes in gene expression respect to siGLO (control) used as calibrator (=1). Data are the mean ± SD of three separate experiments. *p < 0.01 vs siGLO cells. D) The TRPV1 downregulation was also assessed by western blot analysis. Immunoblots are representative of separate experiments. GAPDH was used as loading control. Data of the densitometric analysis are the mean ± SD of three different experiments and are expressed as fold by using siGLO as control (=1). *p < 0.01 vs siGLO cells. E,F) Cell viability assay in siTRPV2 (E), siTRPV1 (F) and siGLO cells treated for 24h with CBD at IC50 dose or vehicle. Data are the mean ± SD of three different experiments. *p<0.05 vs vehicle, °p<0.05 vs CBD-treated siGLO cells.*

In general, the use of a specific therapy is often limited by toxic side-effects caused to healthy cells. In this regard, previous findings already showed that CBD does not target normal hematopoietic progenitor $CD34^+$ cells [151]. However, to further investigate CBD effects on healthy cells, we also performed biparametric analysis of the Annexin V versus PI staining in PBMCs treated with CBD at 25 µM, the highest IC_{50} dose used in our models. Our results indicated that CBD treatment does not induce increase in Annexin V or PI fluorescence (Figure 18 A and B). Given that the conventional treatments can induce also erythrocyte toxicity [152], apoptosis and oxidative stress induction were evaluated in healthy erythrocytes. No enhancement in the Annexin V fluorescence or ROS production was found in CBD- respect to vehicle-treated normal red blood cells (Figure 18 C and D).

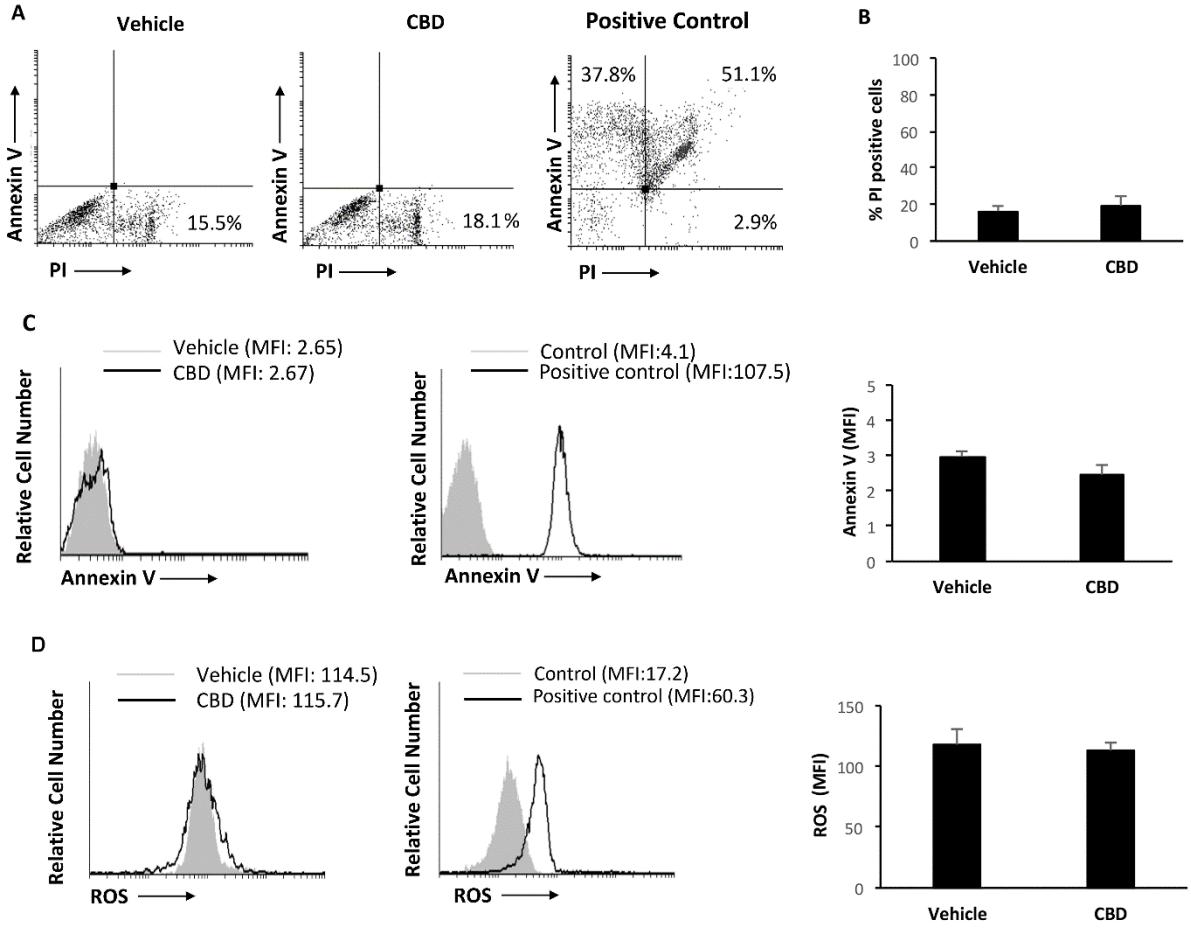

Figure 18. Effect of CBD treatment in PBMCs or red blood cells from blood of healthy donors. *A) Biparametric analysis of Annexin V vs PI staining in PBMCs treated with CBD 25 µM or vehicle for 24h. Treatment with H_2O_2 was used as positive control. Numbers in quadrants represent the percentage of: lower right single PI positive, upper right double positive; lower left double negative, upper left single Annexin positive cells. B) Statistical analysis of the percentage of PI positive cells found in CBD- or vehicle-treated cells. Data are the mean ± SD of three different experiments. C) Cytofluorimetric analysis by using Annexin V staining of red blood cells treated for 24h with CBD 25 µM or vehicle. Treatment with H2O2 was used as positive control. Bars represent the statistical analysis of the MFI values shown as mean ± SD of three different experiments. D) ROS production was analyzed by using DCFDA staining and cytofluorimetric analysis in red blood cells treated with CBD 25 µM or vehicle. Treatment with H_2O_2 was used as positive control. Bars represent the statistical analysis of the MFI values shown as mean ± SD of three different experiments.*

TRPV2 is a calcium permeable channel [53] and to better understand the signaling pathway induced by CBD, we performed calcium mobilization assay up to three minutes. Our results showed that CBD induced a rapid increase in $[Ca^{2+}]_i$ with the maximum 1 minute after the stimulation. This effect was inhibited by tranilast supporting the TRPV2 involvement in CBD-induced effects. (Fig. 19A, B). Moreover, the calcium overload was associated with a marked

enhancement in ROS production after 1 h of CBD treatment as shown by the increase in DCFDA fluorescence (Fig. 19 C, D).

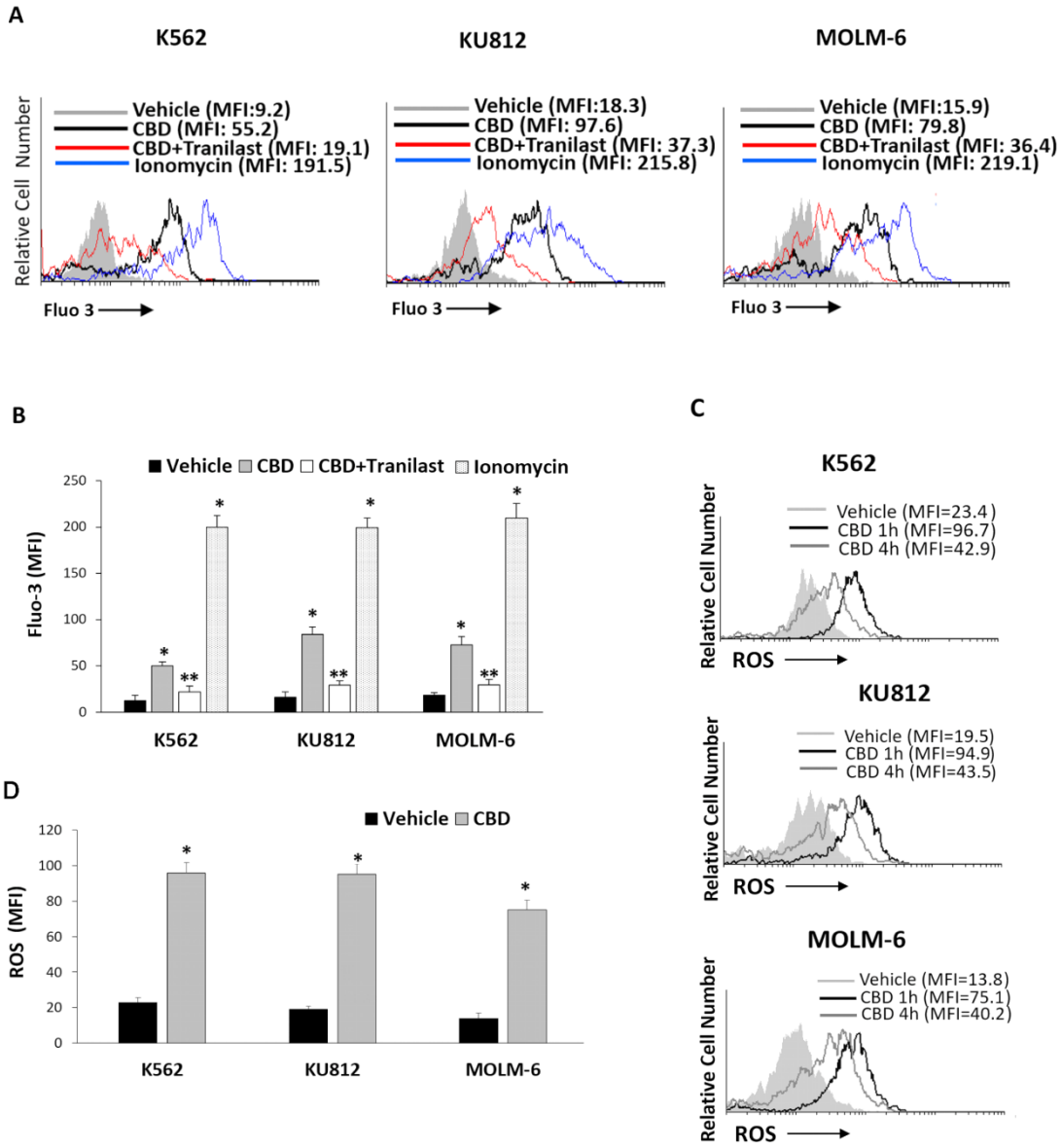

Figure 19. CBD treatment induces calcium overload and ROS production in CML cells. *A) $[Ca2+]_i$ influx was evaluated by Fluo-3 staining and FACS analysis in CML cells treated for 1 min with CBD (IC_{50} dose) or pretreated with tranilast and then stimulated with CBD. B) [Ca2+]i mobilization assay was performed by Fluo-3 staining in CML cells treated with CBD or pretreated with tranilast and then stimulated with CBD for 1 min. Bars represent the statistical analysis of the MFI values shown as mean ± SD of three different experiments. *p<0.05 vs vehicle-treated cells; **p<0.05 vs CBD-treated cells. C) ROS production was assessed by DCFDA staining and FACS analysis in CML cells treated with vehicle or with CBD (IC_{50}) for 1 and 4h. D) Bars represent the statistical analysis of the MFI values shown as mean ± SD of three different experiments. *p<0.05 vs vehicle-treated cells. MFI= Mean Fluorescence Intensity.*

CBD inhibits cell proliferation in CML cell lines

We assessed cell death and proliferation by using PI and BrdU incorporation assay, respectively. Cytofluorimetric analysis, performed in CML cells treated for 24 h with CBD and stained with PI (Figure 20 A and B), demonstrated that CBD is able to mildly stimulate cell death only in KU812 cells but not in K562 and MOLM-6, as shown by the MFI values comparing CBD- with vehicle-treated cells. In addition, we also found that apoptosis is the mechanism of cell death induced by CBD in KU812 as shown the presence of cleaved caspase 3 fragment in CBD-treated cells (Figure 20 C). CDB-induced cell death in KU812 is reverted in siTRPV2 cells, underlying the involvement of this channel in the CBD-mediated effects (Figure 20 D).

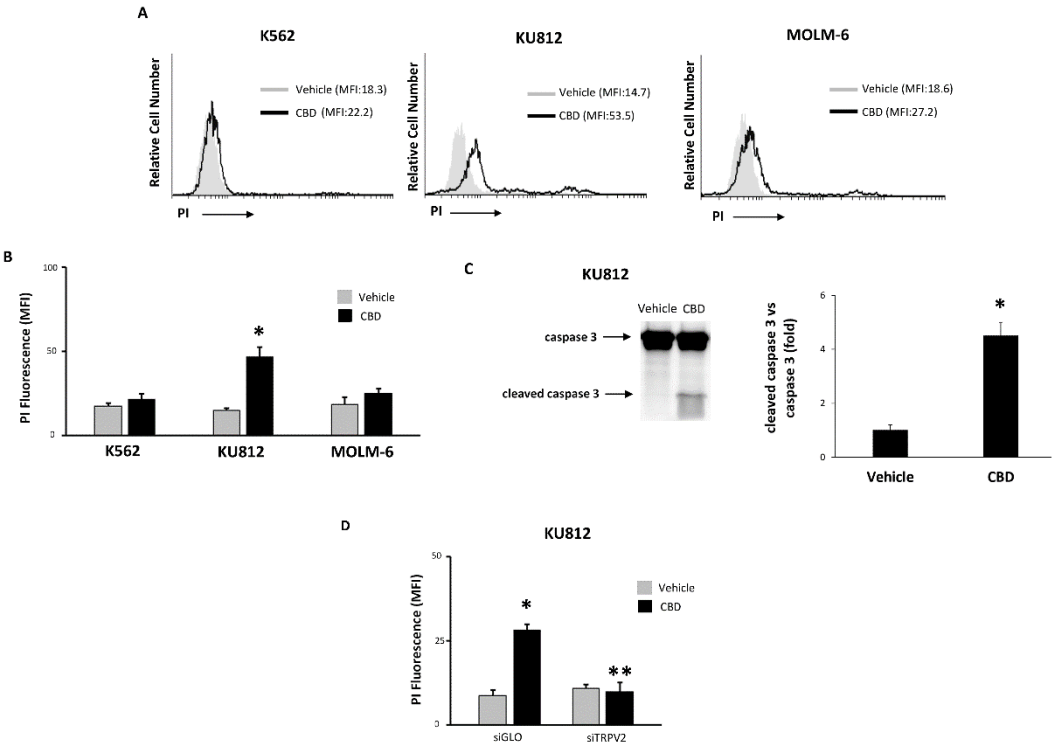

Figure 20. CBD treatment inhibits cell proliferation in CML cells. *A) Cell death was assessed by PI staining and cytofluorimetric analysis in CML cells treated with CBD at IC_{50} dose or with vehicle used as control for 24 h. Data are representative of three separate experiments. MFI= Mean Fluorescence Intensity. B) Statistical analysis of the MFI values found in CBD- or vehicle-treated CML cells for 24 h after staining with PI. Data are the mean ± SD of three different experiments. *p<0.05 vs vehicle-treated cells. C) Caspase 3 cleavage was analyzed by western blot analysis in KU812 cells treated with CBD for 24h. Blot is representative of three separate experiments. Statistical analysis of the cleaved caspase 3 densitometry values normalized to uncleaved caspase 3 levels. Folds represent changes respect to vehicle-treated cells (=1). D) PI assay was performed in CBD (IC_{50} dose)- or vehicle-treated for 24 h siGLO and siTRPV2 KU812 by cytofluorimetric analysis. Data are the mean ± SD of three different experiments. *p<0.05 vs vehicle; **p<0.05 vs CBD-treated siGLO.*

This result prompted us to investigate cell proliferation. We found that CBD markedly inhibits BrdU incorporation (Figure 21 A, B) in all three CML cell lines indicating that the reduction in cell viability is mainly associated with a strong decrease in cell proliferation.

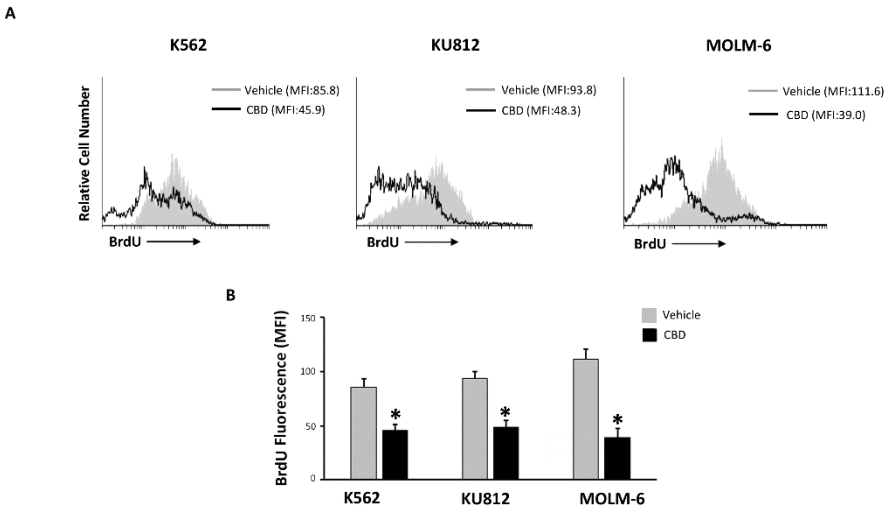

Figure 21. CBD treatment block cell proliferation in CML cells. *A) Cell proliferation was evaluated by BrdU incorporation assay and FACS analysis in CML cells treated with CBD at IC_{50} dose or with vehicle used as control for 24 h. Histograms are representative of three separate experiments. B) Statistical analysis of the MFI values found in CBD- or vehicle-treated CML cells for 24 h after BrdU assay. Data are the mean ± SD of three different experiments. *p<0.05 vs vehicle-treated cells.*

We also analyzed cell cycle phases in leukemia cells treated with CBD or with vehicle used as control. CBD treatment induced a strong cell cycle arrest by reducing the percentage of cells in S and G2/M phases and increasing the percentage of cells stopped in the G0/G1 phase (Figure 22A). This effect involved the activation of TRPV2 as demonstrated by the ability of tranilast to revert the accumulation of cells in G0/G1 phase (Figure 22B).

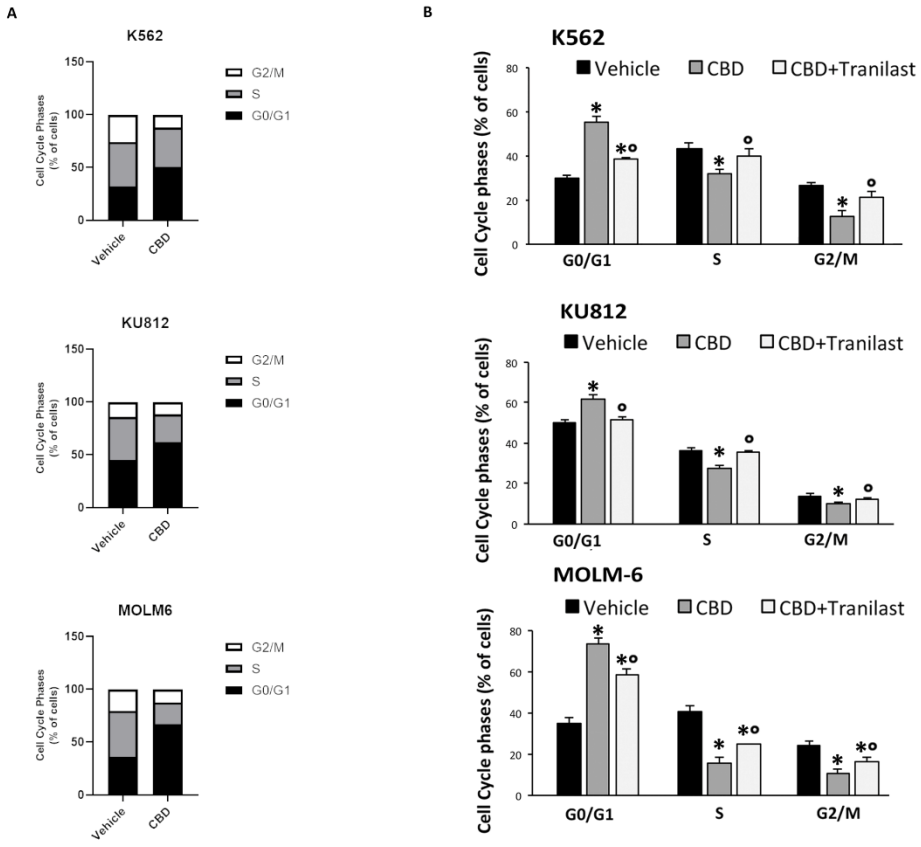

Figure 22. CBD treatment block the cell cycle. *A) Cell cycle analysis was performed in CML cells treated with CBD at IC_{50} dose or with vehicle used as control for 24 h. Numbers indicate the percentage of cells in each cell cycle step. Data are representative of three separate experiments. B) Statistical analysis of cell cycle phases investigated in CML cells treated with CBD at IC_{50} dose or vehicle used as control for 24 h or pretreated with tranilast for 1 h before the addition of CBD. Data are the mean ± SD of three separate experiments. *p<0.05 vs vehicle: °p<0.05 vs CBD.*

The cell cycle arrest induced by CBD treatment is associated with mitochondria impairment

CBD is able to target mitochondria promoting mitochondrial depolarization (ΔΨm) [88], and, together with calcium overload and the consequent ROS production, play a pivotal role in the mitochondria dysfunction [153]. Thus, by using JC-1 staining, we found that the treatment of CML cell lines with the IC_{50} dose of CBD induces a time-dependent ΔΨm with decreased red fluorescence (depolarization). The CBD-induced ΔΨm dissipation was evident at 8 h, increased at 12 h and slightly decreased at 24 h (Figure 23 A, B). CCCP was used as positive control.

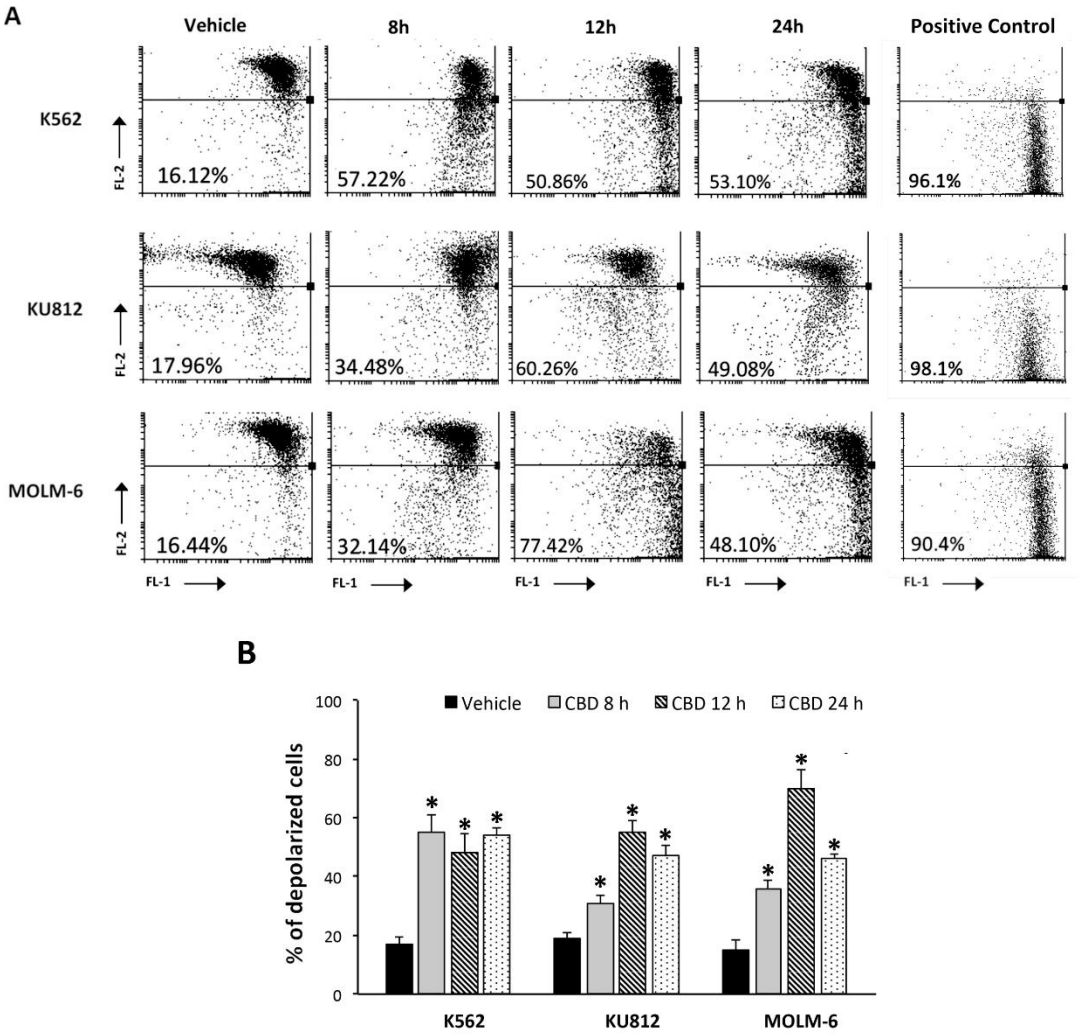

Figure 23. CBD treatment impairs mitochondrial integrity. *A) Time course analysis of ΔΨm changes on CBD-treated CML cells at different times (8, 12 or 24 h) after treatment was evaluated by JC-1 staining and biparametric FL-2(red)/FL-1(green) flow cytometric analysis. Drop of ΔΨm decreases the J-aggregate emission at 590 nm (red fluorescence). Numbers indicating the percentage of gated cells showing a decline in the ΔΨm-related red fluorescence intensity denotes depolarization. Data are representative of three separate experiments. CCP was used as positive control. B) Statistical analysis of the % of depolarized cells found in CBD- or vehicle-treated CML cells for 24 h after JC-1 staining. Data are the mean ± SD of three different experiments. *p<0.05 vs vehicle-treated cells.*

The CBD-induced effect on mitochondria was also assessed by JC-1 in healthy PBMCs treated with the highest dose of CBD used. Our results showed a barely noticeable decrease in red fluorescence in the CBD-treated cells and the total absence of cells in the lower right quadrant thus indicating the absence of cells with fully depolarized mitochondria (Figure 24).

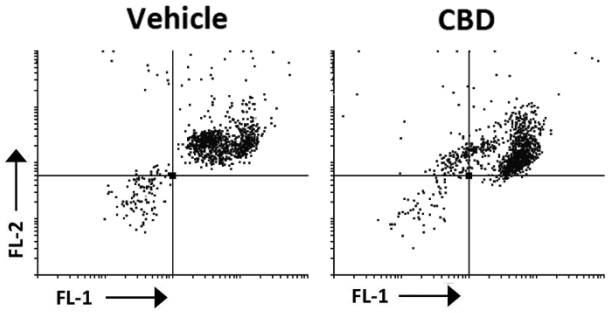

Figure 24. CBD treatment does not impair mitochondrial integrity in PBMCs*. The mitochondrial integrity was evaluated by JC-1 staining and cytofluorimetric analysis in healthy PBMCs treated with CBD at 25 µM or with vehicle used as control for 24 h. Data are representative of three separate experiments.*

To further support the role of TRPV2, we evaluated the drop of ΔΨm in siGLO and siTRPV2 cells treated with vehicle or with CBD (IC_{50} dose) for 12h. Our results showed that the CBD-induced mitochondrial impairment is markedly reduced in siTRPV2 respect to siGLO cells (Figure 25).

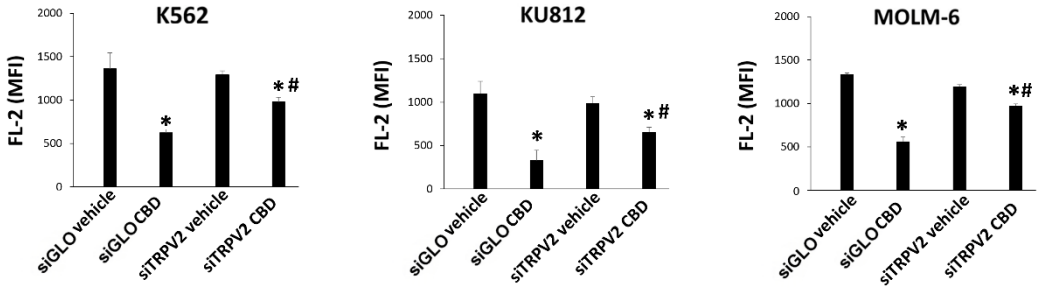

Figure 25. TRPV2 silencing reduced the mitochondrial impairment CBD-mediated*. The decrease of FL-2 fluorescence indicating the drop of ΔΨm was evaluated by JC-1 in siGLO and siTRPV2 cells treated with vehicle or CBD for 12h. Data are the mean ± SD of three different experiments *p<0.05 vs vehicle; #p<0.05 vs CBD-treated siGLO cells.*

The mitochondrial dysfunction was also investigated by labeling CML cell lines with Mitobright. A marked reduction in MFI values and an increased percentage of cells with diminished green fluorescence in CBD-treated respect to vehicle-treated cells were found indicating mitochondrial impairment (Figure 26 A and B). These changes were TRPV2-dependent. In fact, no statistically significant differences in MFI values are present in CBD- respect to vehicle-treated siTRPV2 cells. Whereas in siGLO cells, the treatment with CBD was able to promote reduction in the green fluorescence after staining with Mitobright (Figure 26 C).

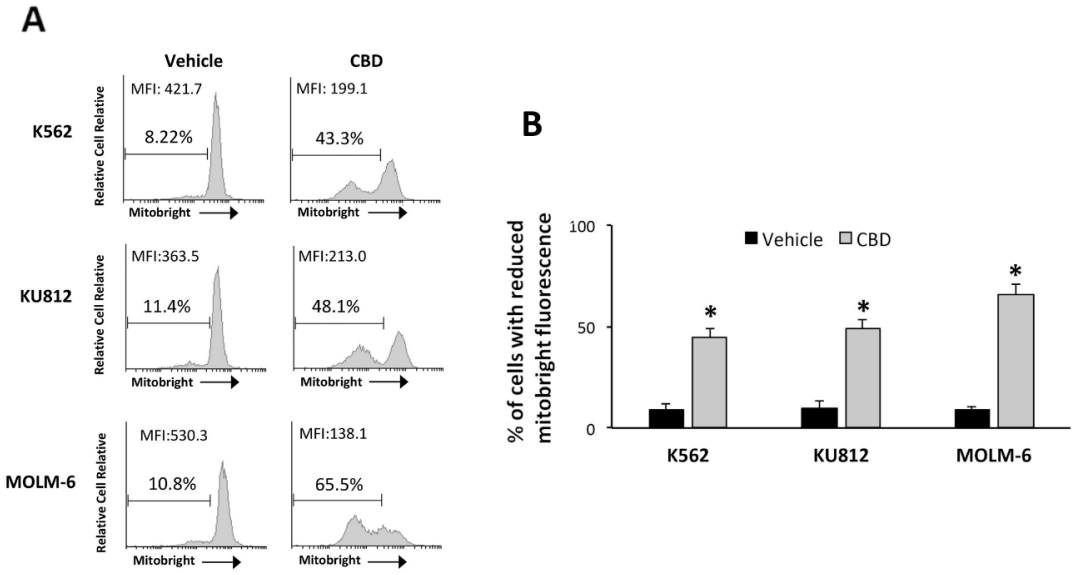

C

Mitobright (MFI)	siGLO+Vehicle	siGLO+CBD	siTRPV2+Vehicle	siTRPV2+CBD
K562	505.5±14.5	420.5±10.6*	569.7±15.4	551.3±12.2
KU812	286.7±7.8	195.8±5.2*	235.8±9.8	226.8±7.6
MOLM-6	609.6±12.5	519.1±.7*	671.4±16.7	658.0±11.4

***Figure 26. CBD treatment induces mitochondrial dysfunction in CML cells**. A) The mitochondrial integrity was evaluated by cytofluorimetric analysis in CML cells treated with CBD at IC_{50} dose or with vehicle for 24 h and labeled with Mitobright. B) Statistical analysis of the percentage of cells with reduced Mitobright fluorescence found in CBD- or vehicle-treated CML cells for 24 h after Mitobright staining. Data are the mean ± SD of three different experiments. *p<0.05 vs vehicle-treated cells. C) MFI values of the Mitobright fluorescence were evaluated in siGLO and siTRPV2 CML cells treated with CBD or vehicle for 24 h and stained with Mitobright. Data are the mean ± SD of three different experiments. *p<0.05 vs vehicle-treated cells.*

The CBD induces mitophagy in CML cells

To assess if the mitochondrial impairment was associated with mitochondrial mass reduction, we labeled cells with the specific anti-COX IV Ab. COX IV is a mitochondrial protein widely used as mitochondrial mass marker [154]. A marked down-regulation in COX IV expression in CBD respect to vehicle-treated CML cells was found demonstrating the stimulation of mitochondria removal (Figure 27 A and B).

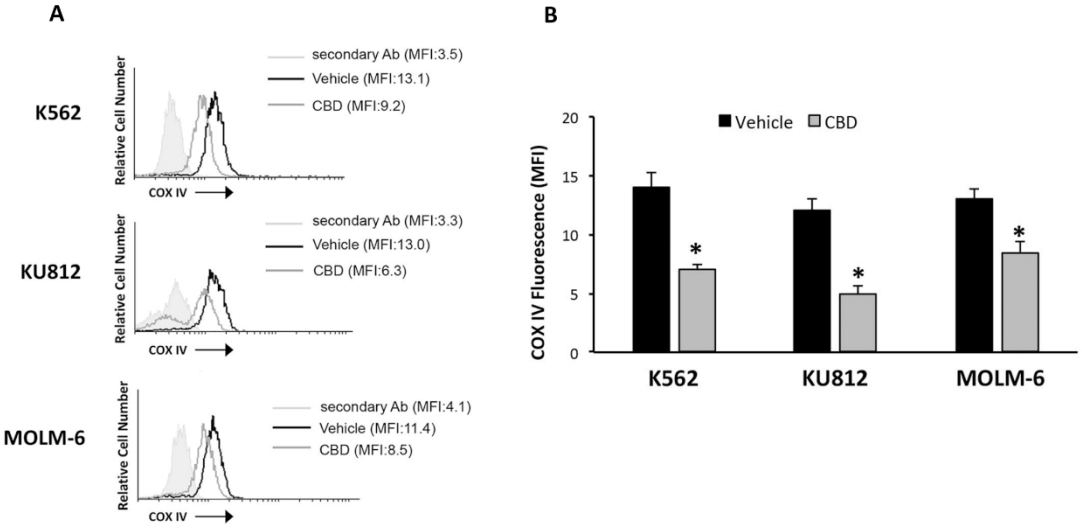

Figure 27. CBD treatment induces mitochondrial mass reduction in CML cells. *A) The mitochondrial mass in CML cells, treated as above described, was investigated by FACS analysis using specific anti-COX IV Ab. Data are representative of three separate experiments. C) Statistical analysis of the MFI values found in CBD- or vehicle-treated CML cells for 24 h after COX IV staining. Data are the mean ± SD of three different experiments. *p<0.05 vs vehicle-treated cells.*

Thus, we decided to investigate whether CBD treatment promotes mitophagy in CML cells. To this purpose, cytofluorimetric analysis was performed by labelling cells before CBD treatment with the specific Mtphagy Dye. Mtphagy Dye accumulates in intact mitochondria and emits weak fluorescence in normal pH condition; however, when mitophagy is induced, the damaged mitochondria fuse

to lysosome and, in acidic microenvironment, Mtphagy Dye increases the fluorescence. Our results demonstrated that the fluorescence enhancement occurs in CBD-treated respect to vehicle-treated CML cells as shown by the MFI values (Figure 28 A and B).

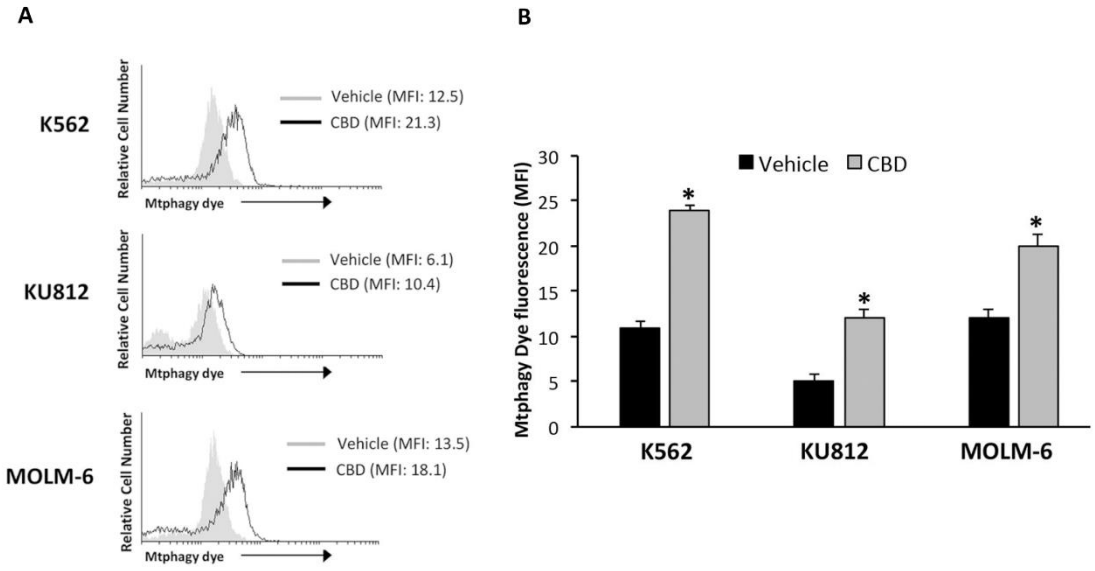

Figure 28. CBD treatment induces mitophagy in CML cells *A) Mtphagy dye and cytofluorimetric analysis were used to assess mitophagy induced by CBD treatment for 24 h in CML cells. Data are representative of three separate experiments. B) Statistical analysis of the MFI values found in CBD- or vehicle-treated CML cells for 24 h after Mtphagy dye staining. Data are the mean ± SD of three different experiments. *p<0.05 vs vehicle-treated cells.*

To confirm the fusion of Mtphagy Dye–labeled mitochondria and lysosomes, cells were also stained with Lyso Dye and then analyzed by confocal microscopy. Data confirmed that Mtphagy dye fluorescence is strongly increased in CBD-treated compared to vehicle-treated CML cells. Moreover, Mtphagy and Lyso dyes colocalized in CBD-treated cells indicating that damaged mitochondria are driven inside lysosomes by mitophagy (Figure 29).

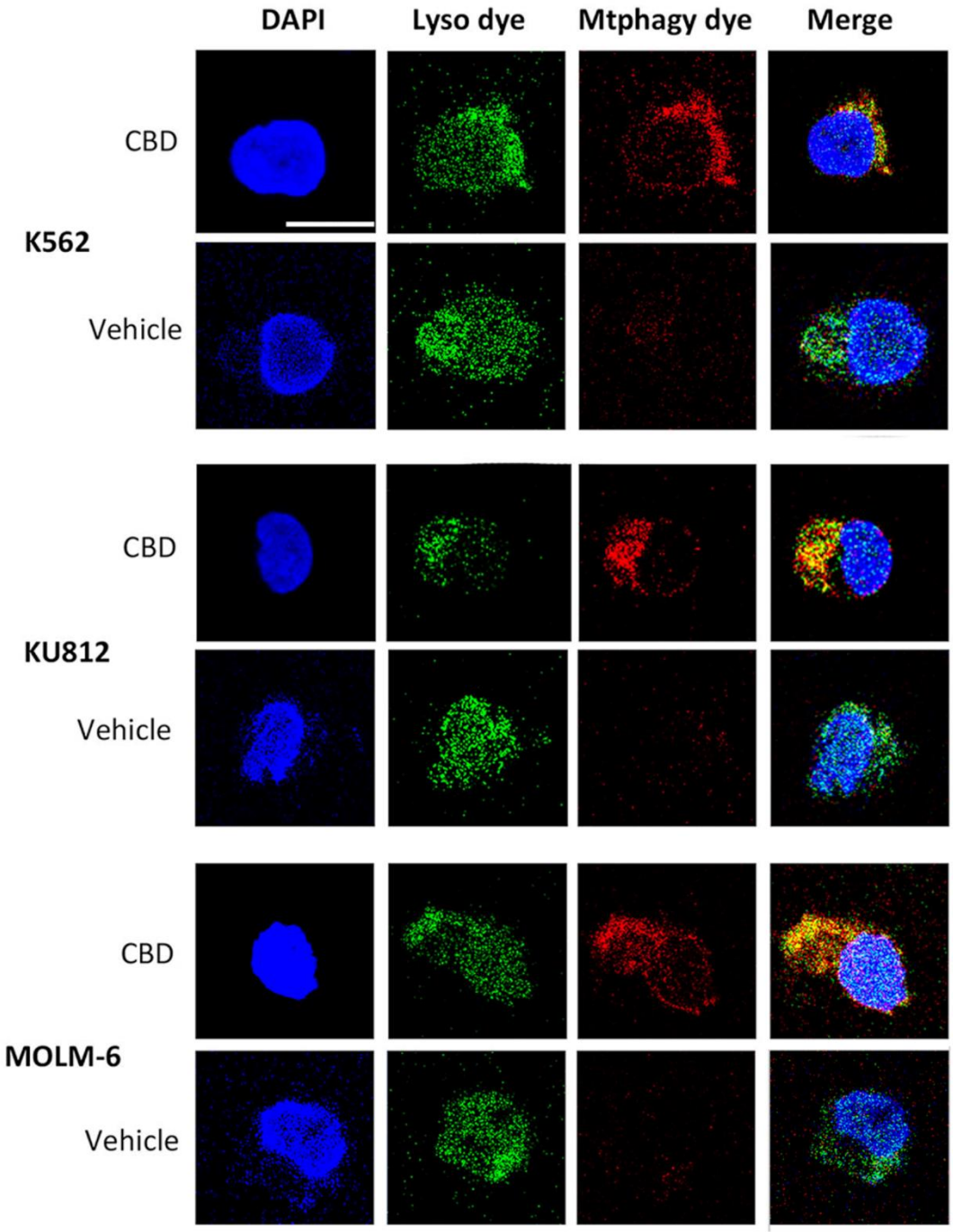

Figure 29. Mitophagy induction by CBD treatment in CML. *CML cells treated with CBD at IC_{50} dose or with vehicle for 24 h were stained with Mtphagy dye and Lyso dye and then analyzed by confocal microscopy. Images are representative of three separate experiments. Magnification: 100X. Bar: 20 µm.*

The CBD-induced mitophagy is TRPV2-dependent in CML cells

Mitophagy is a type of cargo-specific autophagy [155]. To better characterize the autophagic process induced by CBD treatment, we examined the conversion of the soluble form of LC3-I to the lipidated and autophagosome-associated form (LC3-II) (Figure 30 A). CBD treatment increased the expression of LC3-II in all three CML cell lines. The autophagy inhibitor bafilomycin A (BAF), by blocking the autophagic degradation activity, was able to increase the LC3-II form in all the three lines (Figure 30 B), demonstrating that LC3-II levels were strictly dependent from the autophagic flux and not the result of an increased protein synthesis.

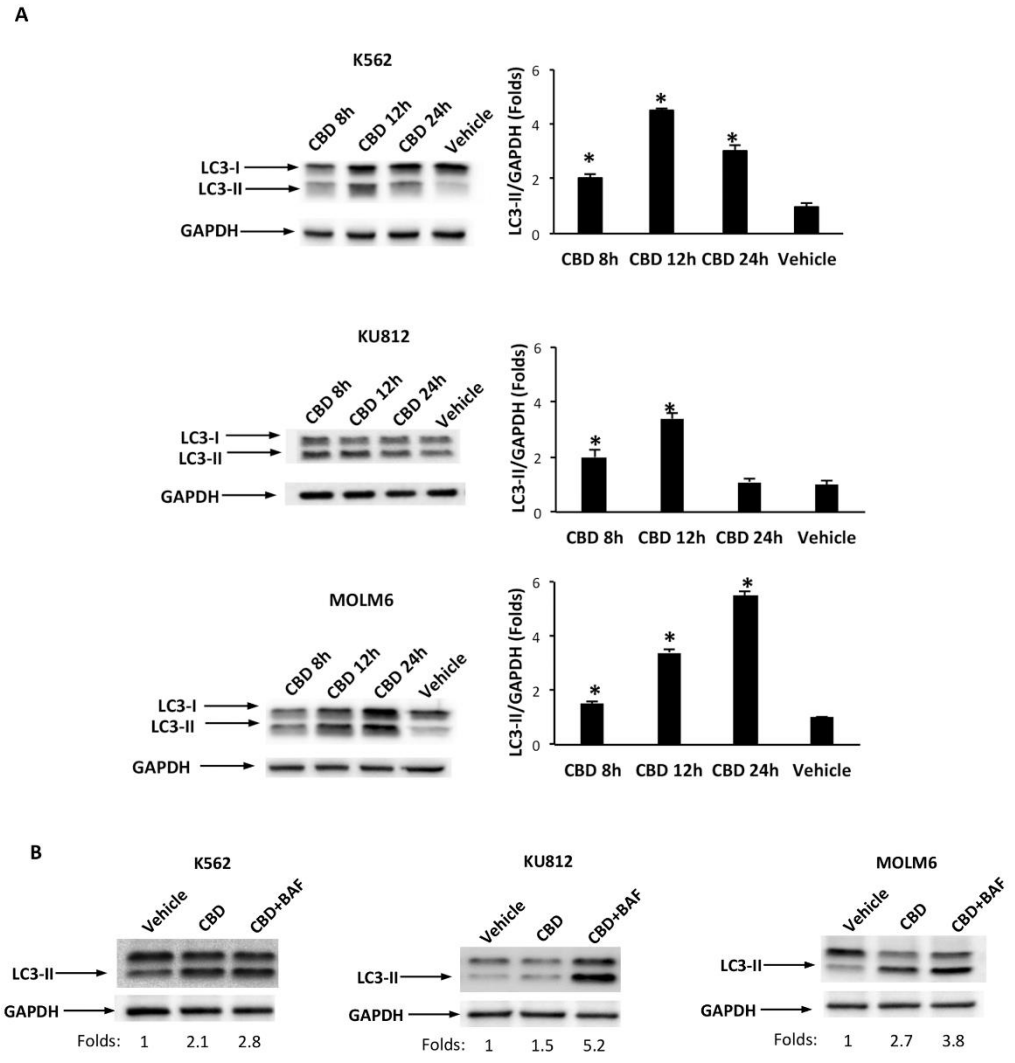

Figure 30. CBD treatment increases the expression of LC-3 II protein. *A) Western blot analysis of LC-3 II protein levels in CML cells treated with CBD at IC_{50} dose or with vehicle (used as control) for different times. Blots are representative of one of three separate experiments. GAPDH was used as loading control. Statistical analysis represents the LC-3 II densitometry values normalized to GAPDH levels, expressed as folds changes respect to vehicle-treated cells (=1). Data are the mean ± SD of three different experiments. *p < 0.01 vs vehicle-treated cells. B) Western blot analysis of LC-3 II protein levels in CML cells pretreated with BAF for 1 h before the addition of CBD at IC_{50} dose for 12 h. Blots are representative of one of three separate experiments. LC-3 II densitometry values were normalized to GAPDH used as loading control. Folds represent changes respect to vehicle-treated cells (=1).*

In addition, in siTRPV2 cells, the treatment with CBD was unable to increase markedly the expression of LC3-II respect to vehicle-treated cells at comparable level as in siGLO cells indicating the involvement of TRPV2 activation (Figure 31).

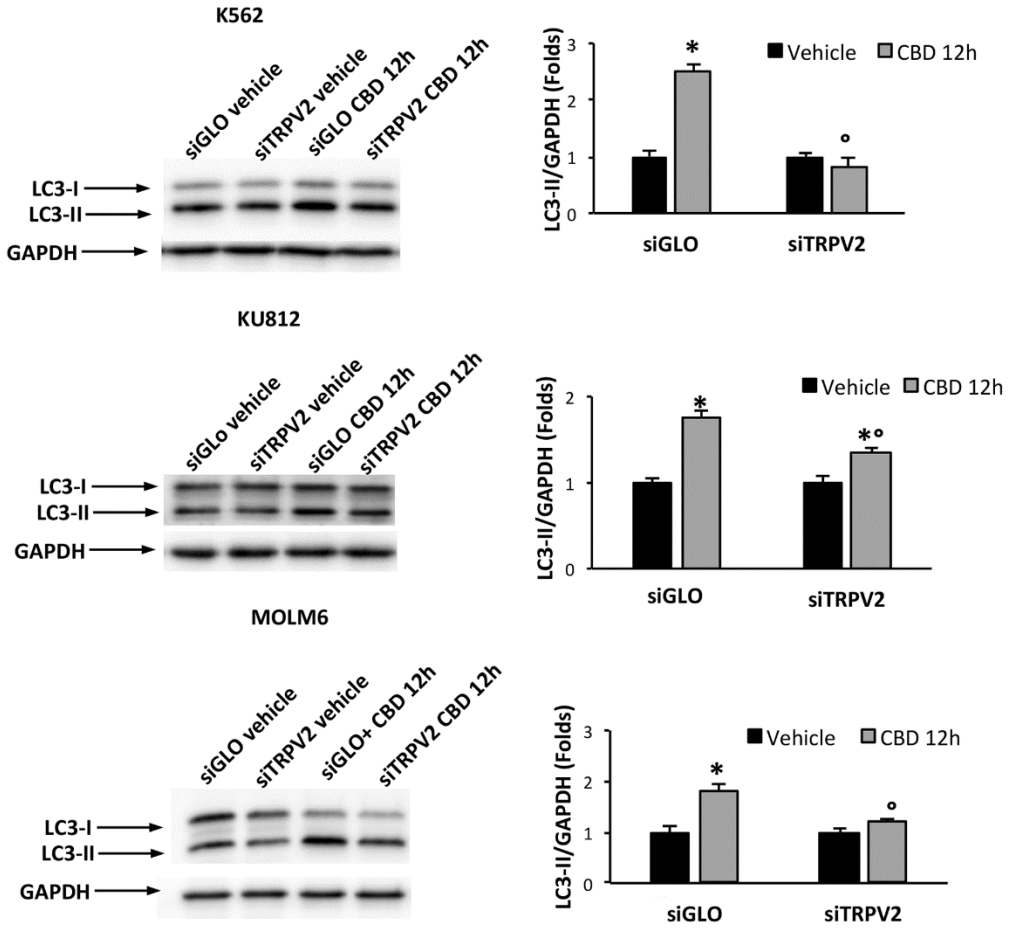

Figure 31. Block of the autophagic flux in siTRPV2 CML cells treated with CBD. *Western blot analysis of LC-3 II protein levels in siGLO and siTRPV2 CML cells treated with CBD at IC_{50} dose or with vehicle (used as control) for 12 h. Blots are representative of one of three separate experiments. In statistical analysis LC-3 II densitometry values were normalized to GAPDH used as loading control. Folds represent changes respect to vehicle-treated cells (=1). Data are the mean ± SD of three different experiments. *p < 0.01 vs vehicle-treated cells; °p < 0.05 vs CBD-treated siGLO cells.*

The autophagic process was also investigated by analyzing ATG16L1 and ATG5/ATG12 essential for the formation of the autophagosomes [156]. CBD treatment also induced up-regulation of ATG16L1 and ATG5/ATG12 expression indicating the execution of canonical autophagy (Figure 32).

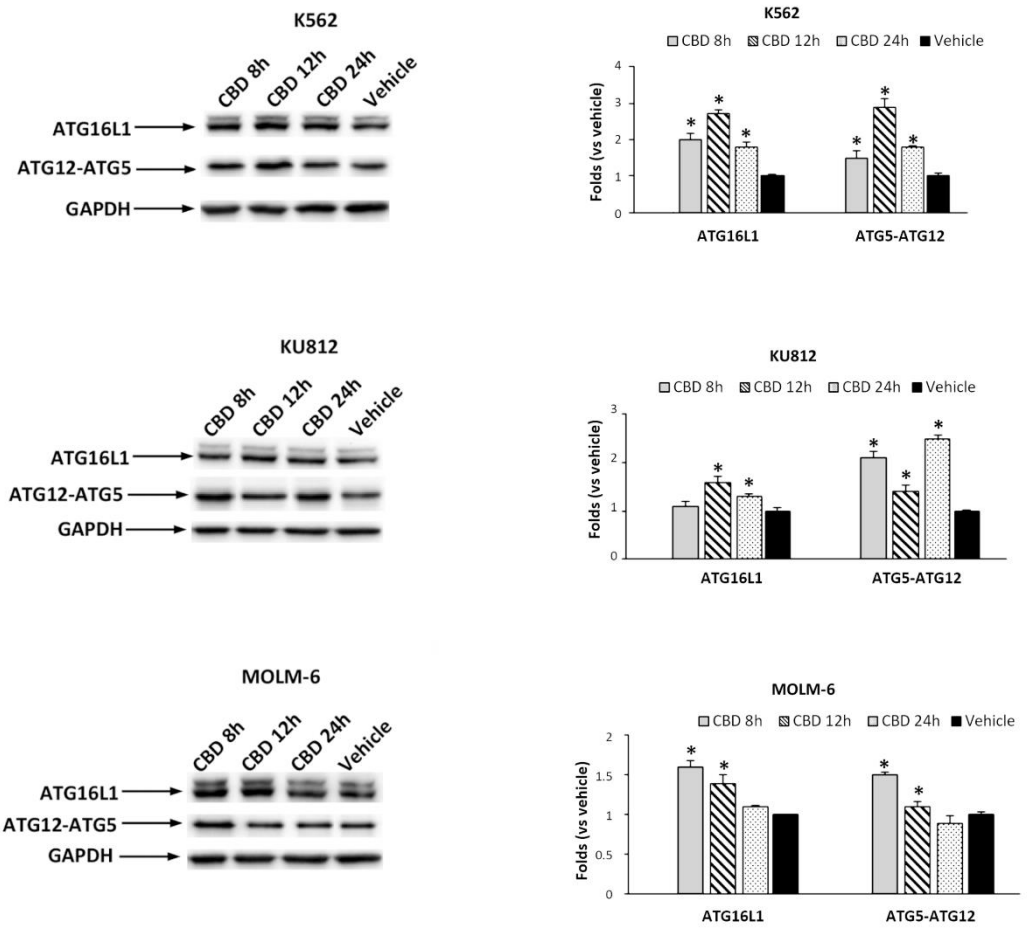

Figure 32. Increase expression of ATG proteins in CBD treated cells. *Western blot analysis of ATG16L-1 and ATG12/ATG5 complex protein levels in CML cells treated with CBD at IC_{50} dose for different times. Blots are representative of one of three separate experiments. In statistical analysis ATG16L-1 and ATG12/ATG5 complex protein densitometric values were normalized to GAPDH levels used as loading control. Folds represent changes respect to vehicle-treated cells (=1). Data are the mean ± SD of three different experiments. *p < 0.01 vs vehicle-treated cells.*

Moreover, given that mitophagy is regulated by parkin and pink1 that mediate ubiquitination of proteins on the membrane of damaged mitochondria and promote autophagosome formation around optineurin-labeled damaged mitochondria [157], we evaluated the expression of these proteins in CML cells treated or not with CBD. Our findings showed that CBD treatment stimulates an increased expression of parkin, PINK1 and optineurin (Figure 33) indicating the activation of mitophagy.

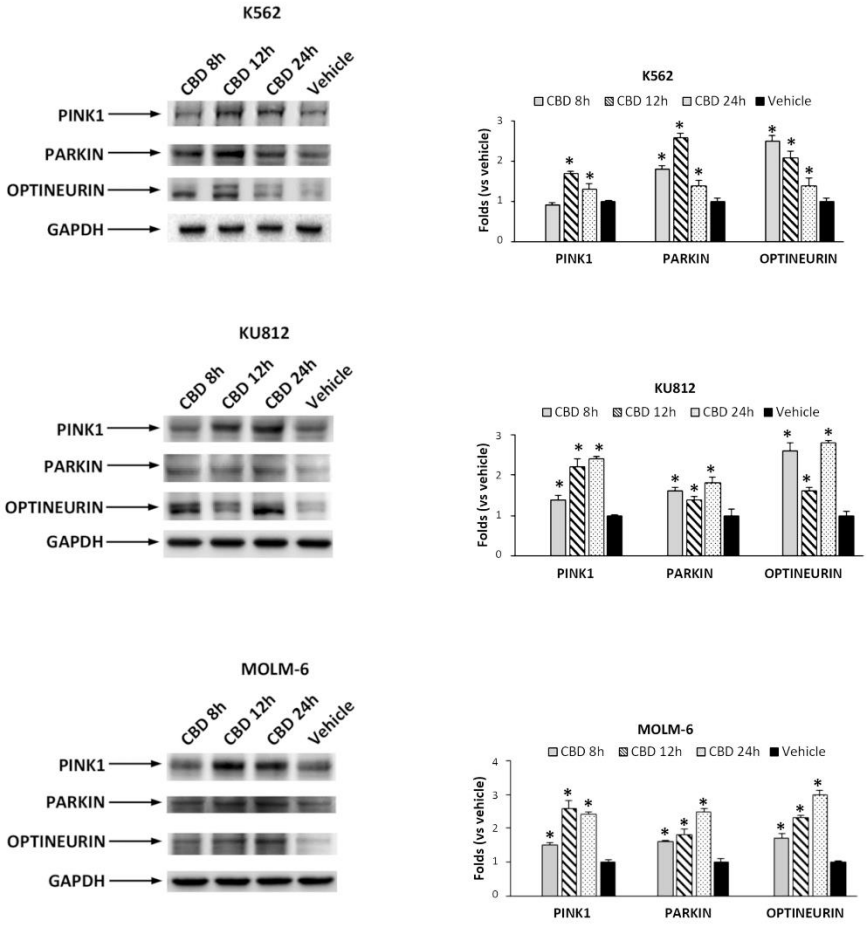

Figure 33. Expression of mitophagy markers in CBD treated cells. *Western blot analysis of pink1, parkin and optineurin protein levels in CML cells treated with CBD at IC_{50} dose for different times. Blots are representative of one of three separate experiments. In statistical analysis pink1, parkin and optineurin densitometric values were normalized to GAPDH levels used as loading control. Folds represent changes respect to vehicle-treated cells (=1). Data are the mean ± SD of three different experiments. *p < 0.01 vs vehicle-treated cells.*

Moreover, the inhibition of autophagy strongly reverted the cell growth inhibition stimulated by CBD treatment (Fig. 34) markedly supporting the role of autophagy in the CBD-mediated effects.

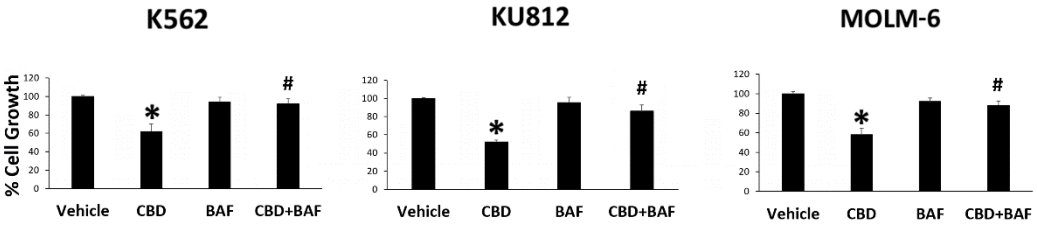

Figure 34. Reduction in cell viability is influenced by autophagy. *Cell viability assay was performed in CML cells pretreated for 1h with BAF and then treated for 24h with CBD (IC_{50} dose). *p<0.05 vs vehicle-treated cells; **p<0.05 vs CBD-treated cells.*

The CBD-induced mitophagy modulates differentiation and pluripotency marker expression

The levels of pluripotency-associated proteins are modulated during autophagy [158]. Thus, we also investigated whether CBD treatment was able to induce modulation of the expression of transcription factors involved in the maturation of CML cells. We found by cytofluorimetric analysis that CBD markedly reduces the expression of the stemness-related protein OCT-4 in CML cells as shown by the reduction in MFI values in CBD treated respect to vehicle-treated cells (Figure 35).

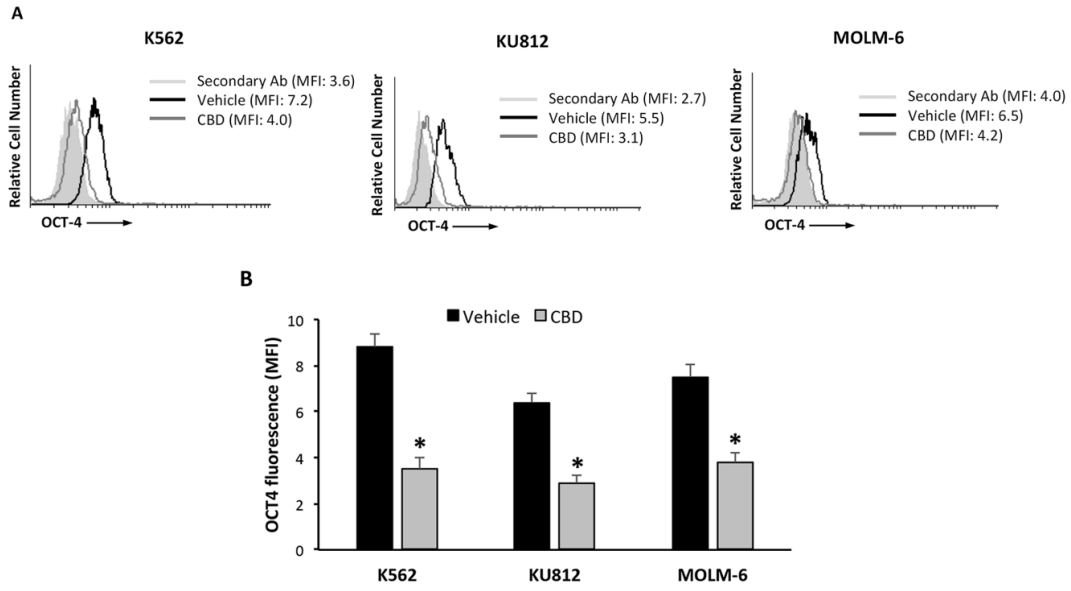

Figure 35. CBD treatment in CML cells reduces the expression of the stem cell marker OCT-4. *A) Cytofluorimetric analysis was performed to evaluate the OCT-4 expression levels in CML cells treated for 24 h with CBD at IC_{50} dose or vehicle. Data are representative of one of three separate experiments. MFI= Mean Fluorescence Intensity. B) Statistical analysis of the MFI values found in CBD- or vehicle-treated CML cells for 24 h after OCT-4 staining. Data are the mean ± SD of three different experiments. *p<0.05 vs vehicle-treated cells.*

Since our CML cell line are all in blast crisis phase, we investigated if even the LSC population is affected by the action of CBD treatment. To date this, we analyzed

the CD34 stemness marker expression via qRT-PCR. Results show that KU812 expressed the highest amount of CD34 gene ($p<0.0001$) among the three cell lines, MOLM6 is barely detectable and K562 is CD34 negative, as previously reported [159]. Since KU812 has the highest expression of CD34, we investigated the expression of this marker after CBD treatment. Indeed, the treatment with CBD for 8 and 12 hours reduce the expression of CD34 in KU812 at genetic level, as demonstrated in Figure 36 A and B.

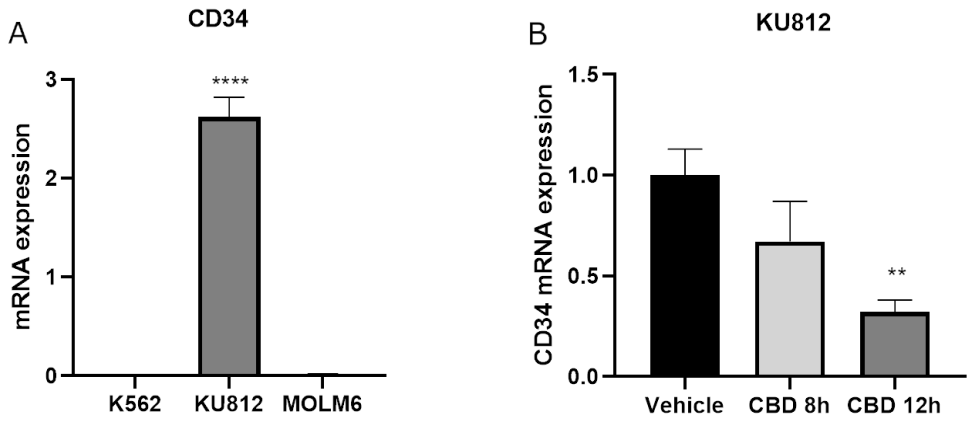

Figure 36. CD34 expression in CML. *A) CD34 mRNA expression was evaluated by qRT-PCR in CML cell lines. mRNA levels were normalized for GAPDH expression. Data are expressed as fold mean ± SD of three separate experiments. ****p < 0.0001 using one-way ANOVA. B) CD34 mRNA expression in KU812 after CBD treatment for 8 and 12 hours, was evaluated by qRT-PCR. mRNA levels were normalized for GAPDH expression. Data are expressed as fold mean ± SD of three separate experiments. **p < 0.005 vs vehicle-treated cells.*

Another protein essential for myeloid cell development is PU.1 [160]. By western blot analysis and confocal microscopy, we demonstrated that CBD treatment markedly increases the expression of PU.1 in CML cells showing that the cell proliferation inhibition and cell cycle blockage are associated with enhancement in CML cell maturation (Figures 37 and 38).

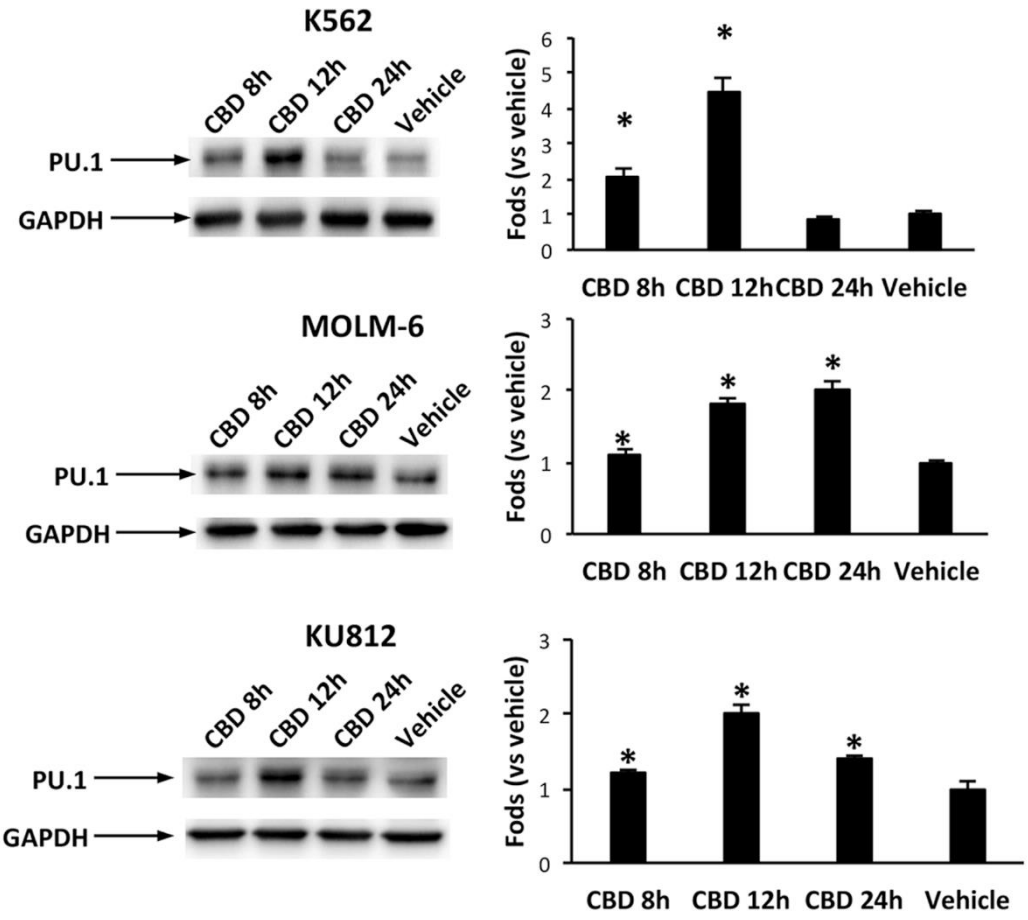

Figure 37. CBD treatment in CML increases the levels of PU.1 involved in cell differentiation. *Western blot analysis of PU.1 in CML cells treated with CBD at IC_{50} dose or vehicle for different times. Blots are representative of one of three separate experiments. Statistical analysis of the PU.1 densitometric values normalized to GAPDH levels used as loading control. Folds represent changes respect to vehicle-treated cells (=1). Data are the mean ± SD of three different experiments. *p < 0.05 vs vehicle-treated cells.*

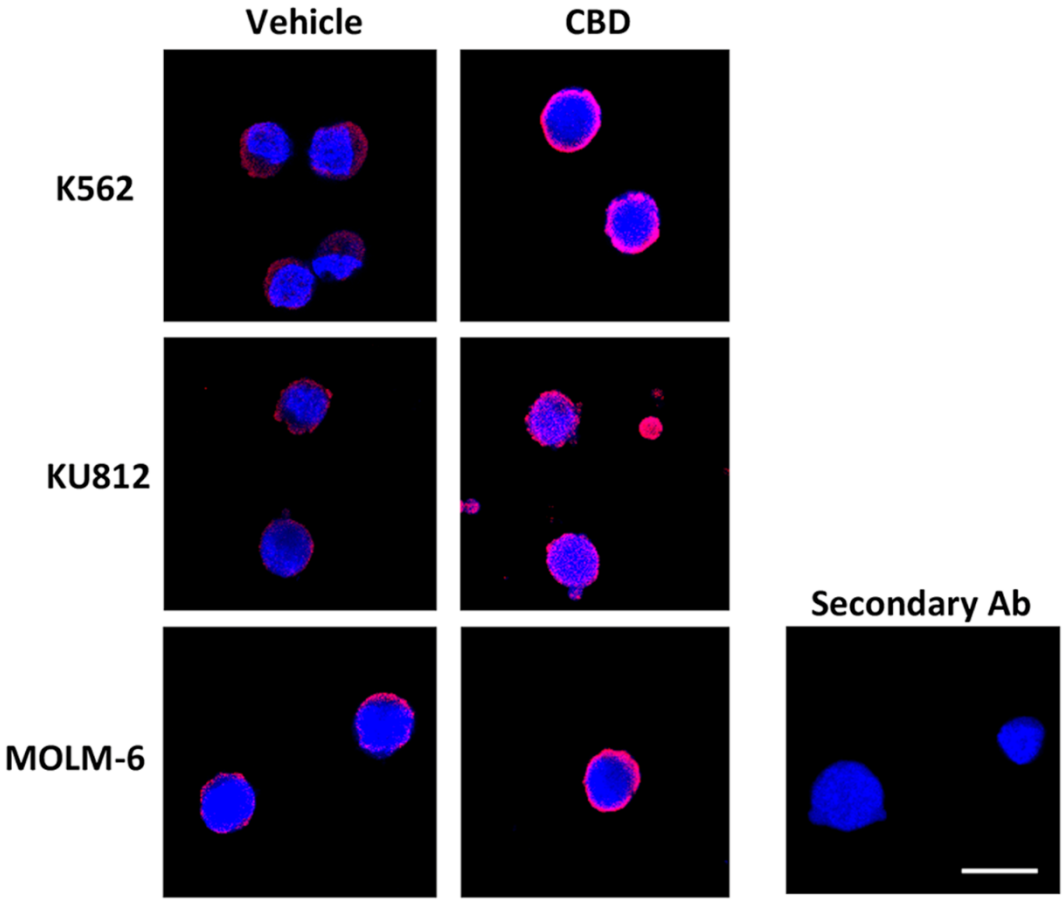

Figure 38. Confocal analysis of PU.1 expression after CBD treatment. *PU.1 protein expression level was also evaluated by confocal microscopy by using specific anti-PU.1 Ab. Images are representative of three separate experiments. Magnification= 100X. Bar= 20 µm.*

The ability of CBD to stimulate a more differentiated cellular state in CML cells was also evaluated by using colony forming assay useful to test the clonogenic activity of undifferentiated cells [161]. Our results demonstrated that CBD strongly reduces the ability to form colonies in all CML cell lines (Figure 39 A and B).

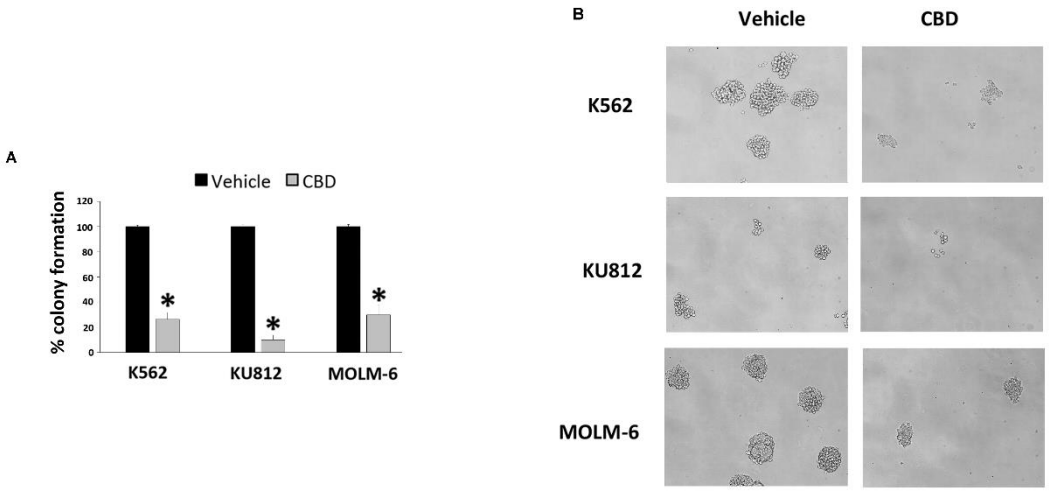

Figure 39. Colony formation assay analysis after CBD treatment. *A) Colony formation assay was performed in CML cells treated with CBD (IC50 dose) for 24h and then plated in Methocult for 10 days. Data are the mean ± SD of three different experiments. *p<0.05 vs vehicle-treated cells. B) Representative images of the colony formation in CML cells treated as above described by inverted microscope. Magnification=10X.*

CBD treatment modulates expression of CD274 gene in CML lines

Given that autophagy can modulate the expression of immune-check point [162], in particular we focused the attention on CD274 (PD-L1) gene expression. As reported in Figure 40 A, CD274 is barely expressed in CML cells respect to THP-1 ($p<0.0001$), and, among them, only in KU812 cell line is consistent ($p<0.0001$). After the treatment with CBD, we evaluated the modulation of CD274 gene in CML cells after 8 and 12h treatment via qRT-PCR. Our preliminary results show that CBD treatment in KU812 increase the expression of CD274 after 8h, which then decrease after 12h, whereas in K562 and MOLM6 the CD274 mRNA expression is barely the same respect to the vehicle (Figure 40 B).

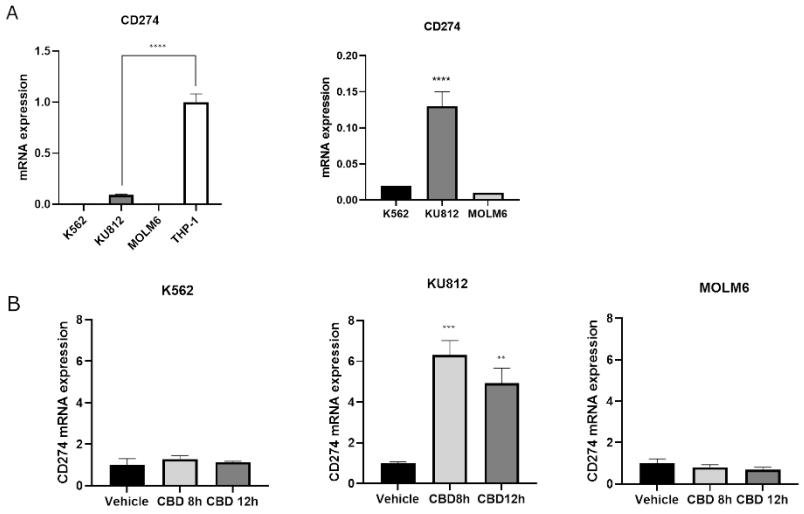

Figure 40. Expression of CD274 in CML. *A) CD274 mRNA expression was evaluated by qRT-PCR in CML cell lines. mRNA levels were normalized for GAPDH expression. Data are expressed as fold mean ± SD of three separate experiments. *p < 0.0001 vs THP-1. B) CD274 mRNA expression in CML after CBD treatment for 8 and 12 hours, was evaluated by qRT-PCR. mRNA levels were normalized for GAPDH expression. Data are expressed as fold mean ± SD of three separate experiments. ***p<0.001; **p < 0.005 vs vehicle-treated cells.*

CBD synergizes with imatinib in reducing cell viability in CML cell lines

Currently, the standard therapy of CML consist of TKI inhibitors such as imatinib. We evaluated the possible synergism between CBD and imatinib in the three CML cell lines. Cells were exposed to various concentrations of CBD and imatinib for 24 h. The administrations were performed in sequential and in combined protocol.

For the sequential administration, cells were treated for 24h with the proper IC_{50} dose of CBD or vehicle, followed by 24h of treatment with different doses of imatinib (5 nM - 2.5 µM). Cell viability were analyzed with Tripan blue exclusion assay. As reported in Figure 41, the sequential administration is not effective respect to the imatinib alone.

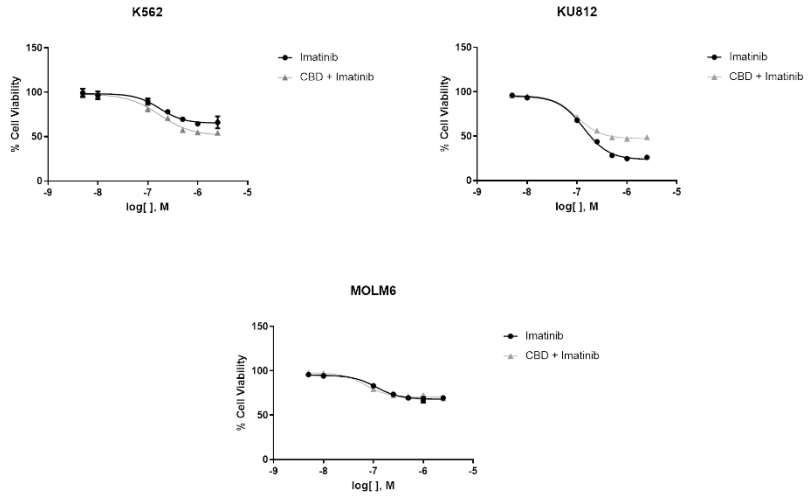

Figure 41. CBD and imatinib sequential administration do not affected cell viability respect to Imatinib alone. *Tripan blue Exclusion assay was used to evaluate cell growth in CML cells treated with CBD at IC_{50} dose for 24h and imatinib at different doses for other 24 h. Data are the mean ± SD of three different experiments.*

Since the sequential administration did not ameliorate the effect of imatinib, we proceed with a combined administration. To date, cells were treated for 24h with different doses of CBD at IC_{50} and Imatinib (10 nM – 1 µM).

The isobologram analysis was performed, and results showed that several combinations of the two drugs induce increased levels of cytotoxicity, as compared with single treatments with either CBD or imatinib alone (Figure 42 A). The CI values obtained by combining the CBD at IC_{50} dose with all the doses of imatinib are <1 indicating from slight to moderate synergistic effects (Figure 42 B).

A

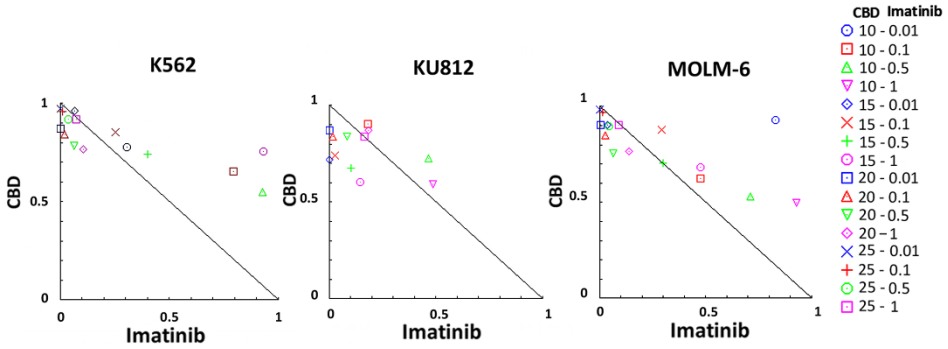

B

K562

CBD (µM)	Imatinib (µM)	CI
10	0.01	1.08
10	0.1	1.45
10	0.5	1.48
10	1	1.94
15	0.01	1.03
15	0.1	1.11
15	0.5	1.14
15	1	1.68
20	0.01	0.87
20	0.1	0.86
20	0.5	0.84
20	1	0.87
25	0.01	0.97
25	0.1	0.96
25	0.5	0.95
25	1	0.99

KU812

CBD (µM)	Imatinib (µM)	CI
10	0.01	1.06
10	0.1	1.08
10	0.5	1.19
10	1	1.07
15	0.01	0.72
15	0.1	0.77
15	0.5	0.78
15	1	0.75
20	0.01	0.87
20	0.1	0.85
20	0.5	0.92
20	1	1.05
25	0.01	1.01
25	0.1	1.11
25	0.5	1.13
25	1	1

MOLM-6

CBD (µM)	Imatinib (µM)	CI
10	0.01	1.76
10	0.1	1.1
10	0.5	1.24
10	1	1.42
15	0.01	0.94
15	0.1	1.16
15	0.5	1
15	1	1.15
20	0.01	0.9
20	0.1	0.87
20	0.5	0.81
20	1	0.9
25	0.01	0.98
25	0.1	0.98
25	0.5	0.93
25	1	0.99

Figure 42. The combination between CBD and imatinib synergism. *A) Isobologram plots for combination treatments of CBD and imatinib in CML cell lines. On the lower left of the hypotenuse synergism, on the hypotenuse additive effect, and on the upper right of the hypotenuse antagonism. Data are representative of three separate experiments. B) CI values for the CBD-imatinib combination assessed by CompuSyn software. CI = 1, <1 and >1 indicates additive effect, synergism and antagonism, respectively. Data are representative of three separate experiments.*

The fraction affected for these selected combinations is between 0.45 and 0.65. In fact, the percentage of cell growth was markedly reduced when imatinib, even at

the lowest dose, is combined with CBD at IC_{50} dose (Figure 43 A). To strengthen these data, we also performed cell viability assay in K562 cells resistant to imatinib (K562 IR) treated with different doses of CBD for 24h. Firstly, we confirmed the acquisition of the resistant phenotype by comparing cell viability between K562 IR and the normal K562 cells treated with different doses of imatinib (Fig. 43 B). Then, as shown in Figure 43 C, we found that CBD treatment also inhibits cell growth in this resistant cell model.

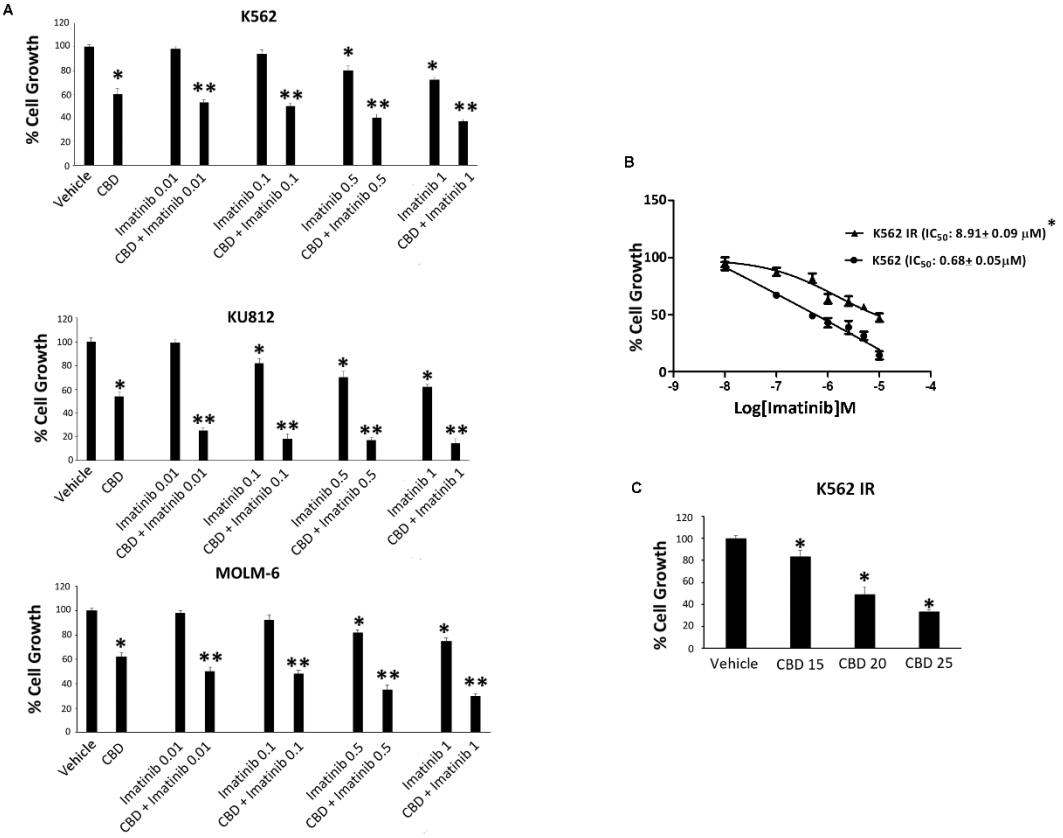

Figure 43. CBD and imatinib combination induce cell growth reduction even in K562 IR. A) Cell viability assay in CML cells treated with CBD at IC50 dose and imatinib at different doses for 24h. Data are the mean ± SD of three different experiments. *p<0.01 vs vehicle; **p < 0.01 vs CBD or imatinib. B) Cell viability assay performed in K562 resistant to imatininb (K562 IR) or K562 cells treated with different dose of imatinib or vehicle. *p<0.01 vs K562 cells. C) Cell viability assay in K562 IR treated with CBD at IC50 doses for 24h. Data are the mean ± SD of three different experiments. *p<0.01 vs vehicle.

These results support the hypothesis that CBD could represent a new potential adjuvant in the treatment of CML and TRPV2 a potential new molecular target.

PART II: TRPV1

TRPV1 agonist induces cell growth inhibition in CML cell lines

CPS and OLDA are TRPV1 agonists [81,163]. In order to evaluate their effects on CML, a cell viability assay was performed. CML cells were treated with different doses of OLDA (0.5 - 100 µM) and CPS (10 - 300 µM) for 24 h and cell viability was analyzed by Tripan blue exclusion assay. High resistance was shown for CPS with IC_{50} of 140.1 µM (K562), 129.8 µM (KU812) and 173.8 µM (MOLM-6) (Figure 44 A); whereas OLDA induced a significant decrease of cell viability with an IC_{50} of 14.1 µM (K562), 1.4 µM (KU812) and 8.4 µM (MOLM-6) (Figure 44 B). 10 and 20 µM doses of OLDA were used for the subsequent experiments.

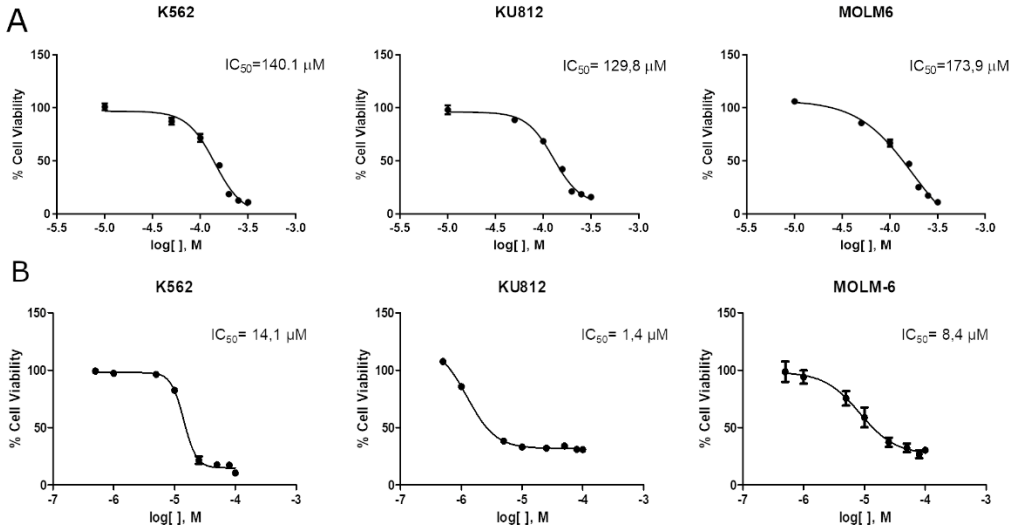

Figure 44. CPS and OLDA treatments reduce cell viability in CML cells. *A) Tripan blue exclusion assay was performed in CML cells treated for 24 h with different doses of CPS. IC_{50} values were analyzed by GraphPad software. Data are the mean ± SD of three different experiments. B) Tripan blue exclusion assay was performed in CML cells treated for 24 h with different doses of OLDA. IC_{50} values were analyzed by GraphPad software. Data are the mean ± SD of three different experiments.*

OLDA induces cell death

To better investigate the reduction in cell viability induced by OLDA, we decided to evaluate cell death by using PI. Cytofluorimetric analysis, performed in CML cells treated for 24h with OLDA and stained with PI (Figure 45 A), demonstrated that OLDA is able to markedly stimulate cell death especially when used at 20 µM ($p<0.0001$) in all CML cell lines. In fact, the treatment with OLDA induced a progressive increase in the red fluorescence measured with the MFI and in the percentage of PI positive cells (Figure 45 B).

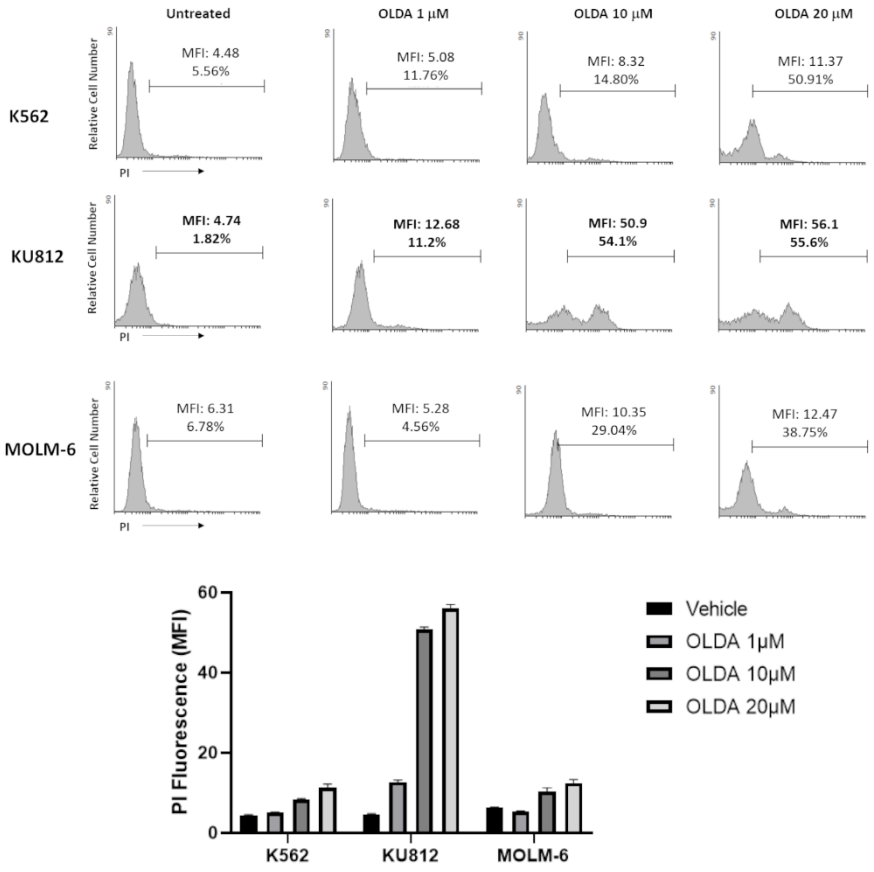

Figure 45. OLDA induce cell death in CML cells. *A) Cell death was assessed by PI staining and cytofluorimetric analysis in CML cells treated with OLDA at 1, 10, 20 µM dose or with vehicle used as control for 24 h. Data are representative of three separate experiments. MFI= Mean Fluorescence Intensity. B) Statistical analysis of the MFI values found in OLDA- or vehicle-treated CML cells for 24 h after PI staining. Data are the mean ± SD of three different experiments. ****p<0.0001 vs vehicle-treated cells.*

OLDA treatment stimulates ROS production.

Given that TRPV1 receptor is a cation channel able to enhance free intracellular calcium concentration strictly connected with ROS increase and cell death [164], we then investigated the ability of OLDA treatment to promote ROS production in CML cell lines. To this aim, cells were treated for 6 h with OLDA 10 µM and then ROS level was assessed by cytofluorimetric analysis. Our data showed that OLDA is able to markedly increase the production of ROS (Figure 46 A) as shown by the enhancement of the MFI values in OLDA- respect to vehicle-treated cells (Figure 46 B).

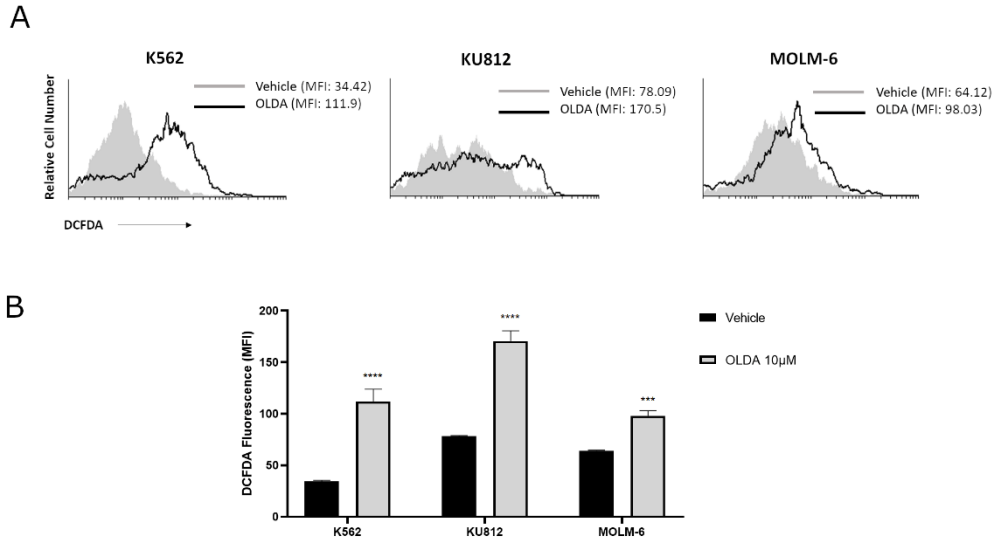

Figure 46. ROS level assessment through cytofluorimetric analysis. *A) Cytofluorimetric analysis was performed to evaluate the ROS production in CML cells treated for 6h with OLDA at 10 µM dose or vehicle. Data are representative of one of three separate experiments. MFI= Mean Fluorescence Intensity. B) Statistical analysis of the MFI values found in OLDA- or vehicle-treated CML cells for 6h after DCFDA staining. Data are the mean ± SD of three different experiments. ****p<0.0001; ***p<0.005 vs vehicle-treated cells.*

ROS production induced by OLDA treatment is associated with DNA damage and cell death.

ROS overload is responsible for the induction of the DNA damage response. To assess if the oxidative stress induced by OLDA leads to DNA damage, we performed western blot analysis in CML treated cells to detect the phosphorylation of γH2AX associated with DNA double strand breaks.

Our data clearly showed that OLDA is able to induce a strong enhancement in the phosphorylated form of γH2AX respect to vehicle ($p<0.0001$) indicating that the oxidative stress promoted by OLDA is responsible for DNA damage (Figure 47).

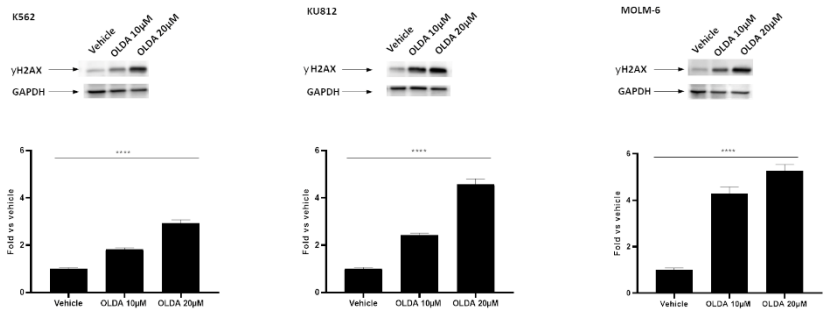

Figure 47. γH2AX and GAPDH expression in the three cell lines treated with OLDA for 24h. *Western blot analysis of γH2AX in CML cells treated with OLDA at 10 and 20μM dose or vehicle for 24h. Blots are representative of one of three separate experiments. Statistical analysis of the γH2AX densitometric values normalized to GAPDH levels used as loading control. Folds represent changes respect to vehicle-treated cells (=1). Data are the mean ± SD of three different experiments. ****p < 0.0001 vs vehicle-treated cells.*

Given that apoptosis is a secondary response to DNA damage [165], we investigated if apoptosis is the mechanism of cell death induced by OLDA in CML. CML cells were treated for 24h with OLDA at doses 10 and 20μM. Results has shown that

there is the presence of cleaved caspase 3 fragment in OLDA respected vehicle-treated cells (Figure 48) corroborating the apoptosis cell death.

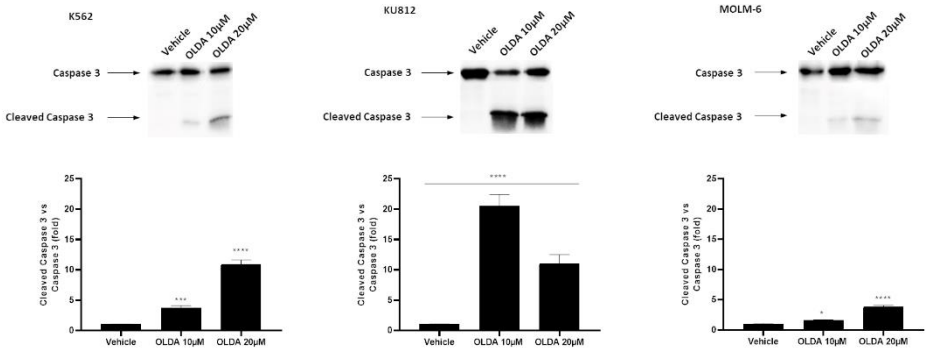

Figure 48. Caspase 3 cleavage in CML cell lines treated with OLDA for 24h. *Western blot analysis of Caspase 3 in CML cells treated with OLDA at 10 and 20μM dose or vehicle for 24h. Blots are representative of one of three separate experiments. Statistical analysis of the cleaved caspase 3 densitometry values normalized to uncleaved caspase 3 levels. Folds represent changes respect to vehicle-treated cells (=1). Data are the mean ± SD of three different experiments. *p<0.02; ***p<0.001; ****p < 0.0001 vs vehicle-treated cells.*

OLDA induces ER stress in CML cells

Alteration in the genome integrity has been associated with disruption of the endoplasmic reticulum (ER) proteostasis [166]. Indeed, production of ROS has been linked to ER stress and the Unfolding Protein Response (UPR) [167]. As described above, CML cells were treated with OLDA for 24h and then an immunoblot was performed, and the expression of two ER stress marker were investigated. BiP, also known as GRP78 or HSPA5, is a major ER chaperone protein important for ER protein quality control, and it is considered the master regulator of the UPR [168]. The degradation in endoplasmatic reticulum protein 1 (Derlin 1) is a component of the endoplasmatic reticulum-associated degradation (ERAD) system for misfolded luminal proteins, and it is involved in the retrotraslocation of specific misfolded proteins into the cytosol leading them to the proteasome degradation system [169]. BiP expression increase in all CML lines respect to the vehicle ($p<0.0001$) after 24h and with both OLDA treatments, whereas Derlin 1 is overexpressed in K562 ($p<0.001$) and KU812 ($p<0.001$) with 20µM dose and in MOLM-6 ($p<0.001$) with the 10µM dose with respect to the vehicle (Figure 49). Altogether, these results confirm the induction of the ER stress response by OLDA treatment.

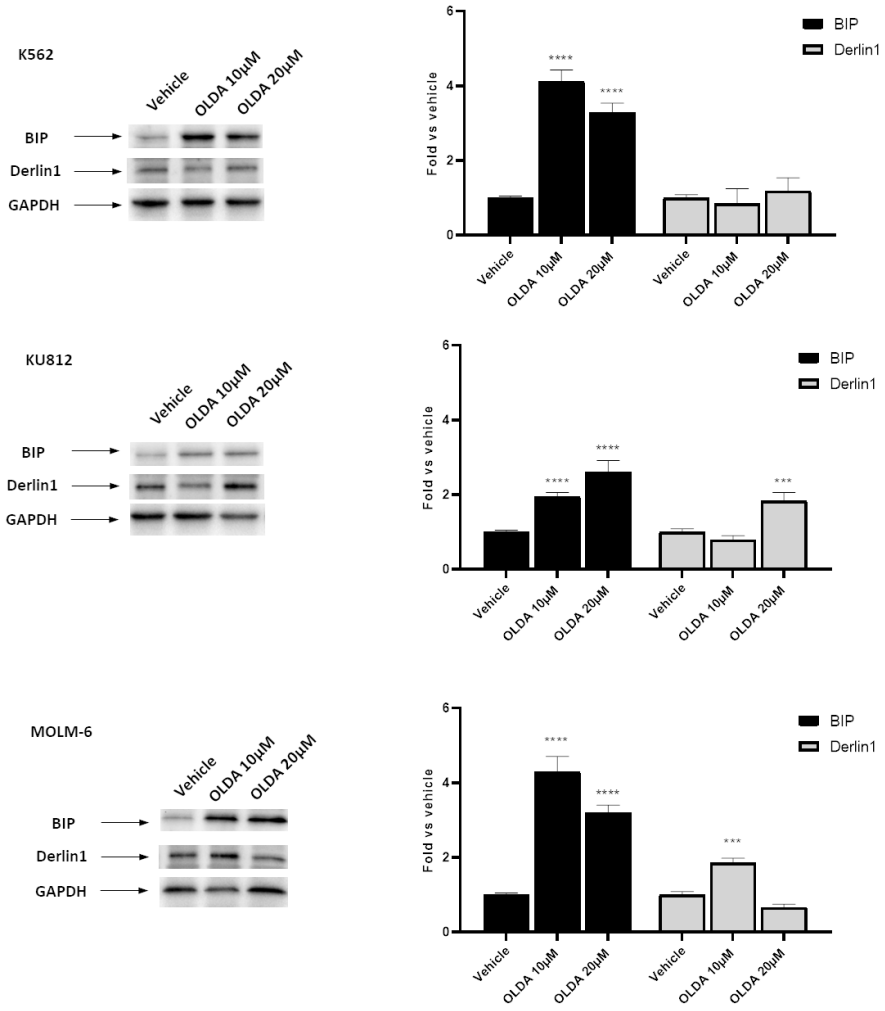

Figure 49. ER stress proteins expression in CML cell lines treated with OLDA for 24h. *Western blot analysis of BiP and Derlin 1 proteins in CML cells treated with OLDA at 10 and 20μM dose or vehicle for 24h. Blots are representative of one of three separate experiments. Statistical analysis of the BIP and Derlin1 protein densitometry values normalized to GAPDH levels. Folds represent changes respect to vehicle-treated cells (=1). Data are the mean ± SD of three different experiments. ***p<0.001; ****p < 0.0001 vs vehicle-treated cells.*

Discussion

CML is a myeloproliferative disorder originating from an incomplete differentiation process of hematopoietic progenitors to adult cells with consequent accumulation of immature ones in the bone marrow and in the peripheral blood.

Although successful results were obtained with the introduction of TKI inhibitors in therapy, several patients show or develop during time TKI resistance causing a reduction in survival expectancy [170,171]. Thus, the discovery of new anti-cancer compounds to be included in the clinical use and the identification of potential new drug targets represent an interesting challenge and a motivated goal.

It is known that TRPV1 and TRPV2 channels are expressed in normal immune cells [172,173] and in some leukemia cell lines [53,72,147,174].

Bioinformatic analysis provides other essential information's regarding their regulation during the normal differentiation, and during the evolution of the CML disease. From our analysis, during normal hematopoiesis and differentiation, both TRPV1 and TRPV2 channels are modulated. In particular, TRPV1 is expressed in less amount respect to TRPV2, and both decrease in expression with progenitor's differentiation. Since the block in differentiation, which occurs during the CML onset, interests the myeloid progenitors, we investigated if TRPV1 and TRPV2 expression could vary during the disease progression. Interestingly, the expression of these two Ca^{2+} channels show an opposite trend, indeed TRPV1 expression declines during the progression of CML, especially in the accelerated phase, in all the three progenitors; whereas TRPV2 expression rise during CML evolution, specifically during the accelerated phase. It is already assessed that TRPV2 can be implicated in many functions of immune cells such as phagocytosis, degranulation, chemotaxis, cytokine secretion and proliferation, and in cancer it can drive the tumorogenesis in various type of tumors, sustaining their fast growth [175,176]. Little is known about the TRPV2 role in the

leukemogenesis, even though an oncogenic function related to its involvement in cell proliferation has been suggested [53]. In opposite direction, in cancer the TRPV1 expression has been demonstrated to be linked to apoptosis cell death and suppression of cell proliferation [177].

Our analyses demonstrate that TRPV2 seem to be overexpressed in order to support the huge cancer cell proliferation which occurred during the accelerated phase of CML, whereas TRPV1 seems to be down regulated in order to avoid cell death. Moreover, our data confirm the expression of both receptors in the three CML cell lines used, in common myeloid progenitors and normal myeloid cells suggesting the importance of TRPV channels in the modulation of blood cells activities. Although TRPV2 expression is higher in K562 respect to KU812 and MOLM-6 cells, the ability of CBD to inhibit cell growth is very similar among the three CML lines. It is well known that mRNA and protein expression levels are not enough to suppose differences in the TRPV functionality. In fact, the status of activation of TRPV2 can be influenced by several post-translational modifications such as glycosylation, phosphorylation and binding with lipids [178].

CBD is one of the phytochemicals extracted from Cannabis sativa whose use as herbal medicine dates back to 500 BC [94]. It displays several effects such as anti-inflammatory, antioxidant, analgesic, anxiolytic, anticonvulsive and neuroprotective. Moreover, it is now well accepted that CBD can be also considered a promising anti-cancer drug alone or in combinations with conventional chemotherapies. In fact, several findings demonstrated that CBD is able to induce cell death, inhibit cell migration *in vitro*, decrease tumor size and vascularization in glioma models [91,94,179]. Moreover, similar interesting results have been obtained in other cancer types [94].

Few data on CBD-mediated effects in leukemia and lymphoma have been provided [170,171,180–182] and no findings are present about the role of TRPV2 in CBD-induced effects on CML cells. Our data showed that CBD, by activating TRPV2, induces

calcium influx, ROS production, cell cycle arrest, cell proliferation blockage, mitophagy and changes in the expression of differentiation markers in different CML cell lines.

Although CBD belongs to the family of phytocannabinoids able to bind the CB1 and CB2 receptors, controversial data are present about its ability to bind them. The idea that CBD has no affinity for these receptors and at most, based on *in vitro* studies, can have a weak antagonistic effect, is gaining strength [89]. Instead, it has been well accepted that it functions as an agonist for TRPV1 and TRPV2 receptor [148,149].

Interestingly, we demonstrated that CBD, used at the IC_{50} dose, induces inhibition of cell proliferation and blockage of cell cycle by activating only the TRPV2 receptor. These results are also supported by previous conclusions in glioma cells indicating that the CBD-induced effects are TRPV2-dependent [149] enforcing the role of this receptor in the signaling pathways activated by CBD.

We showed for the first time that the inhibition of cell proliferation in cells treated with CBD is TRPV2 dependent, and is associated with activation of mitophagy and mitochondrial mass reduction in CML cell lines. The ability of CBD to cause mitochondrial damage was also recently investigated in Jurkat cells [88] and, in addition, CBD has been found to interact directly with freshly isolated mitochondria to promote organelle dysfunction [88]. Here we demonstrated that CBD stimulates, via TRPV2, calcium overload and oxidative stress strongly leading to the mitochondrial dysfunction [153]. Mitochondria dynamics is essential to regulate cellular metabolism, ATP production and redox homeostasis [118]. It has been found that the number of mitochondria, the total mitochondrial mass, bioenergetics, biogenesis, membrane potential and ROS are increased in chronic lymphatic leukemia respect to normal naïve B lymphocytes suggesting the importance of mitochondria to fulfill the energy requirements [183]. Moreover, the targeting of mitochondrial metabolic enzymes could represent an effective therapeutic strategy to target acute myeloid leukemia cells, given that they have higher copy number of mitochondrial DNA, more mitochondria and increased

oxygen consumption compared with normal HSC [184]. Finally, the upregulation of mitochondrial key proteins and the influence of the mitochondrial mass are responsible for the promotion of drug resistance in Hodking lymphoma [185]. Thus, our data show that the CBD treatment, via TRPV2, induces mitochondria dysfunction, and promotes the elimination of unfunctional mitochondria by mitophagy. These two aspects meet the overall need to use therapies leniting exaggerated mitochondrial activity in leukemia [118].

Depolarization of potential mitochondrial membrane, as we detected in CBD-treated CML cells, is the essential requirement for mitophagy. Mitophagy, a specialized form of macro autophagy characterized by the engulfment of dysfunctional mitochondria, is a quality control mechanism for the recognition and selective removal of damaged mitochondria [155,182]. Proteins of the ATG family such as LC3, ATG5 and ATG12 are involved in the regulation of autophagy by participating in the formation of autophagosomes. LC3, localized in the cytosol, during autophagy is conjugated with phosphatidylethanolamine and this lipidated form, known as LC3-II, is placed within the autophagosomal membrane [186]. In addition, ATG5 forms a complex with ATG12 and ATG16-L1 at the membrane of the developing autophagosome [187]. In our study, the CBD treatment, via TRPV2, markedly increased the expression of the LC3-II, indicating the activation of autophagy. Moreover, our data showed enhancement in the expression of ATG16-L1 and the complex ATG5-ATG12 strongly supporting the stimulation of the autophagic machinery. These results are in agreement with previous findings demonstrating the upregulation of LC3-II, ATG5 and ATG12 after inducing photodamages in mitochondria [188]. In addition, during mitophagy pink1 expression is increased and it accumulates on the depolarized mitochondria facilitating the recruitment of parkin. The pink1 and parkin upregulation and accumulation are essential to promote mitophagy so much that their mutations are associated with the pathological accumulation of damaged mitochondria [189]. Mitophagy is also regulated by the autophagic receptor optineurin that, with its ubiquitin-binding domain, binds polyubiquitinated damaged mitochondria to

selectively promote their elimination. Optineurin expression enhances LC3 recruitment and stimulates the degradation of damaged mitochondria by increasing autophagic engulfment [160]. In a similar way, we demonstrated that CBD treatment is able to enhance the expression of pink1, parkin and optineurin indicating the selectively removal of depolarized mitochondria.

Given that mitophagy is responsible for the mitochondrial turn over and homeostasis, it is also found to be involved in the regulation of stem cell survival and cell differentiation [190]. Although findings suggest that mitophagy plays an important role in the maintenance of stem cell populations in cancer including leukemia [191], it is also well accepted that mitophagy also participates in the cellular differentiation. At this regard, it is implicated in maturation of erythrocytes and primitive myoblasts [190]. In line with these results, we showed that the inhibition of cell proliferation, and the stimulation of mitophagy induced by CBD in CML cells, are associated with changes in differentiation markers. We found a reduction of the stem associated marker OCT-4 and CD34 levels, and a counteract enhancement of PU.1 differentiation marker. OCT-4 is a transcription factor, involved leukemogenesis and in the induction of cell differentiation arrest, found to be overexpressed in acute myeloid leukemia [192]. CD34 is a transmembrane phosphoglycoprotein which identify hematopoietic stem and progenitor cells, and it is considered an independent prognostic factor in AML [193]. PU.1 is considered a master myeloid regulator because it stimulates myeloid differentiation and inhibits cell growth [194]. We found a reduction of the stem-associated marker OCT-4 and CD34 levels and the enhancement of PU.1 suggesting that CBD drives, through mitochondrial damages, CML cells to a more differentiated state. This was also confirmed by colony formation assay that demonstrated the ability of CBD treatment to markedly reduce the clonogenic activity of CML cells.

In addition to them, autophagy can regulate the expression of immune-check point [124,128,162], and our preliminary data show that the expression of CD274 (PD-L1) can be modulated at genetic levels increasing its expression in KU812 after

treatment with CBD, whereas in K562 and MOLM6 the genetic changes are barely perceptible. This could come in help as novel approaches with combined immune-target therapies, increasing their clinical effects [195–199].

The presence of poorly differentiated cells is strongly associated with the acquisition of chemoresistance, and even worse prognosis. TKI resistance develops due to secondary BCR-ABL mutations and/or BCR-ABL independent mechanism including the activation of signaling pathway able to sustain the growth of progenitors [200]. Given that several studies suggest that TKI treatment, surprisingly, induces stemness gene expression in CML cells, and that it might be involved in residual disease [201]. This highlights the need to develop new-targeted therapies that could overcome these stemness-promoting effects. Among possible strategies to overcome chemotherapy and TKI resistance, CD274 expression could help clinicians to overcome therapy resistance [202,203]. It is already aware that expression of CD274 in cancer correlates with worse prognosis, relapses and immune system escape [197]. However, recent studies have demonstrated that CD274 is involved in multiple cellular pathways which lead to TKI resistance [202], thus where CD274 is highly expressed, TKIs have better therapeutic effects [204]. Our cells express low amount of CD274 respect to spontaneously immortalized monocyte-like cell line THP-1 [205], used as calibrator, and are in agreement with the fact that CD274 expression is low in HSC and increase during cell maturation [206]. Thus, our preliminary data demonstrate that there is a correlation between higher expression of CD274 and higher efficacy of imatinib. In fact, KU812 cells are more sensible to imatinib respect to K562 and MOLM6, and in combination with CBD, imatinib treatment exert a powerful cytotoxicity effect respect to the other cell lines. Our results, showing a synergistic effect by combining CBD with imatinib, represent a promising resource to ameliorate the effectiveness of TKIs.

CPS is well known as the active compound of chili peppers, and is responsible for the usual burn and pungent sensation given by TRPV1 channel activation. It is widely used as analgesic since is able to donate temporary relief modulating the

pains transmission [207]. Furthermore, its role as anti-cancer compound in many types of tumors has grown over decades [208]. OLDA has first discovered in bovine striatal extract and is an endogenous compound in the mammalian brain which activate selectively TRPV1 [97]. It has been used mainly in the modulation of synaptic transmission in the spinal cord and in nocifensive behavior studies [95,97,209], however its role as anticancer compound is not still prove. Our preliminary results show that K562, KU812 and MOLM6 are more sensible to OLDA respect to CPS. TRPV1 channel is able to boost free intracellular Ca^{2+} concentration, which has been strictly connected with ROS increase and cell death [164]. ROS generation is supposed to cause DNA damage and phosphorylation of γH2AX. Growing evidences suggest that γH2AX phosphorylation is not only a DNA damage marker, but also plays an important role in the regulation of cell death [210]. Our data showed that treatment with OLDA enhance markedly ROS overload causing a significant increase in phosphorylated γH2AX form triggering the apoptosis cell death.

The excessive production of ROS can cause the disruption of protein homeostasis in the ER, leading to the accumulation of misfolded proteins. This accumulation, perturbating the ER homeostasis, activate the UPR machinery which alters the expression of many genes involved in ER quality control [211]. The UPR consists in a complex network of interconnected signaling pathways. In physiological condition, the three ER stress sensors (IRE1α, PERK and ATF6α) are bound to the the ER chaperone BiP and are inhibited. When ER stress occurs, BiP dissociate from the ER stress sensors, then is sequester by the misfolded peptides, and the three sensors are released starting the UPR signal transduction with the aim to restore protein homeostasis [211]. When ER stress is prolonged and misfolded proteins start to aggregate and accumulate, the endoplasmatic reticulum-associated degradation (ERAD) is activated. Among ERAD pathway, there is a particular family of proteins implicated in the retrotraslocation of specific misfolded proteins. This family is the Derlin family that is composed by Derlin 1, 2 and 3 and they mediate the degradation of misfolded luminal proteins within ER. The misfolded protein is retrotraslocated in the cytosol where complexes transiently with BiP and enters in

the ubiquitin-proteasome pathway [212–215]. Our data, in agreement with previous findings, demonstrate that with the OLDA treatment there is an increase expression of BiP and Derlin1 proteins confirming the ER stress activation. More investigations are required to better clarify the involvement of TRPV1 channel and OLDA effects on CML cell lines, but our preliminary data suggests that CML cells are more sensible to OLDA respect to CPS, moreover OLDA, through the activation of TRPV1, induce cell death via ROS production, ER stress and DNA damages.

Conclusion

Overall, our study demonstrated that TRPV1 and TRPV2 are modulated during normal hematopoiesis and during the progression of CML cancer. In particular, the activation of the TRPV2 channel, by treatment with the natural compound CBD, induces cell proliferation arrest, mitochondrial impairment, removal by mitophagy of damaged mitochondria and reduction in the stemness-related markers OCT-4 and CD34 in CML cells. Even more interesting, our results also highlighted the ability of CBD to act synergistically with imatinib. This supports the interesting chance to modulate TRPV2 activity to enhance conventional therapy and improve the prognosis of patients. Therefore, a better awareness of the TRP-dependent autophagy process and a subsequent interest in the network between immunosuppressive molecules expression and autophagy, will allow the acquisition of information useful to improve therapeutic efficacy and to discover new possible therapeutic targets for further pharmacological treatments both as adjuvants and as new healings.

Even if preliminary data, for the first time we demonstrated the anticancer effects of OLDA on TRPV1 through the DNA damage and oxidative stress induction. More investigations are required to better clarify the involvement of TRPV1 using specific TRPV1 antagonists and gene silencing.

In conclusion, these findings represent a strong support and stimulate the interest in further efforts to go on in this research field by using patient samples.

Bibliography

1. Keykhaei, M. *et al.* A global, regional, and national survey on burden and Quality of Care Index (QCI) of hematologic malignancies; global burden of disease systematic analysis 1990-2017. *Experimental hematology & oncology* **10**, 11 (2021).
2. Arber, D. A. *et al.* The 2016 revision to the World Health Organization classification of myeloid neoplasms and acute leukemia. *Blood* **127**, 2391–2405 (2016).
3. Bray, F. *et al.* Global cancer statistics 2018: GLOBOCAN estimates of incidence and mortality worldwide for 36 cancers in 185 countries. *CA: A Cancer Journal for Clinicians* **68**, 394–424 (2018).
4. De Kouchkovsky, I. & Abdul-Hay, M. 'Acute myeloid leukemia: a comprehensive review and 2016 update.' *Blood Cancer Journal* **6**, e441–e441 (2016).
5. Ferrara, F., Lessi, F., Vitagliano, O., Birkenghi, E. & Rossi, G. Current Therapeutic Results and Treatment Options for Older Patients with Relapsed Acute Myeloid Leukemia. *Cancers* **11**, 224 (2019).
6. Riether, C., Schürch, C. M. & Ochsenbein, A. F. Regulation of hematopoietic and leukemic stem cells by the immune system. *Cell Death and Differentiation* vol. 22 187–198 (2015).
7. Tefferi, A. The history of myeloproliferative disorders: before and after Dameshek. *Leukemia* **22**, 3–13 (2008).
8. Westerweel, P. E., Te Boekhorst, P. A. W., Levin, M.-D. & Cornelissen, J. J. New Approaches and Treatment Combinations for the Management of Chronic Myeloid Leukemia. *Frontiers in oncology* **9**, 665 (2019).
9. Cortes, J. & Kantarjian, H. Chronic myeloid leukemia: sequencing of TKI therapies. *Hematology. American Society of Hematology. Education Program* **2016**, 164–169 (2016).
10. García-Gutiérrez, V. & Hernández-Boluda, J. C. Tyrosine Kinase Inhibitors Available for Chronic Myeloid Leukemia: Efficacy and Safety. *Frontiers in oncology* **9**, 603 (2019).
11. Harris, N. L. *et al.* The World Health Organization Classification of Neoplasms of the Hematopoietic and Lymphoid Tissues: Report of the Clinical Advisory Committee Meeting - Airlie House, Virginia, November, 1997. *Hematology Journal* **1**, 53–66 (2000).
12. Taylor, J., Xiao, W. & Abdel-Wahab, O. Diagnosis and classification of hematologic malignancies on the basis of genetics. *Blood* **130**, 410–423 (2017).
13. Carter, B. Z., Mak, D. H., Cortes, J. & Andreeff, M. The Elusive Chronic Myeloid Leukemia Stem Cell: Does It Matter and How Do We Eliminate It? *Seminars in Hematology* **47**, 362–370 (2010).
14. Hochhaus, A. *et al.* A novel BCR-ABL fusion gene (e6a2) in a patient with Philadelphia chromosome-negative chronic myelogenous leukemia. *Blood* **88**, 2236–40 (1996).

15. Cilloni, D. & Saglio, G. Molecular Pathways: BCR-ABL. *Clinical Cancer Research* **18**, 930–937 (2012).

16. Albano, F. *et al.* Gene expression profiling of chronic myeloid leukemia with variant t(9;22) reveals a different signature from cases with classic translocation. *Molecular Cancer* **12**, 36 (2013).

17. Nilius, B. TRP channels in disease. *Biochimica et Biophysica Acta (BBA) - Molecular Basis of Disease* **1772**, 805–812 (2007).

18. Zheng, J. Molecular Mechanism of TRP Channels. in *Comprehensive Physiology* vol. 3 221–242 (John Wiley & Sons, Inc., 2013).

19. Duan, J. *et al.* Structure of the mammalian TRPM7, a magnesium channel required during embryonic development. *Proceedings of the National Academy of Sciences* **115**, E8201–E8210 (2018).

20. Nilius, B. TRP channels in disease. *Biochimica et Biophysica Acta - Molecular Basis of Disease* **1772**, 805–812 (2007).

21. Montell, C. & Rubin, G. M. Molecular characterization of the drosophila trp locus: A putative integral membrane protein required for phototransduction. *Neuron* **2**, 1313–1323 (1989).

22. Ferrandiz-Huertas, C., Mathivanan, S., Wolf, C. J., Devesa, I. & Ferrer-Montiel, A. Trafficking of Thermo TRP channels. *Membranes* **4**, 525–564 (2014).

23. Méndez-Reséndiz, K. A. *et al.* Steroids and TRP Channels: A Close Relationship. *International Journal of Molecular Sciences* **21**, 3819 (2020).

24. Nagatomo, K. & Kubo, Y. Caffeine activates mouse TRPA1 channels but suppresses human TRPA1 channels. *Proceedings of the National Academy of Sciences* **105**, 17373–17378 (2008).

25. Talavera, K. *et al.* Nicotine activates the chemosensory cation channel TRPA1. *Nature Neuroscience* **12**, 1293–1299 (2009).

26. Bandell, M. *et al.* Noxious Cold Ion Channel TRPA1 Is Activated by Pungent Compounds and Bradykinin. *Neuron* **41**, 849–857 (2004).

27. Rubaiy, H. N. Treasure troves of pharmacological tools to study transient receptor potential canonical 1/4/5 channels. *British Journal of Pharmacology* **176**, 832–846 (2019).

28. Venkatachalam, K., Zheng, F. & Gill, D. L. Regulation of Canonical Transient Receptor Potential (TRPC) Channel Function by Diacylglycerol and Protein Kinase C. *Journal of Biological Chemistry* **278**, 29031–29040 (2003).

29. Leuner, K. *et al.* Hyperforin—a key constituent of St. John's wort specifically activates TRPC6 channels. *The FASEB Journal* **21**, 4101–4111 (2007).

30. Leuner, K. *et al.* Simple 2,4-Diacylphloroglucinols as Classic Transient Receptor Potential-6 Activators—Identification of a Novel Pharmacophore. *Molecular Pharmacology* **77**, 368–377 (2010).

31. García-Ávila, M. & Islas, L. D. What is new about mild temperature sensing? A review of recent findings. *Temperature* **6**, 132–141 (2019).

32. Kraft, R., Grimm, C., Frenzel, H. & Harteneck, C. Inhibition of TRPM2 cation channels by N -(p -amylcinnamoyl)anthranilic acid. *British Journal of Pharmacology* **148**, 264–273 (2006).

33. Hill, K., McNulty, S. & Randall, A. D. Inhibition of TRPM2 channels by the antifungal agents clotrimazole and econazole. *Naunyn-Schmiedeberg's Archives of Pharmacology* **370**, 227–237 (2004).

34. Hill, K., Benham, C. D., McNulty, S. & Randall, A. D. Flufenamic acid is a pH-dependent antagonist of TRPM2 channels. *Neuropharmacology* **47**, 450–460 (2004).

35. Malysz, J., Maxwell, S., Yarotskyy, V. & Petkov, G. V. Compound-dependent Effects of TRPM4 Channel Modulators on Guinea Pig Detrusor Smooth Muscle Excitability and Contractility. *The FASEB Journal* **33**, 837.4-837.4 (2019).

36. Takezawa, R. *et al.* A Pyrazole Derivative Potently Inhibits Lymphocyte Ca 2+ Influx and Cytokine Production by Facilitating Transient Receptor Potential Melastatin 4 Channel Activity. *Molecular Pharmacology* **69**, 1413–1420 (2006).

37. Wong, R., Turlova, E., Feng, Z.-P., Rutka, J. T. & Sun, H.-S. Activation of TRPM7 by naltriben enhances migration and invasion of glioblastoma cells. *Oncotarget* **8**, 11239–11248 (2017).

38. Saldanha, S. *et al.* Agonists of Transient Receptor Potential Channels 3 and 2 (TRPML3 & TRPML2). *Probe Reports from the NIH Molecular Libraries Program [Internet]* **2**, 1–21.

39. Plesch, E. *et al.* Selective agonist of TRPML2 reveals direct role in chemokine release from innate immune cells. *eLife* **7**, e39720 (2018).

40. Kaneko, Y. & Szallasi, A. Transient receptor potential (TRP) channels: a clinical perspective. *British Journal of Pharmacology* **171**, 2474–2507 (2014).

41. Chow, J., Norng, M., Zhang, J. & Chai, J. TRPV6 mediates capsaicin-induced apoptosis in gastric cancer cells--Mechanisms behind a possible new "hot" cancer treatment. *Biochimica et biophysica acta* **1773**, 565–576 (2007).

42. Gees, M., Colsoul, B. & Nilius, B. The Role of Transient Receptor Potential Cation Channels in Ca2+ Signaling. *Cold Spring Harbor Perspectives in Biology* **2**, a003962–a003962 (2010).

43. Lev, S. *et al.* Constitutive Activity of the Human TRPML2 Channel Induces Cell Degeneration. *Journal of Biological Chemistry* **285**, 2771–2782 (2010).

44. Dong, X. P., Wang, X. & Xu, H. TRP channels of intracellular membranes. *Journal of Neurochemistry* **113**, 313–328 (2010).

45. Caterina, M. J. & Pang, Z. TRP channels in skin biology and pathophysiology. *Pharmaceuticals* **9**, (2016).

46. Cui, C., Merritt, R., Fu, L. & Pan, Z. Targeting calcium signaling in cancer therapy. *Acta Pharmaceutica Sinica B* **7**, 3–17 (2017).

47. Smani, T., Shapovalov, G., Skryma, R., Prevarskaya, N. & Rosado, J. A. Functional and physiopathological implications of TRP channels. *Biochimica et Biophysica Acta - Molecular Cell Research* **1853**, 1772–1782 (2015).

48. Di Paola, S., Scotto-Rosato, A. & Medina, D. L. TRPML1: The Ca(2+)retaker of the lysosome. *Cell Calcium* **69**, 112–121 (2018).

49. Morelli, M. B. *et al.* Expression and function of the transient receptor potential ion channel family in the hematologic malignancies. *Current molecular pharmacology* **6**, 137–148 (2013).

50. Maggi, F. *et al.* Transient Receptor Potential (TRP) Channels in Haematological Malignancies: An Update. *Biomolecules* **11**, 765 (2021).

51. Cabanas, H. *et al.* Deregulation of calcium homeostasis in Bcr-Abl-dependent chronic myeloid leukemia. *Oncotarget* **9**, 26309–26327 (2018).

52. Takahashi, K. *et al.* TRPM7-mediated spontaneous Ca2+ entry regulates the proliferation and differentiation of human leukemia cell line K562. *Physiological Reports* **6**, 1–15 (2018).

53. Siveen, K. S. *et al.* Evaluation of cationic channel TRPV2 as a novel biomarker and therapeutic target in Leukemia-Implications concerning the resolution of pulmonary inflammation. *Scientific reports* **9**, 1554 (2019).

54. Yee, N. S. Role of TRPM7 in cancer: Potential as molecular biomarker and therapeutic target. *Pharmaceuticals* **10**, (2017).

55. Ong, H. L., de Souza, L. B. & Ambudkar, I. S. Role of TRPC Channels in Store-Operated Calcium Entry. in 87–109 (2016). doi:10.1007/978-3-319-26974-0_5.

56. Shim, A. H.-R., Tirado-Lee, L. & Prakriya, M. Structural and Functional Mechanisms of CRAC Channel Regulation. *Journal of Molecular Biology* **427**, 77–93 (2015).

57. Ambudkar, I. S., de Souza, L. B. & Ong, H. L. TRPC1, Orai1, and STIM1 in SOCE: Friends in tight spaces. *Cell Calcium* **63**, 33–39 (2017).

58. Kuang, C. *et al.* Knockdown of Transient Receptor Potential Canonical-1 Reduces the Proliferation and Migration of Endothelial Progenitor Cells. *Stem Cells and Development* **21**, 487–496 (2012).

59. Shapovalov, G., Ritaine, A., Skryma, R. & Prevarskaya, N. Role of TRP ion channels in cancer and tumorigenesis. *Seminars in Immunopathology* **38**, 357–369 (2016).

60. Santoni, G. & Farfariello, V. TRP channels and cancer: new targets for diagnosis and chemotherapy. *Endocrine, metabolic & immune disorders drug targets* **11**, 54–67 (2011).

61. Liberati, S., Morelli, M. B., Nabissi, M., Santoni, M. & Santoni, G. Oncogenic and anti-oncogenic effects of transient receptor potential channels. *Current topics in medicinal chemistry* **13**, 344–366 (2013).

62. Santoni, G. *et al.* Calcium Signaling and the Regulation of Chemosensitivity in Cancer Cells: Role of the Transient Receptor Potential Channels. in *Advances in Experimental Medicine and Biology* 505–517 (2020). doi:10.1007/978-3-030-12457-1_20.

63. Abdoul-Azize, S., Buquet, C., Vannier, J. P. & Dubus, I. Pyr3, a TRPC3 channel blocker, potentiates dexamethasone sensitivity and apoptosis in acute lymphoblastic leukemia cells by disturbing Ca 2+ signaling, mitochondrial membrane potential changes and reactive oxygen species production. *European Journal of Pharmacology* **784**, 90–98 (2016).

64. Gil-Kulik, P. *et al.* Different regulation of PARP1, PARP2, PARP3 and TRPM2 genes expression in acute myeloid leukemia cells. *BMC Cancer* **20**, 1–9 (2020).

65. Yang, S. *et al.* Leukemia cells remodel marrow adipocytes via TRPV4-dependent lipolysis. *Haematologica* haematol.2019.225763 (2019) doi:10.3324/haematol.2019.225763.

66. Debant, M. *et al.* STIM1 at the plasma membrane as a new target in progressive chronic lymphocytic leukemia. *Journal for ImmunoTherapy of Cancer* **7**, 1–13 (2019).

67. Hirai, A. *et al.* Expression of TRPM8 in human reactive lymphoid tissues and mature B-cell neoplasms. *Oncology Letters* **16**, 5930–5938 (2018).

68. Loo, S. K. *et al.* TRPM4 expression is associated with activated B cell subtype and poor survival in diffuse large B cell lymphoma. *Histopathology* **71**, 98–111 (2017).

69. Chatterton, Z. *et al.* Epigenetic deregulation in pediatric acute lymphoblastic leukemia. *Epigenetics* **9**, 459–467 (2014).

70. Almamun, M. *et al.* Integrated methylome and transcriptome analysis reveals novel regulatory elements in pediatric acute lymphoblastic leukemia. *Epigenetics* **10**, 882–890 (2015).

71. Chen, S. *et al.* Transient receptor potential ion channel TRPM2 promotes AML proliferation and survival through modulation of mitochondrial function, ROS, and autophagy. *Cell Death & Disease* **11**, 247 (2020).

72. Punzo, F. *et al.* Effects of CB2 and TRPV1 receptors' stimulation in pediatric acute T-lymphoblastic leukemia. *Oncotarget* **9**, 21244–21258 (2018).

73. Bowen, C. V *et al.* In vivo detection of human TRPV6-rich tumors with anti-cancer peptides derived from soricidin. *PloS one* **8**, e58866 (2013).

74. Bobkov, D. *et al.* Lipid raft integrity is required for human leukemia Jurkat T-cell migratory activity. *Biochimica et Biophysica Acta - Molecular and Cell Biology of Lipids* **1866**, 2–11 (2021).

75. Chen, B. *et al.* TRPM4-specific blocking antibody attenuates reperfusion injury in a rat model of stroke. *Pflügers Archiv - European Journal of Physiology* **471**, 1455–1466 (2019).

76. Samanta, A., Hughes, T. E. T. & Moiseenkova-Bell, V. Y. Transient Receptor Potential (TRP) Channels. *Sub-cellular biochemistry* **87**, 141–165 (2018).

77. Haustrate, A., Prevarskaya, N. & Lehen'kyi, V. Role of the TRPV Channels in the Endoplasmic Reticulum Calcium Homeostasis. *Cells* **9**, (2020).

78. Santoni, G., Maggi, F., Morelli, M. B., Santoni, M. & Marinelli, O. Transient Receptor Potential Cation Channels in Cancer Therapy. *Medical sciences (Basel, Switzerland)* **7**, (2019).

79. Kärki, T. & Tojkander, S. TRPV Protein Family-From Mechanosensing to Cancer Invasion. *Biomolecules* **11**, (2021).

80. Muller, C., Morales, P. & Reggio, P. H. Cannabinoid Ligands Targeting TRP Channels. *Frontiers in Molecular Neuroscience* **11**, 487 (2019).

81. Zhong, B. & Wang, D. H. N-oleoyldopamine, a novel endogenous capsaicin-like lipid, protects the heart against ischemia-reperfusion injury via activation of TRPV1. *American journal of physiology. Heart and circulatory physiology* **295**, H728-35 (2008).

82. Bujak, J. K., Kosmala, D., Majchrzak-Kuligowska, K. & Bednarczyk, P. Functional Expression of TRPV1 Ion Channel in the Canine Peripheral Blood Mononuclear Cells. *International journal of molecular sciences* **22**, (2021).

83. Bertin, S. *et al.* The ion channel TRPV1 regulates the activation and proinflammatory properties of $CD4^+$ T cells. *Nature immunology* **15**, 1055–1063 (2014).

84. Shuba, Y. M. Beyond Neuronal Heat Sensing: Diversity of TRPV1 Heat-Capsaicin Receptor-Channel Functions. *Frontiers in Cellular Neuroscience* **14**, (2021).

85. Omari, S. A., Adams, M. J. & Geraghty, D. P. *TRPV1 Channels in Immune Cells and Hematological Malignancies*. *Advances in Pharmacology* vol. 79 (Elsevier Inc., 2017).

86. Pumroy, R. A. *et al.* Molecular mechanism of TRPV2 channel modulation by cannabidiol. *eLife* **8**, (2019).

87. Perálvarez-Marín, A., Doñate-Macian, P. & Gaudet, R. What do we know about the transient receptor potential vanilloid 2 (TRPV2) ion channel? *FEBS Journal* **280**, 5471–5487 (2013).

88. Olivas-Aguirre, M. *et al.* Cannabidiol directly targets mitochondria and disturbs calcium homeostasis in acute lymphoblastic leukemia. *Cell Death & Disease* **10**, 779 (2019).

89. Stasiłowicz, A., Tomala, A., Podolak, I. & Cielecka-Piontek, J. Cannabis sativa L. as a Natural Drug Meeting the Criteria of a Multitarget Approach to Treatment. *International Journal of Molecular Sciences* **22**, 778 (2021).

90. Pisanti, S. *et al.* Cannabidiol: State of the art and new challenges for therapeutic applications. *Pharmacology & therapeutics* **175**, 133–150 (2017).

91. Solinas, M. *et al.* Cannabidiol, a Non-Psychoactive Cannabinoid Compound, Inhibits Proliferation and Invasion in U87-MG and T98G Glioma Cells through a Multitarget Effect. *PLoS ONE* **8**, e76918 (2013).

92. Gallily, R. *et al.* Gamma-irradiation enhances apoptosis induced by cannabidiol, a non-psychotropic cannabinoid, in cultured HL-60 myeloblastic leukemia cells. *Leukemia & lymphoma* **44**, 1767–73 (2003).

93. McKallip, R. J. *et al.* Cannabidiol-induced apoptosis in human leukemia cells: A novel role of cannabidiol in the regulation of p22phox and Nox4 expression. *Molecular pharmacology* **70**, 897–908 (2006).

94. Seltzer, E. S., Watters, A. K., MacKenzie, D., Granat, L. M. & Zhang, D. Cannabidiol (CBD) as a Promising Anti-Cancer Drug. *Cancers* **12**, 3203 (2020).

95. de Luca, R. *et al.* Mechanisms of N-oleoyldopamine activation of central histaminergic neurons. *Neuropharmacology* **143**, 327–338 (2018).

96. Szolcsányi, J. *et al.* Direct evidence for activation and desensitization of the capsaicin receptor by N-oleoyldopamine on TRPV1-transfected cell, line in gene deleted mice and in the rat. *Neuroscience Letters* **361**, 155–158 (2004).

97. Chu, C. J. *et al.* N-Oleoyldopamine, a Novel Endogenous Capsaicin-like Lipid That Produces Hyperalgesia. *Journal of Biological Chemistry* **278**, 13633–13639 (2003).

98. Chang, A., Rosani, A. & Quick, J. *Capsaicin*. *StatPearls* (2021).

99. Zhang, S., Wang, D., Huang, J., Hu, Y. & Xu, Y. Application of capsaicin as a potential new therapeutic drug in human cancers. *Journal of Clinical Pharmacy and Therapeutics* **45**, 16–28 (2020).

100. Bootman, M. D., Chehab, T., Bultynck, G., Parys, J. B. & Rietdorf, K. The regulation of autophagy by calcium signals: Do we have a consensus? *Cell Calcium* **70**, 32–46 (2018).

101. Folkerts, H., Hilgendorf, S., Vellenga, E., Bremer, E. & Wiersma, V. R. The multifaceted role of autophagy in cancer and the microenvironment. *Medicinal Research Reviews* **39**, 517–560 (2019).

102. Li, C. J., Liao, W. T., Wu, M. Y. & Chu, P. Y. New insights into the role of autophagy in tumor immune microenvironment. *International Journal of Molecular Sciences* **18**, (2017).

103. Auberger, P. & Puissant, A. Autophagy, a key mechanism of oncogenesis and resistance in leukemia. *Blood* **129**, 547–552 (2017).

104. Nazio, F., Bordi, M., Cianfanelli, V., Locatelli, F. & Cecconi, F. Autophagy and cancer stem cells: molecular mechanisms and therapeutic applications. *Cell Death and Differentiation* **26**, 690–702 (2019).

105. Galluzzi, L., Buqué, A., Kepp, O., Zitvogel, L. & Kroemer, G. Immunological Effects of Conventional Chemotherapy and Targeted Anticancer Agents. *Cancer Cell* **28**, 690–714 (2015).

106. Pitt, J. M. *et al.* Resistance Mechanisms to Immune-Checkpoint Blockade in Cancer: Tumor-Intrinsic and -Extrinsic Factors. *Immunity* **44**, 1255–1269 (2016).

107. Naka, K. *et al.* TGF-β–FOXO signalling maintains leukaemia-initiating cells in chronic myeloid leukaemia. *Nature* **463**, 676–680 (2010).

108. Pellicano, F. *et al.* The Antiproliferative Activity of Kinase Inhibitors in Chronic Myeloid Leukemia Cells Is Mediated by FOXO Transcription Factors. *STEM CELLS* **32**, 2324–2337 (2014).

109. van der Vos, K. E. & Coffer, P. J. FOXO-binding partners: it takes two to tango. *Oncogene* **27**, 2289–2299 (2008).

110. Maycotte, P., Jones, K. L., Goodall, M. L., Thorburn, J. & Thorburn, A. Autophagy Supports Breast Cancer Stem Cell Maintenance by Regulating IL6 Secretion. *Molecular Cancer Research* **13**, 651–658 (2015).

111. Iliopoulos, D., Hirsch, H. A., Wang, G. & Struhl, K. Inducible formation of breast cancer stem cells and their dynamic equilibrium with non-stem cancer cells via IL6 secretion. *Proceedings of the National Academy of Sciences* **108**, 1397–1402 (2011).

112. Codony-Servat, J. & Rosell, R. Cancer stem cells and immunoresistance: clinical implications and solutions. *Translational lung cancer research* **4**, 689–703 (2015).

113. Viry, E. *et al.* Autophagy: An adaptive metabolic response to stress shaping the antitumor immunity. *Biochemical Pharmacology* **92**, 31–42 (2014).

114. Lorin, S., Hamaï, A., Mehrpour, M. & Codogno, P. Autophagy regulation and its role in cancer. *Seminars in Cancer Biology* **23**, 361–379 (2013).

115. Dikic, I. & Elazar, Z. Mechanism and medical implications of mammalian autophagy. *Nature Reviews Molecular Cell Biology* **19**, 349–364 (2018).

116. Porporato, P. E., Filigheddu, N., Pedro, J. M. B. S., Kroemer, G. & Galluzzi, L. Mitochondrial metabolism and cancer. *Cell Research* **28**, 265–280 (2018).

117. Chourasia, A. H., Boland, M. L. & Macleod, K. F. Mitophagy and cancer. *Cancer & Metabolism* **3**, 4 (2015).

118. Barbato, A. *et al.* Mitochondrial Bioenergetics at the Onset of Drug Resistance in Hematological Malignancies: An Overview. *Frontiers in Oncology* **10**, 604143 (2020).

119. Vara-Perez, M., Felipe-Abrio, B. & Agostinis, P. Mitophagy in Cancer: A Tale of Adaptation. *Cells* **8**, (2019).

120. Dougan, M. & Dranoff, G. Immune Therapy for Cancer. *Annual Review of Immunology* **27**, 83–117 (2009).

121. Bardhan, K., Anagnostou, T. & Boussiotis, V. A. The PD1:PD-L1/2 Pathway from Discovery to Clinical Implementation. *Frontiers in Immunology* **7**, 550 (2016).

122. Tang, H. *et al.* PD-L1 on host cells is essential for PD-L1 blockade–mediated tumor regression. *Journal of Clinical Investigation* **128**, 580–588 (2018).

123. Bellmunt, J., Powles, T. & Vogelzang, N. J. A review on the evolution of PD-1/PD-L1 immunotherapy for bladder cancer: The future is now. *Cancer Treatment Reviews* **54**, 58–67 (2017).

124. Robainas, M., Otano, R., Bueno, S. & Ait-Oudhia, S. Understanding the role of PD-L1/PD1 pathway blockade and autophagy in cancer therapy. *OncoTargets and Therapy* **10**, 1803–1807 (2017).

125. Choi, D., Tremblay, D., Iancu-Rubin, C. & Mascarenhas, J. Programmed cell death-1 pathway inhibition in myeloid malignancies: implications for myeloproliferative neoplasms. *Annals of Hematology* **96**, 919–927 (2017).

126. Grzywnowicz, M. *et al.* Expression of Programmed Death 1 Ligand in Different Compartments of Chronic Lymphocytic Leukemia. *Acta Haematologica* **134**, 255–262 (2015).

127. Mumprecht, S., Schürch, C., Schwaller, J., Solenthaler, M. & Ochsenbein, A. F. Programmed death 1 signaling on chronic myeloid leukemia-specific T cells results in T-cell exhaustion and disease progression. *Blood* **114**, 1528–1536 (2009).

128. Wang, X. *et al.* Autophagy inhibition enhances PD-L1 expression in gastric cancer. *Journal of Experimental and Clinical Cancer Research* **38**, 1–14 (2019).

129. Sutherland, J. A., Turner, A. R., Mannoni, P., McGann, L. E. & Turc, J. M. Differentiation of K562 leukemia cells along erythroid, macrophage, and megakaryocyte lineages. *Journal of biological response modifiers* **5**, 250–62 (1986).

130. Blom, T., Huang, R., Aveskogh, M., Nilsson, K. & Hellman, L. Phenotypic characterization of KU812, a cell line identified as an immature human basophilic leukocyte. *European journal of immunology* **22**, 2025–32 (1992).

131. Nakazawa, M. *et al.* KU 812: a pluripotent human cell line with spontaneous erythroid terminal maturation. *Blood* **73**, 2003–2013 (1989).

132. Tsuji-Takayama, K. *et al.* Establishment of multiple leukemia cell lines with diverse myeloid and/or megakaryoblastoid characteristics from a single Ph1 positive chronic myelogenous leukemia blood sample. *Human cell* **7**, 167–71 (1994).

133. Dong, Y. *et al.* Semi-random mutagenesis profile of BCR-ABL during imatinib resistance acquirement in K562 cells. *Molecular medicine reports* **16**, 9409–9414 (2017).

134. Dircio-Maldonado, R. *et al.* Functional Integrity and Gene Expression Profiles of Human Cord Blood-Derived Hematopoietic Stem and Progenitor Cells Generated In Vitro. *STEM CELLS Translational Medicine* **7**, 602–614 (2018).

135. de Abreu Costa, L. *et al.* Dimethyl Sulfoxide (DMSO) Decreases Cell Proliferation and TNF-α, IFN-γ, and IL-2 Cytokines Production in Cultures of Peripheral Blood Lymphocytes. *Molecules* **22**, 1789 (2017).

136. Bagger, F. O. *et al.* BloodSpot: a database of gene expression profiles and transcriptional programs for healthy and malignant haematopoiesis. *Nucleic Acids Research* **44**, (2016).

137. Choi, J. *et al.* Stemformatics: visualize and download curated stem cell data. *Nucleic Acids Research* **47**, (2019).

138. Cramer-Morales, K. *et al.* Personalized synthetic lethality induced by targeting RAD52 in leukemias identified by gene mutation and expression profile. *Blood* **122**, (2013).

139. Majeti, R. *et al.* Dysregulated gene expression networks in human acute myelogenous leukemia stem cells. *Proceedings of the National Academy of Sciences of the United States of America* **106**, (2009).

140. Andersson, A., Edén, P., Olofsson, T. & Fioretos, T. Gene expression signatures in childhood acute leukemias are largely unique and distinct from those of normal tissues and other malignancies. *BMC medical genomics* **3**, (2010).

141. Hu, X. *et al.* Integrated regulation of Toll-like receptor responses by Notch and interferon-gamma pathways. *Immunity* **29**, (2008).

142. Wildenberg, M. E., van Helden-Meeuwsen, C. G., van de Merwe, J. P., Drexhage, H. A. & Versnel, M. A. Systemic increase in type I interferon activity in Sjögren's syndrome: a putative role for plasmacytoid dendritic cells. *European journal of immunology* **38**, (2008).

143. Khanduja, K. L. *et al.* Anti-apoptotic activity of caffeic acid, ellagic acid and ferulic acid in normal human peripheral blood mononuclear cells: A Bcl-2 independent mechanism. *Biochimica et Biophysica Acta (BBA) - General Subjects* **1760**, 283–289 (2006).

144. Sun, Y. *et al.* Erythropoietin Protects Erythrocytes Against Oxidative Stress-Induced Eryptosis In Vitro. *Clinical Laboratory* **64**, (2018).

145. Santoni, G. *et al.* The role of transient receptor potential vanilloid type-2 ion channels in innate and adaptive immune responses. *Frontiers in immunology* **4**, 34 (2013).

146. Park, K. S. *et al.* Identification and functional characterization of ion channels in CD34+ hematopoietic stem cells from human peripheral blood. *Molecules and Cells* **32**, 181–188 (2011).

147. Kunde, D. A., Yingchoncharoen, J., Jurković, S. & Geraghty, D. P. TRPV1 mediates capsaicin-stimulated metabolic activity but not cell death or inhibition of interleukin-1β release in human THP-1 monocytes. *Toxicology and Applied Pharmacology* **360**, 9–17 (2018).

148. Iannotti, F. A. *et al.* Nonpsychotropic Plant Cannabinoids, Cannabidivarin (CBDV) and Cannabidiol (CBD), Activate and Desensitize Transient Receptor Potential Vanilloid 1 (TRPV1) Channels in Vitro: Potential for the Treatment of Neuronal Hyperexcitability. *ACS Chemical Neuroscience* **5**, 1131–1141 (2014).

149. Nabissi, M. *et al.* Cannabidiol stimulates Aml-1a-dependent glial differentiation and inhibits glioma stem-like cells proliferation by inducing autophagy in a TRPV2-dependent manner. *International journal of cancer* **137**, 1855–1869 (2015).

150. Amantini, C. *et al.* Distinct thymocyte subsets express the vanilloid receptor VR1 that mediates capsaicin-induced apoptotic cell death. *Cell Death & Differentiation* **11**, 1342–1356 (2004).

151. Morelli, M. B. *et al.* The effects of cannabidiol and its synergism with bortezomib in multiple myeloma cell lines. A role for transient receptor potential vanilloid type-2. *International journal of cancer* **134**, 2534–2546 (2014).

152. Barber, N. A., Afzal, W. & Akhtari, M. Hematologic toxicities of small molecule tyrosine kinase inhibitors. *Targeted Oncology* **6**, 203–215 (2011).

153. Brookes, P. S., Yoon, Y., Robotham, J. L., Anders, M. W. & Sheu, S.-S. Calcium, ATP, and ROS: a mitochondrial love-hate triangle. *American Journal of Physiology-Cell Physiology* **287**, C817–C833 (2004).

154. Dannheisig, D. P. *et al.* Loss of Peter Pan (PPAN) Affects Mitochondrial Homeostasis and Autophagic Flux. *Cells* **8**, 894 (2019).

155. Youle, R. J. & Narendra, D. P. Mechanisms of mitophagy. *Nature Reviews Molecular Cell Biology* **12**, 9–14 (2011).

156. Kharaziha, P. & Panaretakis, T. Dynamics of Atg5–Atg12–Atg16L1 Aggregation and Deaggregation. *Methods in Enzymology* **587**, 247–255 (2017).

157. Wong, Y. C. & Holzbaur, E. L. F. Optineurin is an autophagy receptor for damaged mitochondria in parkin-mediated mitophagy that is disrupted by an ALS-linked mutation. *Proceedings of the National Academy of Sciences* **111**, E4439–E4448 (2014).

158. Cho, Y.-H. *et al.* Autophagy Regulates Homeostasis of Pluripotency-Associated Proteins in hESCs. *STEM CELLS* **32**, 424–435 (2014).

159. Gerber, J. M. *et al.* Characterization of chronic myeloid leukemia stem cells. *American Journal of Hematology* **86**, (2011).

160. Albajar, M. *et al.* PU.1 expression is restored upon treatment of chronic myeloid leukemia patients. *Cancer Letters* **270**, 328–336 (2008).

161. Rajendran, V. & Jain, M. V. In Vitro Tumorigenic Assay: Colony Forming Assay for Cancer Stem Cells. *Methods in molecular biology (Clifton, N.J.)* **1692**, 89–95 (2018).

162. Gou, Q. *et al.* PD-L1 degradation pathway and immunotherapy for cancer. *Cell Death & Disease* **11**, (2020).

163. Jung, J. *et al.* Capsaicin Binds to the Intracellular Domain of the Capsaicin-Activated Ion Channel. *The Journal of Neuroscience* **19**, (1999).

164. Zhai, K., Liskova, A., Kubatka, P. & Büsselberg, D. Calcium Entry through TRPV1: A Potential Target for the Regulation of Proliferation and Apoptosis in Cancerous and Healthy Cells. *International journal of molecular sciences* **21**, (2020).

165. Wang, J. DNA damage and apoptosis. *Cell Death & Differentiation* **8**, (2001).

166. González-Quiroz, M. *et al.* When Endoplasmic Reticulum Proteostasis Meets the DNA Damage Response. *Trends in Cell Biology* **30**, (2020).

167. Cao, S. S. & Kaufman, R. J. Endoplasmic reticulum stress and oxidative stress in cell fate decision and human disease. *Antioxidants & redox signaling* **21**, (2014).

168. Wang, M., Wey, S., Zhang, Y., Ye, R. & Lee, A. S. Role of the Unfolded Protein Response Regulator GRP78/BiP in Development, Cancer, and Neurological Disorders. *Antioxidants & Redox Signaling* **11**, (2009).

169. Ye, Y., Shibata, Y., Yun, C., Ron, D. & Rapoport, T. A. A membrane protein complex mediates retro-translocation from the ER lumen into the cytosol. *Nature* **429**, (2004).

170. Osman, A. E. G. & Deininger, M. W. Chronic Myeloid Leukemia: Modern therapies, current challenges and future directions. *Blood Reviews* 100825 (2021) doi:10.1016/j.blre.2021.100825.

171. Apperley, J. F. Chronic myeloid leukaemia. *The Lancet* **385**, 1447–1459 (2015).

172. Amantini, C. *et al.* The TRPV1 ion channel regulates thymocyte differentiation by modulating autophagy and proteasome activity. *Oncotarget* **8**, 90766–90780 (2017).

173. Cai, X. *et al.* Transient Receptor Potential Vanilloid 2 (TRPV2), a Potential Novel Biomarker in Childhood Asthma. *Journal of Asthma* **50**, 209–214 (2013).

174. Pottosin, I. *et al.* Mechanosensitive Ca2 +-permeable channels in human leukemic cells: Pharmacological and molecular evidence for TRPV2. *Biochimica et Biophysica Acta - Biomembranes* **1848**, 51–59 (2015).

175. Santoni, G. *et al.* The TRPV2 cation channels: from urothelial cancer invasiveness to glioblastoma multiforme interactome signature. *Laboratory Investigation* (2020) doi:10.1038/s41374-019-0333-7.

176. Liberati, S. *et al.* Advances in transient receptor potential vanilloid-2 channel expression and function in tumor growth and progression. *Current protein & peptide science* **15**, 732–737 (2014).

177. Li, L. *et al.* The Impact of TRPV1 on Cancer Pathogenesis and Therapy: A Systematic Review. *International Journal of Biological Sciences* **17**, (2021).

178. Huynh, K. W. *et al.* Structure of the full-length TRPV2 channel by cryo-EM. *Nature Communications* **7**, 11130 (2016).

179. Deng, L., Ng, L., Ozawa, T. & Stella, N. Quantitative Analyses of Synergistic Responses between Cannabidiol and DNA-Damaging Agents on the Proliferation and Viability of Glioblastoma and Neural Progenitor Cells in Culture. *Journal of Pharmacology and Experimental Therapeutics* **360**, 215–224 (2017).

180. Kalenderoglou, N., Macpherson, T. & Wright, K. L. Cannabidiol Reduces Leukemic Cell Size – But Is It Important? *Frontiers in Pharmacology* **8**, 144 (2017).

181. Scott, K. A., Dalgleish, A. G. & Liu, W. M. Anticancer effects of phytocannabinoids used with chemotherapy in leukaemia cells can be improved by altering the sequence of their administration. *International Journal of Oncology* **51**, 369–377 (2017).

182. Togano, T. *et al.* The evaluation of Cannabidiol's effect on the immunotherapy of Burkitt lymphoma. *Biochemical and Biophysical Research Communications* **520**, 225–230 (2019).

183. Nakajima, K. *et al.* Glycolytic enzyme hexokinase II is a putative therapeutic target in B-cell malignant lymphoma. *Experimental Hematology* **78**, 46-55.e3 (2019).

184. Sriskanthadevan, S. *et al.* AML cells have low spare reserve capacity in their respiratory chain that renders them susceptible to oxidative metabolic stress. *Blood* **125**, 2120–2130 (2015).

185. Mikkilineni, L. *et al.* Hodgkin lymphoma: A complex metabolic ecosystem with glycolytic reprogramming of the tumor microenvironment. *Seminars in Oncology* **44**, 218–225 (2017).

186. Tanida, I., Ueno, T. & Kominami, E. LC3 conjugation system in mammalian autophagy. *The International Journal of Biochemistry & Cell Biology* **36**, 2503–2518 (2004).

187. Hanada, T. *et al.* The Atg12-Atg5 Conjugate Has a Novel E3-like Activity for Protein Lipidation in Autophagy. *Journal of Biological Chemistry* **282**, 37298–37302 (2007).

188. Mai, S., Muster, B., Bereiter-Hahn, J. & Jendrach, M. Autophagy proteins LC3B, ATG5 and ATG12 participate in quality control after mitochondrial damage and influence lifespan. *Autophagy* **8**, 47–62 (2012).

189. Narendra, D. P. & Youle, R. J. Targeting Mitochondrial Dysfunction: Role for PINK1 and Parkin in Mitochondrial Quality Control. *Antioxidants & Redox Signaling* **14**, 1929–1938 (2011).

190. Naik, P. P., Birbrair, A. & Bhutia, S. K. Mitophagy-driven metabolic switch reprograms stem cell fate. *Cellular and Molecular Life Sciences* **76**, 27–43 (2019).

191. Pei, S. *et al.* AMPK/FIS1-Mediated Mitophagy Is Required for Self-Renewal of Human AML Stem Cells. *Cell Stem Cell* **23**, 86-100.e6 (2018).

192. Picot, T. *et al.* Potential Role of OCT4 in Leukemogenesis. *Stem Cells and Development* **26**, 1637–1647 (2017).

193. Amer, A., Abdelhaleim, ayman & Salah, hossam E. CD34 Expression in Adult Acute Myeloid Leukemia is an Independent Poor Prognostic Factor. *Zagazig University Medical Journal* **0**, (2019).

194. Trinh, B. Q. *et al.* Myeloid lncRNA LOUP Mediates Opposing Regulatory Effects of RUNX1 and RUNX1-ETO in t(8;21) AML. *Blood* (2021) doi:10.1182/blood.2020007920.

195. Herbst, R. S. *et al.* Atezolizumab for First-Line Treatment of PD-L1–Selected Patients with NSCLC. *New England Journal of Medicine* **383**, 1328–1339 (2020).

196. Giannopoulos, K. Targeting Immune Signaling Checkpoints in Acute Myeloid Leukemia. *Journal of Clinical Medicine* **8**, 236 (2019).

197. Ju, X., Zhang, H., Zhou, Z. & Wang, Q. *Regulation of PD-L1 expression in cancer and clinical implications in immunotherapy*. *Am J Cancer Res* vol. 10 www.ajcr.us/ (2020).

198. Chen, J., Jiang, C. C., Jin, L. & Zhang, X. D. Regulation of PD-L1: A novel role of pro-survival signalling in cancer. *Annals of Oncology* vol. 27 409–416 (2016).

199. Shi, L., Chen, S., Yang, L. & Li, Y. The role of PD-1 and PD-L1 in T-cell immune suppression in patients with hematological malignancies. *Journal of Hematology and Oncology* vol. 6 (2013).

200. Arrigoni, E. *et al.* Concise Review: Chronic Myeloid Leukemia: Stem Cell Niche and Response to Pharmacologic Treatment. *STEM CELLS Translational Medicine* **7**, 305–314 (2018).

201. Charaf, L. *et al.* Effect of tyrosine kinase inhibitors on stemness in normal and chronic myeloid leukemia cells. *Leukemia* **31**, 65–74 (2017).

202. Yuan, Y., Adam, A., Zhao, C. & Chen, H. Recent advancements in the mechanisms underlying resistance to pd-1/pd-l1 blockade immunotherapy. *Cancers* vol. 13 1–18 (2021).

203. Liu, H. *et al.* Epigenetic treatment-mediated modulation of PD-L1 predicts potential therapy resistance over response markers in myeloid malignancies: A molecular mechanism involving effectors of PD-L1 reverse signaling. *Oncology Letters* (2018) doi:10.3892/ol.2018.9841.

204. Lin, C. *et al.* Programmed Death-Ligand 1 Expression Predicts Tyrosine Kinase Inhibitor Response and Better Prognosis in a Cohort of Patients With Epidermal Growth Factor Receptor Mutation-Positive Lung Adenocarcinoma. *Clinical lung cancer* **16**, (2015).

205. Tsuchiya, S. *et al.* Establishment and characterization of a human acute monocytic leukemia cell line (THP-1). *International journal of cancer* **26**, (1980).

206. Tober, J. *et al.* Maturation of hematopoietic stem cells from prehematopoietic stem cells is accompanied by up-regulation of PD-L1. *Journal of Experimental Medicine* **215**, (2018).

207. Fattori, V., Hohmann, M. S. N., Rossaneis, A. C., Pinho-Ribeiro, F. A. & Verri, W. A. Capsaicin: Current Understanding of Its Mechanisms and Therapy of Pain and Other Pre-Clinical and Clinical Uses. *Molecules (Basel, Switzerland)* **21**, (2016).

208. Clark, R. & Lee, S.-H. Anticancer Properties of Capsaicin Against Human Cancer. *Anticancer research* **36**, (2016).

209. Spicarova, D. & Palecek, J. Tumor necrosis factor alpha sensitizes spinal cord TRPV1 receptors to the endogenous agonist N-oleoyldopamine. *Journal of neuroinflammation* **7**, (2010).

210. Kang, M. A., So, E.-Y., Simons, A. L., Spitz, D. R. & Ouchi, T. DNA damage induces reactive oxygen species generation through the H2AX-Nox1/Rac1 pathway. *Cell Death & Disease* **3**, (2012).

211. Zhang, Z. *et al.* Redox signaling and unfolded protein response coordinate cell fate decisions under ER stress. *Redox Biology* **25**, (2019).

212. Oda, Y. *et al.* Derlin-2 and Derlin-3 are regulated by the mammalian unfolded protein response and are required for ER-associated degradation. *The Journal of cell biology* **172**, (2006).

213. Ye, Y., Shibata, Y., Yun, C., Ron, D. & Rapoport, T. A. A membrane protein complex mediates retro-translocation from the ER lumen into the cytosol. *Nature* **429**, (2004).

214. Lilley, B. N. & Ploegh, H. L. A membrane protein required for dislocation of misfolded proteins from the ER. *Nature* **429**, (2004).

215. Cox, J. S., Shamu, C. E. & Walter, P. Transcriptional induction of genes encoding endoplasmic reticulum resident proteins requires a transmembrane protein kinase. *Cell* **73**, (1993).

Other projects and pubblications

Pubblications

Maggi F, Morelli MB, Tomassoni D, Marinelli O, Aguzzi C, Zeppa L, Nabissi M, Santoni G and Amantini C. The effects of cannabidiol via TRPV2 channel in chronic myeloid leukemia cells and its combination with imatinib. Cancer Science 2022. **Accepted for pubblication**. https://doi.org/10.1111/cas.15257

Faloppi L, Nabissi M, Santoni M, **Maggi F**, Galizia E, Miccini F, Bianconi M, Puzzoni M, Astara G, Battelli N, Santoni G, Scartozzi M (2019). RISE-HEP project part 1: Treatment sequences evaluation in hepatocellular carcinoma cell lines. JOURNAL OF CLINICAL ONCOLOGY, ISSN:0732-183X, doi:10.1200/JCO.2019.37.15_suppl.e15663.

Maggi F, Amantini C, Nabissi M, Marinelli O, Santoni G and Morelli MB. Typical and Atypical Circulating Tumour Cells in Bladder Cancer. Why Improve our Knowledge? Clin Oncol. 2019; 2(2): 1008.

Amantini C, Morelli MB, Nabissi M, Piva F, Marinelli O, **Maggi F**, Bianchi F, Bittoni A, Berardi R, Giampieri R and Santoni G. 2019. Expression Profiling of Circulating Tumor Cells in Pancreatic Ductal Adenocarcinoma Patients: Biomarkers Predicting Overall Survival. Front. Oncol. 9:874. doi: 10.3389/fonc.2019.00874

Marinelli O, Annibali D, Aguzzi C, Tuyaerts S, Amant F, Morelli MB, Santoni G, Amantini A, **Maggi F**, Nabissi M. The Controversial Role of PD-1 and Its Ligands in Gynecological Malignancies. Front Oncol. 2019;9:1073. doi:10.3389/fonc.2019.01073

Santoni G, **Maggi F**, Morelli MB, Santoni M, Marinelli O. Transient Receptor Potential Cation Channels in Cancer Therapy. Med. Sci. 2019, 7, 108. doi:10.3390/medsci7120108

Santoni G, Amantini C, **Maggi F**, Marinelli O, Santoni M, Nabissi M, Morelli MB. The TRPV2 cation channels: from urothelial cancer invasiveness to glioblastoma multiforme interactome signature. Lab Invest. 2020;100(2):186–198. doi:10.1038/s41374-019-0333-7.

Santoni G, **Maggi F**, Amantini C, Marinelli O, Nabissi M, Morelli MB. Pathophysiological Role of Transient Receptor Potential Mucolipin Channel 1 in Calcium-mediated Stress-Induced Neurodegenerative Disease. Front. Physiol. 2020 Mar 24; 11:251. doi: 10.3389/fphys.2020.00251. eCollection 2020.

Santoni G, Santoni M, **Maggi F**, Marinelli O and Morelli MB (2020). Emerging Role of Mucolipins TRPML Channels in Cancer. Front. Oncol. 10:659. doi:10.3389/fonc.2020.00659

Martinelli I, Micioni Di Bonaventura MV, Moruzzi M, Amantini C, **Maggi F**, Gabrielli MG, Fruganti A, Marchegiani A, Dini F, Marini C, Polidori C, Lupidi G, Amenta F, Tayebati SK, Cifani C, Tomassoni D. Effects of Prunus cerasus L. Seeds and Juice on Liver Steatosis in an Animal Model of Diet-Induced Obesity. Nutrients 2020, 12, 1308.

Santoni G, Morelli MB, Nabissi M, **Maggi F**, Marinelli O, Santoni M, Amantini C. Cross-talk between microRNAs, long non-coding RNAs and p21Cip1 in glioma: diagnostic, prognostic and therapeutic roles. J Cancer Metastasis Treat 2020; 6:22. http://dx.doi.org/10.20517/2394-4722.2020.49.

Marinelli O, Morelli MB, Annibali D, Aguzzi C, Zeppa L, Tuyaerts S, Amantini C, Amant F, Ferretti B, **Maggi F**, Santoni G, Nabissi M. The Effects of Cannabidiol and Prognostic Role of TRPV2 in Human Endometrial Cancer. Int. J. Mol. Sci. 2020, 21, 5409.

Marinelli O, Annibali D, Morelli MB, Zeppa L, Tuyaerts S, Aguzzi C, Amantini C, Maggi F, Ferretti B, Santoni G, Amant F, Nabissi M. Biological Function of PD-L2 and Correlation With Overall Survival in Type II Endometrial Cancer. Front Oncol. 2020 Oct 28;10:538064. doi: 10.3389/fonc.2020.538064.

Marinelli O, Romagnoli E, **Maggi F**, Nabissi M, Amantini C, Morelli MB, Santoni M, Battelli N, Santoni G. Exploring treatment with Ribociclib alone or in sequence/combination with Everolimus in ER+HER2-Rb wildtype and knock-down in breast cancer cell lines. BMC Cancer. 2020 Nov 19;20(1):1119. doi: 10.1186/s12885-020-07619-1.

Santoni G, Amantini C, Nabissi M, **Maggi F**, Arcella A, Marinelli O, Eleuteri AM, Santoni M and Morelli MB. Knock-Down of Mucolipin 1 Channel Promotes Tumor Progression and Invasion in Human Glioblastoma Cell Lines. Front. Oncol. 2021; 11:578928. doi: 10.3389/fonc.2021.578928

Cocci P, Moruzzi M, Martinelli I, **Maggi F**, Micioni Di Bonaventura MV, Cifani C, Mosconi G, Tayebati SK, Damiano S, Lupidi G, Amantini C, Tomassoni D, Palermo FA. Tart cherry (Prunus cerasus L.) dietary supplement modulates visceral adipose tissue CB1 mRNA levels along with other adipogenesis-related genes in rat models of diet-induced obesity. Eur J Nutr. 2021; 60(5):2695-2707. doi: 10.1007/s00394-020-02459-y.

Maggi F, Morelli MB, Nabissi M, Marinelli O, Zeppa L, Aguzzi C, Santoni G, Amantini C. Transient Receptor Potential (TRP) Channels in Haematological Malignancies: An Update. Biomolecules. 2021; 11(5):765. https://doi.org/10.3390/biom11050765

Santoni G, Amantini C, Santoni M, **Maggi F**, Morelli MB and Santoni A (2021) Mechanosensation and Mechanotransduction in Natural Killer Cells. Front. Immunol. 12:688918. doi: 10.3389/fimmu.2021.688918

Santoni G, Nabissi M, Amantini C, Santoni M, Ricci-Vitiani L, Pallini R, **Maggi F**, Morelli MB. ERK Phosphorylation Regulates the Aml1/Runx1 Splice Variants and

the TRP Channels Expression during the Differentiation of Glioma Stem Cell Lines. Cells. 2021;10(8):2052. doi: 10.3390/cells10082052.

Cappelli A, Amantini C, **Maggi F**, Favia G, Ricci I. Formulation and Safety Tests of a Wickerhamomyces anomalus–Based Product: Potential Use of Killer Toxins of a Mosquito Symbiotic Yeast to Limit Malaria Transmission. Toxins 2021, 13, 676. https://doi.org/10.3390/toxins13100676

Roy P, Martinelli I, Moruzzi M, **Maggi F**, Amantini C, Micioni Di Bonaventura MV, Cifani C, Amenta F, Tayebati SK, Tomassoni D. Ion channels alterations in the forebrain of high-fat diet fed rats. Eur J Histochem. 2021;65(s1):3305. doi: 10.4081/ejh.2021.3305.

Morelli MB, Amantini C, Rossi de Vermandois JA, Gubbiotti M, Giannantoni A, Mearini E, **Maggi F**, Nabissi M, Marinelli O, Santoni M, Cimadamore A, Montironi R, Santoni G. Correlation between High PD-L1 and EMT/Invasive Genes Expression and Reduced Recurrence-Free Survival in Blood-Circulating Tumor Cells from Patients with Non-Muscle-Invasive Bladder Cancer. Cancers (Basel). 2021;13(23):5989. doi: 10.3390/cancers13235989.

Santoni G, Amantini C, **Maggi F**, Marinelli O, Santoni M, Morelli MB. The Mucolipin TRPML2 Channel Enhances the Sensitivity of Multiple Myeloma Cell Lines to Ibrutinib and/or Bortezomib Treatment. Biomolecules. 2022;12(1):107. doi: 10.3390/biom12010107.

Santoni G, Amantini C, Nabissi M, Arcella A, **Maggi F**, Santoni M, Morelli MB. Functional In Vitro Assessment of VEGFA/NOTCH2 Signaling Pathway and pRB Proteasomal Degradation and the Clinical Relevance of Mucolipin TRPML2 Overexpression in Glioblastoma Patients. Int J Mol Sci. 2022;23(2):688. doi: 10.3390/ijms23020688.

Oral Presentation

Cannabidiol-Induced Autophagic Pathway in Chronic Myeloid Leukemia Cells; 3rd International Conference on PharmScience Research & Development (Pharma R&D-2021); Virtual, February 22nd-24th, 2021.

Cannabidiol: Promising role as anti-cancer drug in chronic myeloid leukemia cells; 5th Global Summit on Cancer Science and Oncology 2021, Virtual, February 26th.

Cannabidiol extracted from Cannabis sativa induces cell cycle arrest, mitophagy and cell differentiation in chronic myeloid leukemia cells.

Federica Maggi, Maria Beatrice Morelli, Massimo Nabissi, Oliviero Marinelli, Daniele Tomassoni, Cristina Aguzzi, Laura Zeppa, Giorgio Santoni and Consuelo Amantini; 5° Convegno PTA, ALIMENTI E NUTRACEUTICI: SALUTE E PREVENZIONE ATTRAVERSO IL CIBO; Virtual, July 13th, 2021.

Abstracts

Martinelli I, Moruzzi M, **Maggi F**, Amantini C, Palermo F A, Cocci P, Micioni Di Bonaventura M V, Gabrielli G, Fruganti A, Marchegiani A, Kloeting N, Lupidi G, Cifani C, Seyed K T, Tomassoni D (2019). Prunus Cerasus L. modulates adipogenesis and inflammation of visceral adipose tissue in rats fed a high-fat diet. In: CIBO E NUTRACEUTICI: PAROLA CHIAVE "CARATTERIZZAZIONE". vol. 1, ISBN: 9788867680405, Camerino, 9 Luglio 2019.

Grant

"Avvio alla ricerca" grant promoted by Sapienza University with the project entitled "**Transient receptor potential channels (TRP) and autophagy in cancer immunity: possible new targets in chronic myeloid leukaemia (CML) treatment**". D.R. n. 992/2020 Prot. n. 25415 of March 27th, 2020 Deliberaton S.A. 215/2020 of March 13th, 2020. Project duration: 24 months. Founding allocated: 1.000 €

Settore ERC: LS3_7 – Cell death (including senescence) and autophagy

Abstract: Autophagy represents a well conserved self-degradation system critical for cellular homeostasis and survival during stress conditions. In cancer, autophagy plays as "double-edge sword", in fact it can promote or suppress tumor development, by regulating drug resistance and aggressiveness. So far, many studies have shown that cytosolic calcium (Ca^{2+}) oscillations are involved in the regulation of autophagic signals. Several data have demonstrated that cancer cells are able to remodel their Ca^{2+} signalling network and that its disruption contribute to malignant phenotype development. An important role is played by transient receptor potential (TRP) channels which are responsible for ion homeostasis, and their expression has been also associated with tumour progression, metastasis, proliferation and chemoresistance. To date, little is known about their involvement in blood malignancies, especially in chronic myeloid leukaemia (CML), and in autophagy pathway as well. Programmed death ligand 1 (PD-L1) plays a crucial role in cancer, by inhibiting immune response against cancer cell, increasing chemoresistance and relapses. It has been demonstrated that autophagy inhibition prompts PD-L1 expression; moreover, PD-L1 is found to be up regulated in CML. Therefore, the aim of this study is to investigate in myeloid leukaemia the TRP involvement in autophagy pathway, cancer stem cell and PD-L1 expression through molecular and biochemical approaches by using specific TRP ligands, or modulating TRPs specific expression, in leukaemia cell lines treated with conventional drugs.